MELiSSA

TECHNICAL NOTE

Memorandum of Understanding TOS-MCT/2002/3161/In/CL

TECHNICAL NOTE: 86.4.9

FINAL TECHNICAL NOTE

prepared by/*préparé par*	Tobias Albrecht, Gerd Brunner TU Hamburg-Harburg, Thermal Process Engineering

reference/*réference*	14719/00/NL/SH
issue/*édition*	1
revision/*révision*	0
date of issue/*date d'édition*	30/03/06
status/*état*	Draft
Document type/*type dedocument*	Technical Note
Distribution/*distribution*	

CONFIDENTIAL DOCUMENT

APPROVAL

Title *titre*	issue 1 *issue*	revision 0 *revision*

author *auteur*	date 30/03/06 *date*

approved by *approuvé by*	date *date*

CHANGE LOG

reason for change */raison du changement*	issue/*issue*	revision/*revision*	date/*date*

CHANGE RECORD

Issue: 1 Revision: 0

reason for change/*raison du changement*	page(s)/*page(s)*	paragraph(s)/*paragraph(s)*

Table Of Contents

1 INTRODUCTION

Plant biomass is the world's most abundant source of energy and can serve as a direct nourisher as well as a feedstock for chemical products. Therefore numerous attempts to effectively utilize biomass have been undertaken in the past. One of the most promising approaches in converting materials derived from biomass to useful products is the hydrothermal treatment, also known as hydrothermolysis, employing near- and supercritical water as a reaction medium [1]. Subjecting biomass to water near its critical state offers the potential of high degrees of conversion within short residence times, compared to alternative treatment methods like the biodegradation based on microorganisms. With respect to the product distribution, high selectivities can be achieved by adjusting the operating temperature and/or pressure, leading to changes in water density, the ionic product and the dielectric constant over a wide range of conditions and thus favoring different decomposition pathways. Due to these advantages, the hydrothermal treatment becomes especially attractive when a close to complete recycling of all of the components is required, as might be encountered in future, microorganism and higher plant based life support systems. In such applications, biomass offers the potential of an almost complete recycling of all of its components by harvesting and consuming its edible parts, followed by a sub- or supercritical water treatment of the wastes generated and the subsequent, renewed build-up of plant biomass, thus closing the cycle.

Due to the unique features of water near its critical point, the conversion of biomass derived materials in sub-and supercritical water can serve as a supplement or an alternative to biological degradation techniques. The main advantages of subjecting biomass to such a hydrothermal treatment, namely the conversion at high space-time-yields, become of especially high significance when a close to complete recycling of the biomass components is required. Against this background of a fast reutilization of biomass in such systems, the present work was part of a new phase of research and development on MELISSA (Micro-Ecological Life Support System Alternative) conceived by the European Space Agency (ESA). MELISSA constitutes a self contained ecosystem based on micro-organisms and higher plants and is intended as a tool to gain knowledge and understanding about the behavior of artificial ecosystems. If the design of such an artificial ecosystem proves to be feasible and if the test results are satisfactory with respect to the requirements imposed on the project, it is planned to apply this knowledge to the development of a biological life support system in the long-term perspective. In the following the scheme of the MELISSA project thus far is explained in order to get an insight into the main working principles and the problems associated with the current setup. The special needs and requirements of a biological life support system for long-duration manned space missions are also addressed.

In order for long-duration manned space missions, e.g. a lunar base or a mission to Mars, to become possible, a feasible life support system has to be designed. Special emphasis has to be placed on the treatment of waste streams including air purification and the treatment of both

aqueous and solid wastes. This need arises from the problem of limitations of resources as well as from hygienic demands. Therefore a life support system has not only to be capable of guaranteeing hygiene by purifying the waste streams, but it has also to be capable of achieving a high recycling rate of valuable components by degrading the wastes to useful products at a high rate of conversion.

The approach taken by MELISSA is to develop a concept involving the use of a small-scale artificial ecosystem. The main building blocks and the resulting fluxes are depicted schematically in Figure 1.1.

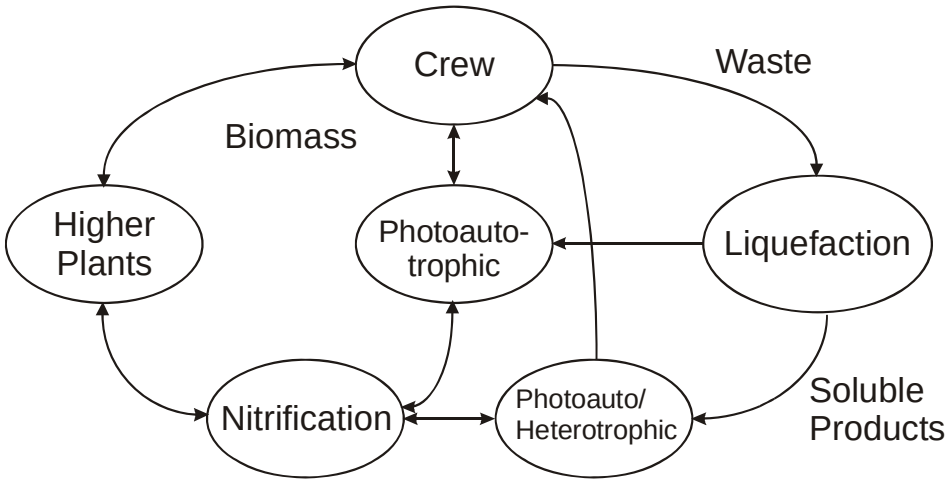

Figure 1.1: Current scheme of the artificial ecosystem of the MELISSA project

The Liquefaction, Nitrification and the Phototrophic biomass production constitute the major compartments of MELISSA. The Liquefaction compartment in the MELISSA loop is responsible for the biodegradation of wastes produced by the crew, e.g. fecal matters and urine as well as non-edible parts of plant material, paper and non-edible biomass. Subsequently, the effluent streams, composed mainly of the product gas carbon dioxide as well as fatty acids and ammonium, are subjected to the phototrophic compartments, e.g. the anaerobic photoauto/heterotrophic compartment II and the photoautotrophic compartment IV. Ammonium produced during the biodegradation of the aqueous and solid wastes is fed to the nitrifying compartment III, where it is oxidized to yield nitrate which in turn can be utilized in the photoautotrophic compartment IV and the higher plant compartment. The higher plant compartment was introduced into the MELISSA cycle to account for the crew's demand for a balanced diet. Higher plants under consideration in this approach include lettuce, wheat, potato, tomato, soybean, rice, spinach, and onion, whose edible parts are consumed by the crew. The inedible fraction of these higher plants, including leaves, roots and stems has to be degraded together with hygienic wastes and fecal matter, by which the overall cycle is closed.

However, the overall performance of the MELISSA cycle is hampered by the liquefying compartment, the part addressed in this project. Due to the particulate structure of plant material and fecal matter, the bacterial strains employed in the liquefaction so far have not proven to be capable of converting the particulate matter at a sufficiently high conversion rate within an acceptable residence time. Indeed, the microorganisms used in the biodegradation are optimally equipped to handle soluble molecules which leads to critical limitations in case that water insoluble substances are involved. The effect of the solubilisation being the rate-controlling step is particularly severe when fibrous components, which make up the major part of the inedible plant material, are subjected to the biological degradation process. Currently, an overall degradation efficiency of 60-65% is accomplished, the overall fibre degradation being about 75% [2].

There are several possible approaches to enhance the conversion of fibrous materials. One thinkable method is the chemical treatment of the wastes by adding certain reagents like Fenton's reagent, Schweizer's reagent or by adjusting the pH such that the acid catalyzed hydrolysis of cellulosic compounds is promoted. Such methods suffer the major drawback that additional treatment steps, e.g. neutralization and precipitation, may become unavoidable in the further processing of the waste water.

The most promising method is the thermal treatment of fibrous materials at elevated temperatures and pressures using water as a solvent. Water near and above its critical point (T_c = 647 K; p_c = 22.1 MPa) serves as an excellent reaction medium due to the high temperature and the increase in the ionic product and a change in the dielectric constant. As a result, compounds which are hardly soluble under ambient conditions can be dissolved to a high degree in water near its critical state. Due to the increased ionic product, water itself acts as an acid leading to an increase in the rate of hydrolysis and consequently to a high degree of decomposition. Since the fluid properties of water near the critical point can be varied over a wide range of conditions the effluent product distribution can possibly be controlled by adjusting operating temperature and/or pressure. Furthermore, the high temperature treatment provides an additional hygienic barrier against hazardous contaminants like pathogens.

The hydrothermal treatment suggested above was initially considered to be embedded in a multi-step biological solubilisation as depicted Figure 1.2.

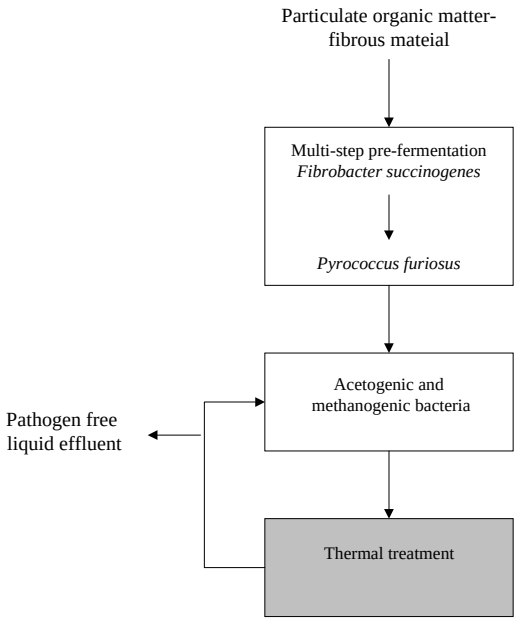

Figure 1.2: Initial scheme of the MAP project

According to the initially proposed scheme the particulate organic matter is subjected to a multi-step pre-fermentation involving Fibrobacter succinogenes, a strictly anaerobic bacterium, and Pyrococcus furiosus, an extremophilic organism growing at temperatures as high as 100°C. These processes can be applied in sequence and it is expected to thereby achieve a high rate of hydrolysis. Subsequently the soluble products are fed to a conventional anaerobic biogas digestion involving acetogenic and methanogenic bacteria. The gaseous products which are mainly composed of hydrogen and methane, can be separated from the liquid phase and can be supplied to the production of microbial protein, the so-called single cell protein or SCP. In the course of the project, the sequence of treatment steps was modified, meaning that the methanogenic reactor became the primary degradation step followed by the Fibrobacter and hydrothermal treatment.

The thermal treatment unit is considered to be implemented in succession to the anaerobic digestion compartment in the frame of the MAP project. By applying the high temperature and high pressure method as an after-treatment it is intended to not only remove any remaining insoluble matter within a short residence time in the order of minutes but also to guarantee an absolutely pathogen free effluent. Extra solubles obtained in the hydrothermal treatment are to be recycled to the anaerobic digestion compartment and subjected to biological degradation in the frame of this MAP-loop.

2 FUNDAMENTALS AND STATE OF KNOWLEDGE

2.1 Sub- and supercritical water

For a pure component, the supercritical state is defined as the state of a fluid above its critical temperature T_c and critical pressure p_c. [3]. The critical point marks the end point of the vapor pressure curve, such that there is no two-phase region but a one-phase supercritical region at conditions above the respective critical values. The supercritical region is denoted as the hatched area in Figure 2.1, which depicts a schematic PT-diagram of a pure component.

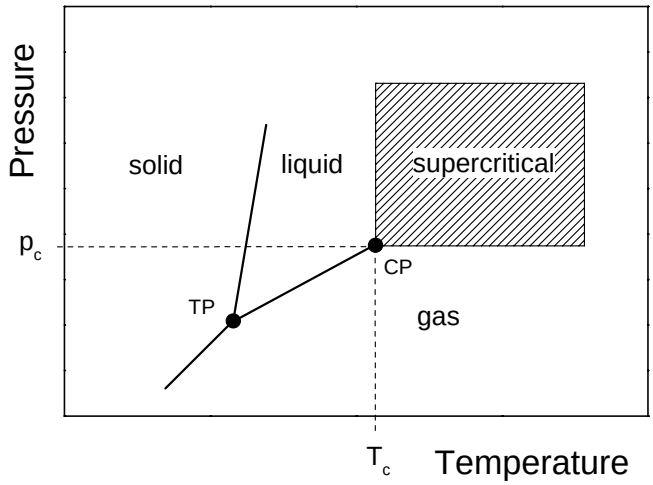

Figure 2.1: PT-diagram of a pure component [3], CP critical point, TP triple point

In many respects, the properties of a supercritical fluid lie in between those of a liquid and a gas. On the one hand the density of a supercritical fluid resembles that of a liquid, on the other hand supercritical fluids exhibit viscosities similar to those of gases. A compilation of important properties in the different states is depicted in Table 2.1.

Table 2.1: Properties of gases, liquids, and supercritical fluids [4]

	Gases	SCF (T_C, P_C)	SCF (T_C, $4P_C$)	Liquids
Density [kg/m^3]	0.6 - 2	200 - 500	400 -900	600 1600
Dynamic viscosity [Pa s]	$(1 – 3)\cdot10^{-5}$	$(1 – 3)\cdot10^{-5}$	$(3 – 9)\cdot10^{-5}$	$(0.2 – 3)\cdot10^{-3}$
Diffusion coefficient [m^2/s]	$(1 – 4)\cdot10^{-5}$	$7\cdot10^{-8}$	$2\cdot10^{-8}$	$(0.2 – 2)\cdot10^{-9}$

Due to the high densities, low viscosities, and the comparatively high diffusion coefficients, supercritical fluids exhibit excellent solvent and transport properties. Furthermore, the fluid properties can be continuously adjusted over a wide range by varying the conditions in terms of temperature and pressure. In the vicinity of the critical point, where the gradients in

physico-chemical properties are the largest, only small changes in temperature and pressure are required to significantly change properties. Supercritical fluids can thus be tuned over a broad range to optimise the properties with respect to the actual process.

Supercritical fluids have therefore been utilised in many applications. While in the past the focus was on extraction and fractionation processes, the use of supercritical fluids as reaction media has been gaining increasing attention during the last two decades. Both decomposition and synthesis reactions in supercritical fluids have been being studied [5, 6] with the objectives to optimise reaction conditions, replace conventional solvents, and allow for reaction pathways which are not feasible with alternative approaches.

Especially water at elevated temperatures and pressures offers many beneficial properties which make it an excellent solvent and reaction medium for a broad variety of applications [7, 8, 9, 10, 11]. Figure 2.2 shows a PT-diagram of water at elevated temperatures and pressures.

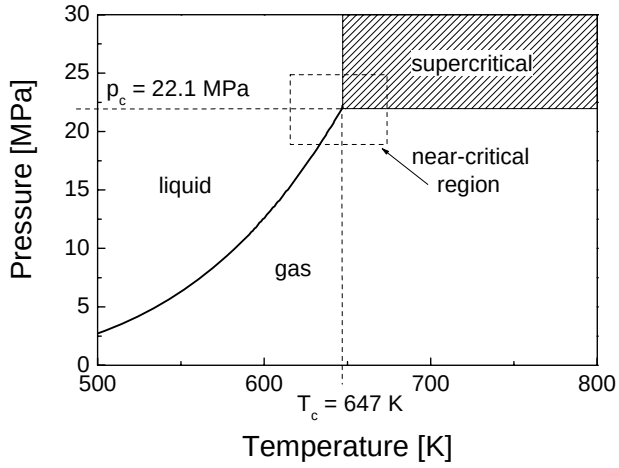

Figure 2.2: PT-diagram of water at elevated temperatures and pressures

Water has characteristically high critical values, which are T_c = 647 K and p_c = 22.1 MPa, respectively. With regard to nomenclature, one refers to “near-critical water” in the region which extends around the critical point, whereas the expression “subcritical water” denotes the non-supercritical, usually liquid state ($T<T_c$). There is, however, no precise definition as where the near-critical region is located. In general, the near-critical condition is referred to as the region in which high gradients in the physico-chemical properties of the substances are observed.

Sub- and supercritical water provides a thermally activated regime for fast kinetics. Besides, it shows a distinctly different behavior compared to water under ambient conditions, which is due to the dramatic changes in thermodynamic properties. One important property with respect

to the polarity of water is its dielectric constant [12, 13]. The dielectric constant ε as a function of temperature and density is depicted in Figure 2.3.

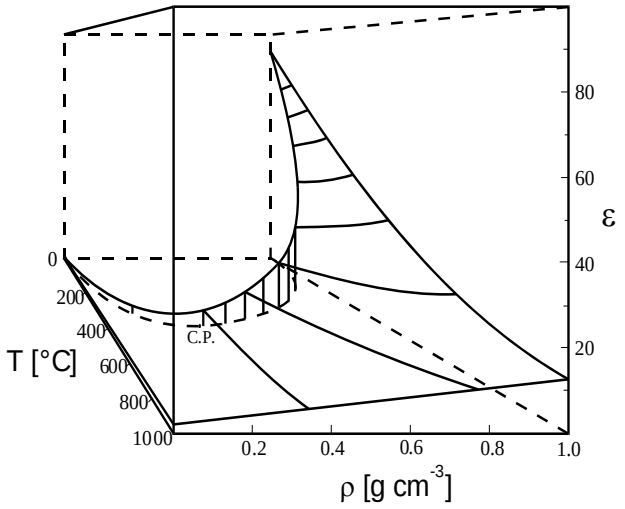

Figure 2.3: Dielectric constant of water [13]

As can be seen, the dielectric constant drops by an order of magnitude from a value of about 80 at ambient conditions, but water still remains a polar fluid. The significant drop in the dielectric strength leads to a much increased solvent power for most organic compounds, thus providing a homogeneous reaction atmosphere. In such cases no phase boundaries impose any mass transfer limitations on the reactions and more chemical bonds are accessible to reaction steps. Many works were therefore focused on the removal and destruction of organic pollutants with supercritical water [14, 15, 16, 17].
Dissociation of water leads to the formation of hydronium and hydroxyl ions and determines the pH of pure water. The ion product changes drastically from ambient to subcritical and supercritical conditions [18, 19] as illustrated in Figure 2.4.

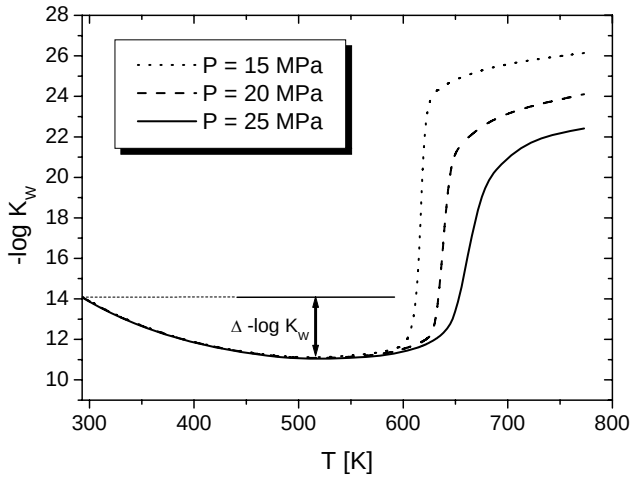

Figure 2.4: Ion product of water at elevated temperatures and pressures [18]

The ion product of water is represented by an empirical equation based on density and two quadratic functions of temperature.

$$\log K_W = A + B/T + C/T^2 + D/T^3 + (E + F/T + G/T^2)\log \rho_W \qquad (2.1)$$

where ρ_W denotes the density of pure water at given temperature and pressure. This equation serves as the background for the international formulation for the ion product of water. It was obtained by fitting several sets of experimental data and it is believed to represent the ion product of water for a temperature range from 0 to 1000°C and pressures ranging from 0.1 to 1,000 MPa.
Figure 2.4 shows that the ion product rises from a value of 10^{-14} at ambient conditions to values up to 10^{-11} in the subcritical region, corresponding to an increase by three orders of magnitude. Due to the associated increase in activity of hydronium- and hydroxyl ions, subcritical water itself promotes acid and base catalysed reactions without any additional catalysts like mineral acids. Accordingly, many ionic reactions, e.g. the hydrolysis of biopolymers, proceed at a maximum rate under subcritical conditions.
In this context, hydrolysis refers to the cleavage of bonds under the influence of water [20] according to the scheme illustrated in Figure 2.5.

$$A - B + H - OH \rightarrow A - H + B - OH$$

Figure 2.5: Formal scheme of the hydrolytic cleavage of bond A-B

Important hydrolysis reactions are the cleavage of glycosidic bonds of polysaccharides, e.g. starch and cellulose [21, 22], of polypeptides to yield protein hydrolyzates and free amino acids [23, 24, 25], as well as the hydrolysis of esters [26].
In contrast, the ion product drastically drops at near- and supercritical conditions as a result of the strong decrease in water density. In general, ionic reaction pathways are favoured at higher water densities, whereas the lower densities at supercritical conditions lead to free radical reaction mechanisms being the preferred reaction pathways [27, 28].
It can also be inferred that pressure does not have a noticeable influence on the ion product at temperatures below 300°C. This observation can be explained by the fact that water still has the character of an incompressible fluid at these conditions, meaning that pressure does not markedly affect density and hence the ion product.

Due to these unique features, near-critical water serves as an excellent reaction medium and is a highly attractive supplement or alternative to biological treatment methods, especially when hardly biodegradable substances like cellulose or related compounds are involved. Near-critical water offers the possibility of controlling and influencing the degradation product distribution by slightly adjusting the operating parameters in terms of pressure and temperature. The treatment in high-temperature water does not only offer the potential of complete conversion at high space-time yields, but it also serves a hygienic barrier, by which the sterility of effluents could be accomplished.
In contrast, the usage of sub- and supercritical water is only associated with limited problems. Salt deposition and corrosion of reactor material are counted among the general drawbacks of supercritical water processes. The precipitation and subsequent deposition of salts is due to the decreased solvent power for ionic species at supercritical conditions.

The degradation of biopolymers and destruction of pollutants can further be enhanced by supplementary means. The acidification by carbon dioxide leads to a decrease in pH, which favours acid catalysed steps like the hydrolysis of ester and ether bonds in biomolecules. The addition of an oxidant to high-temperature water is a very efficient technique to mineralise hydrocarbons by conversion to carbon dioxide, thus achieving a complete destruction of any organic material.

2.2 The system water/carbon dioxide

The pH of the aqueous phase in the system water-CO_2 decreases due to the increased solubility of carbon dioxide in water and the dissociation of carbonic acid according to the following scheme:

$$CO_2 + H_2O \leftrightarrow H_2CO_3 \leftrightarrow H^+ + HCO_3^-$$

Figure 2.6: Reaction scheme of carbonic acid dissociation in water

The acidification by carbon dioxide is assumed to result in a rate enhancement of acid-catalysed reaction steps without the need to add any mineral acids like hydrochloric acid. This approach offers the potential to easily recover carbon dioxide by expansion after treatment and to reuse it by recirculation as opposed to excessive neutralisation and precipitation steps, which become necessary when applying mineral acids.

Investigations on the use of carbon dioxide as a catalyst in water at elevated temperatures and pressures are scarce. Only a limited number of works have been published, e.g. the hydrolysis of starch [29], [30], and the dehydration of cyclohexanol and the alkylation of p-cresol [31]. Besides, water/carbon dioxide-mixtures were successfully employed in the remediation of soils contaminated with heavy metals [32], [33]. As a result of the drop in pH, the mobility of metal ions could be enhanced as compared to the treatment with pure water. The hydrolysis of lignocellulosic materials in water/carbon dioxide-mixtures has not been reported before.

A graphical representation of the pH of aqueous solutions saturated with carbon dioxide is given in [34]. Figure 2.7 shows the pH as a function of temperature for different pressures.

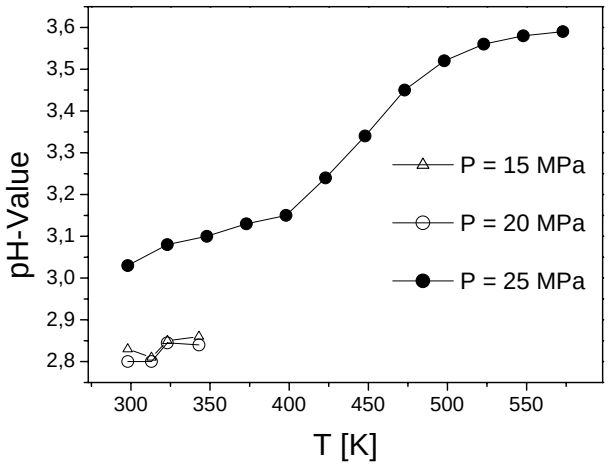

Figure 2.7: pH-value of high-temperature water saturated with carbon dioxide [34]

The values for a pressure of 25 MPa were calculated [32] on the basis of equilibrium data for the system water-CO_2 [35] and the first dissociation constant of carbonic acid [36]. The data depicted for pressures of 15 and 20 MPa were determined experimentally through direct measurement of the pH in a view cell by spectrophotometric methods [37]. The pH-value shows a decrease with increasing pressure and temperature. For the conditions applied in this work, the pH of water saturated with carbon dioxide is in the range of 3.6-3.7.

The pH as a function of the carbon dioxide concentration in the aqueous phase can be determined by solving the respective charge balance:

$$[H^+] = [OH^-] + [HCO_3^-] + 2[CO_3^{2-}] \qquad (2.2)$$

where the values stated in brackets denote the molal concentration of species. The last term on the right hand side, the concentration of bicarbonate, can be neglected because of the low value of the second dissociation constant of carbonic acid.

Both the dissociation of water and the dissociation of carbonic acid contribute to the concentration of hydronium ions according to the following equations:

$$K_W = [H^+][OH^-] \qquad (2.3)$$

$$K_1 = [H^+][HCO_3^-]/[CO_{2,aq}] \qquad (2.4)$$

Isolation for the concentration of hydroxyl ions and carbonate ions, respectively, and substitution into equation 2.2 yields

$$[H^+] = K_W/[H^+] + K_1[CO_{2,aq}]/[H^+] \qquad (2.5)$$

from which the concentration of hydronium ions and the associated pH of the system can be calculated.

Figure 2.8 shows the pH of water/carbon dioxide-mixtures as a function of carbon dioxide concentration.

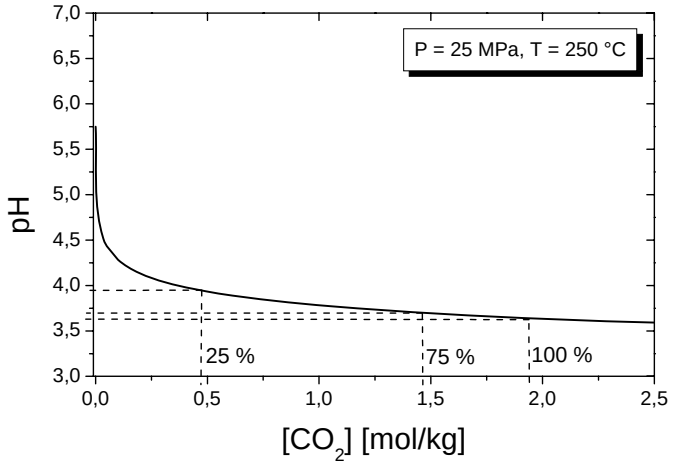

Figure 2.8: pH of water as a function of CO_2-concentration, the percent values are stated with respect to the saturation concentration

The pH decreases by two orders of magnitude up to the saturation level as compared to pure water at the same conditions. Due to the logarithmic character of the underlying equation, the pH initially drops sharply and lowers progressively slower with increasing carbon dioxide addition. Accordingly, addition of carbon dioxide beyond a degree of saturation of 75 % does not significantly contribute to a further decrease in pH and associated rate enhancement of acid catalysed reaction steps.

3 EXPERIMENTAL METHODS

In this work, model compounds, e.g. pure cellulose and lignin, as well as real lignocellulosic wastes were treated in sub- and supercritical water. The experiments were conducted in fully-continuous mode in a tubular reactor at both hydrolytic and oxidative conditions, covering a wide temperature range from 200 to 500°C, residence times in the order of a few seconds up to three minutes, and pressures up to 30 MPa. Because of the continuous processing of particulate matter at flow rates lower than 5 kg/h, the initial biomass concentrations were limited to a maximum of two percent by weight. At higher initial solid concentrations, the narrow architecture of the pump head and the fibrous structure of the solids led to problems due to clogging. The acidification by carbon dioxide as an alternative means to enhance the rate of hydrolysis was also studied. In addition to the fully continuous mode of operation, semi-continuous experiments were performed. In order to increase the residence time of biomass in the reactor, the solid material was retained in a fixed bed set-up and treated by a continuous flow of sub- and supercritical water.

The materials and the experimental set-up used in this work are presented in the following. The analytical methods for the characterization of the input material and the effluents are also discussed.

3.1 Materials

For the experiments on model compound studies, pure cellulose and lignin were employed. Micro-crystalline cellulose (Avicel) with a purity of 99 % was purchased from Merck. Water-insoluble organosolv lignin from the treatment of hardwoods (M_W = 3500 g/mol) and alkali lignin (M_W = 28000 g/mol) were purchased from Sigma-Aldrich. These materials were obtained as a fine powder and could be used as received without additional pre-treatment at initial solid concentrations of up to one wt-%. The suspensions were prepared by weighing the amount of material with a laboratory scale and adding the respective amount of demineralized water. For the experimental studies on the biosafety of effluents, bovine serum albumin and naphthalene were purchased from Merck and were used as received.

Wheat straw was provided by a local farmer. It was first ground in a cutting mill (IKA, MF10 Basic) to particle sizes of less than 250 µm. The obtained powder was subsequently treated in a coffee mill for further size reduction. Particles passing a sieve with a mesh size of 112 µm were used for preparing the suspension.

The composition of the model waste specified by ESA is stated in Table 3.1.

Table 3.1: Composition of model waste and respective suppliers

Component	Portion [wt-%]	Source	DM content [wt-%]
Wheat straw	23.3	Local farmer	94.5
Cabbage	23.3	Market	9.7
Soya	23.3	Oil-mill	91.1
Algae	10	BlueBioTechGmbH	95.5
Faecal material	20	-	27.4

The dry matter content of faecal material was not determined experimentally but calculated from literature data [38]. The composition depicted in the table was based on the original idea of ESA to treat a waste which was as close to reality as possible. Due to hygienic concerns, the faecal material was omitted and the other substrate ingredients were adjusted according to their ratios as specified by ESA.

The preparation of the model waste specified by ESA consisted of a multi-step size reduction procedure in order to obtain sufficiently fine particles that could be handled continuously in the flow reactor. Wheat straw and soya were prepared by dry size reduction methods with a rotary cutter and a conventional coffee mill. This approach was not feasible for the cabbage because of the high water content. The cabbage was first treated with a knife and a grater. The resulting pulp was subsequently subjected to a kitchen mixer with the addition of extra water. The cabbage was finally homogenized by an Ultra-TORAX (Heidolph DIAX 900) together with the algae, which did not require any additional treatment prior to homogenisation.

Digester residues from Partner 1 were received in the form of dry agglomerates or sludge. In the case of agglomerates, the residues were directly treated by dry size reduction, while the sludge was first dewatered by vacuum filtration and subsequent overnight storage in a vacuum dryer.

Hydrogen peroxide was purchased from Merck as an aqueous solution with a concentration of 30 wt-%. It was stored in a cabinet and it was not introduced into the feed vessel until immediately before the start of experiment to avoid decomposition reactions. Carbon dioxide with a purity of 99.95 % (KWD) was taken from the gas phase of the central storage tank of the Institute at a pressure of 6 MPa.

3.2 Experimental set-up

3.2.1 SET-UP OF THE CONTINUOUS REACTION UNIT

A schematic sketch of the tubular reactor for the continuous treatment of lignocellulosic biomass is shown in Figure 3.1.

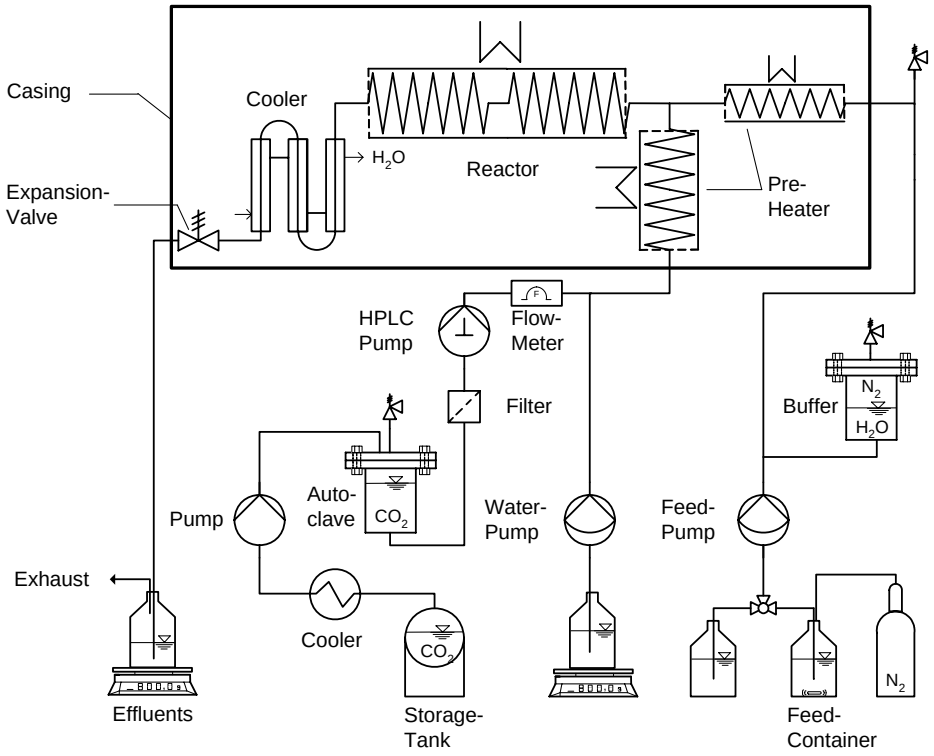

Figure 3.1:Schematic sketch of the experimental apparatus for the continuous treatment of biomass

The main building blocks of the apparatus were the supply lines for the biomass suspension, hot water, and carbon dioxide, the pre-heaters, the tubular reactor, and the downstream processing units, which consisted of the cooler, expansion valve, and the effluent collection system, respectively. The high pressure reaction unit was designed as a tubular reactor made of high temperature/pressure resistant steel (1.4404, OD = 6.35 mm, ID = 3.05 mm). The volume of the tubular reactor could be adjusted by installing coiled high pressure piping of different length. With the coils used in the experiments, which had internal volumes of 8 ml, 50 ml, and 100 ml, residence times in the order of a few seconds up to three minutes could be covered, depending on fluid density and mass flow rates. The flow reactor was capable of withstanding operating pressures up to 30 MPa and temperatures up to 400-450°C.

The feed suspension was fed from a 2 l closed glass flask covered with a plastic layer. The feed was agitated through a magnetic stirrer to prevent the particulate matter from settling and to ensure a homogeneous feed suspension throughout the vessel. In order to secure that no oxygen dissolved in the water and to study the hydrolytic and oxidative treatment separately, the feed suspension was put under a nitrogen atmosphere. This was accomplished by slightly pressurizing the flask with nitrogen gas, which was delivered from a compressed gas cylinder. The water storage tank contained pure demineralized water and served as the water supply until the desired operating conditions were reached and the system worked at steady state conditions in terms of temperature, pressure, and flow rate. The feed suspension was then pumped into the reactor by adjusting the position of a three-way valve in the suction line.

The feed suspension containing the particulate matter was introduced into the system by means of a high pressure membrane pump equipped with double ball valves at the suction and the discharge side (LEWA EK1/V metering pump). This redundant double ball configuration served the purpose of ensuring a reliable operation of the pump even if particles got trapped between one of the balls and its respective seat. In such a case, the second ball-seat pair was intended to secure the closure of the valve. Despite this configuration, it was not possible to reliably process particles larger than 200 µm at flow rates in the order of a few liters per hour. Especially the continuous delivery of real biomass, e.g. wheat straw and complex wastes, led to problems due to the fibrous structure of the material. In general, particles sizes of less than 112 to 180 µm and initial solid concentrations of 0.5 to maximal 2 wt-% were applied and could be satisfactorily processed by the feed pump. Although according to the manufacturer the membrane pump was supposed to exhibit a pressure firm characteristic, the system pressure revealed a noticeable influence on the metered flow rate. At an operating pressure of 25 MPa the maximum flow rate was in the range of 4 l/h.

Before entering the reaction unit the feed suspension was moderately pre-heated in an upstream coil, which had an inner volume of 38 ml and was made of the same piping material as the reactor. The power supply was accomplished by a 0.8 kW electric heating jacket. Typically, the feed suspension was heated up to a maximum temperature of 180-200°C in order to avoid the onset of decomposition reactions in the pre-heater.

In order to obtain meaningful results with respect to the residence time in the reactor at constant temperature conditions, the feed suspension had to be rapidly heated up to operating temperature. For this purpose, pure water was delivered to the apparatus with an additional high pressure metering pump (LEWA EL1) and heated up in two heating coils (45 ml, 2 kW each) to temperatures higher than the desired reaction temperature. Subsequently, this high water stream was mixed with the feed suspension through a mixing-tee at the inlet of the reactor. By this means, the temperature of the influent suspension could be instantaneously raised to the desired level and the temperature gradients along the reactor could be minimized, yielding close to isothermal conditions in the plug flow reactor.

For the experiments on the catalytic influence of carbon dioxide, CO_2 was added to the pure water flow prior to the pre-heater. Gaseous carbon dioxide was taken from the central storage

tank of the Institute and passed to an integrated pump and cooling module, where it was first liquefied and then delivered to a 1 l autoclave at a pressure of 10 to 15 MPa by an air-driven pump. Liquid CO_2 was withdrawn from the autoclave and processed to the reactor by a HPLC pump (Milton Roy miniMetric 1711) at a flow rate of up to 10 ml/min. The actual flow rate was measured by a mass flow meter (Rheonik RHM 015). In order to exclude any disturbances of the metering pumps on the CO_2 flow, a check valve was installed upstream of the mixing point.

The reactor was equipped with two additional heating jackets (2 kW each) in order to compensate for heat losses or to further increase the maximum outlet temperature. Afterwards the reactor effluent was immediately cooled down by passing a double pipe heat exchanger operated with tap water as the cooling medium, thus rapidly terminating the reaction. The effluent subsequently passed a spring-loaded backpressure regulator (IMF-Vatec DV 943/INOX) where it was expanded to ambient pressure. The system pressure could be set by adjusting the load of the spring in the regulator valve. The liquid as well as the gaseous effluents were processed to the effluent collection and measurement system afterwards.

Liquid samples were not taken before a time corresponding to five to ten residence times had passed at steady-state conditions. The effluents were collected in glass flasks and subjected to the respective analytical methods. In order to measure the volumetric gas production as well as the product gas composition, a burette system combined with a sampling vessel was installed. At the beginning of the gas measurement the effluents were passed in an upward direction through the glass vessel (V = 25 ml). This procedure led to the displacement of any air initially present. Afterwards the cylinder was rotated into a horizontal position and gas produced in the course of the reaction was trapped in the upper part of the shell. Gas samples could be taken through a septum with a gas tight syringe (Hamilton gas tight, V = 1000 µl) and were immediately injected into a gas chromatograph for composition analyses. The total volume of the effluents entering the system within a certain time could be determined by reading the difference in the liquid level in the burette. The burette system was connected to a compensator reservoir with adjustable vertical position in order to equalize the pressure within the system to ambient pressure.

In order to minimize pressure fluctuations, which were due to the operation of the pumps and the pressure regulator, the system was connected to a buffer vessel, which had an internal volume of 3.5 l and was filled with a compressible nitrogen headspace.

The pre-heaters and the reaction pipes were electrically heated by means of 5 heating jackets, which could be adjusted separately by a temperature control system (Horst HT-60 controller). In order to decrease the heat losses to the surroundings, the complete high temperature section of the apparatus was thermally insulated.

The system pressure was measured by a pressure transducer. Temperatures at the outlet of the pre-heaters as well as at the inlet and the outlet of the reactor were measured with high temperature resistant NiCrNi-thermocouples, which were inserted into the reaction pipes by

means of tee-connectors. Both pressure and temperatures were constantly measured and recorded by a data acquisition system. The aqueous flow through the reactor was measured gravimetrically by weighing the feed and the sample vessels with laboratory scales, since mass flow meters, which are based on the Coriolis-principle, bear the risk of clogging when suspensions containing larger particles are discharged through their internal tubes.

3.2.2 MODIFICATIONS TO SET-UP FOR CONTINUOUS WATER OXIDATION

For the continuous water oxidation of lignocellulosic biomass, the set-up described above was partially modified. Due to the corrosive atmosphere of high-temperature water in the presence of an oxidant, a new reaction coil made of corrosion-resistant nickel alloy (Inconel, Alloy 600, OD 6.35 mm, ID 2.13 mm) with an internal volume of 20 ml was installed downstream of the mixing point. This reactor could either be connected to the existing reaction coils, in order to extend the residence time and increase the outlet temperature under hydrolytic conditions, or it could be used as a replacement for the existing coils in continuous water oxidation. In the latter case, the reaction coil was directly connected to the mixing point by Inconel pipes and fittings. The reactor was placed in a 4 kW oven (Heraeus RO 7/75), which in principle allows for temperatures up to 1000°C. Under operating conditions, reactor outlet temperatures up to 500°C could be accomplished.
Hydrogen peroxide was used as the oxidant. It was directly introduced into the feed vessel and delivered to the reactor along with the biomass in order to facilitate the experimental procedure.

3.2.3 FIXED BED ASSEMBLY FOR SEMI-CONTINUOUS OPERATION

In some experiments, the reaction coils were replaced by a fixed bed assembly as an alternative means to extend the residence time of solid particulates within the reaction zone. The principle of this set-up is illustrated in Figure 3.2.

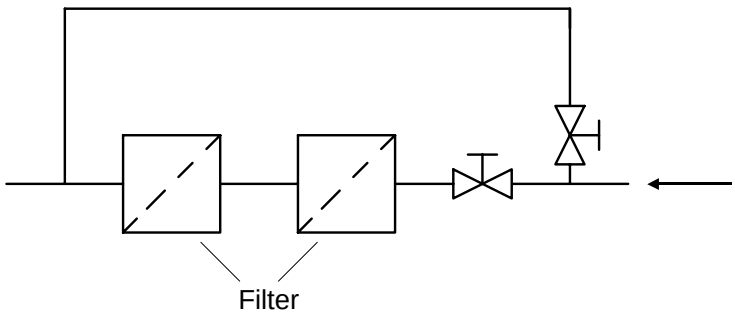

Figure 3.2: Fixed bed assembly for the semi-continuous treatment of biopolymers

The fixed bed was made of two T-filter (Swagelok, model SS-4TF-05) units which were coupled by a piece of high pressure piping. The solid material, e.g. wheat straw and organosolv lignin, was filled in the sinter metal inlet of the upstream unit and was contained between the filters during the experiment. About 0.5 g of solid material could be retained between the filter units. In order to minimize the time required for heating up the assembly to operating temperatures, a bypass was added to the system. During the heating up period pure water was processed through the bypass to avoid the onset of any reactions within the fixed bed. Once the desired temperature was reached, the high temperature valves (Sitec, model 710.5315) were switched and the water stream was allowed to flow through the fixed bed containing the biomass for a preset time period. At the end of this holding time, the second metering pump was turned on to introduce cold water and to rapidly decrease the temperature in the fixed bed. Due to the significant heat capacity of the body of the valve and the filter units, a marked temperature fall could be observed during the first minutes, followed by a temperature increase to the desired level.

3.3 Analytical methods

Different analytical methods were used to characterize the effluents of the hydrothermal treatment. The dissolved organic carbon (DOC), total organic carbon (TOC), total nitrogen (TN) as well as the chemical oxygen demand (COD), ammonia nitrogen (NH_4-N) and nitrate (NO_3-N) were measured to calculate the respective carbon and nitrogen balances. Beside the determination of these lumped parameters, several GC and HPLC methods were employed in order to provide a more detailed insight into the product formation and to identify and quantify main degradation products. The analytical approaches for the different classes of compounds are described in the following.

3.3.1 DETERMINATION OF SUM PARAMETERS

The input materials were characterized with respect to their dry matter content and their elementary composition in terms of carbon, nitrogen, and sulphur. The dry matter content was measured by filling samples in evaporation bowls and subsequent drying in a desiccator cabinet at 105°C. The water content of the material was determined by measuring the weight loss of the samples after a drying period of 48 h. The elementary composition of solid matter was determined in the Central Analytical Laboratory of Technische Universität Hamburg-Harburg by burning samples in a CNS-analyser (Leco-2000-CNS-Analyser) at temperatures from 1000 to 1450°C. The amounts of carbon and sulphur were measured by analysing the concentration of the respective oxidised compounds (CO_2, SO_2) with infrared detectors in the off-gas. The concentration of nitrogen was measured by means of a heat conductivity detector.

Effluents of the hydrothermal degradation of biomass were analysed for their carbon and nitrogen content with fully automated analysers in the Central Analytical Laboratory (Elementar HighTOC + TNb) and at the Institute of Bioprocess and Biochemical Engineering (Multi N/C 3000). For the determination of the dissolved organic carbon (DOC), effluent samples were passed through a 0.45 µm filter prior to injection, in order to retain suspended particles. The samples were first acidified by phosphoric acid to remove any inorganic carbon and afterwards subjected to catalytic incineration. With the instrument available at the Central Laboratory, finely suspended particles could also be injected. Provided that the effluent suspensions had a low concentration of insoluble matter, the total organic carbon (TOC), being the sum of dissolved carbon and insoluble carbon, could thus be determined.

The quantification of chemical oxygen demand (COD), ammonia nitrogen (NH_4-N), and nitrogen in form of nitrate (NO_3-N) was accomplished by using standardized photometric test kits (Dr. Lange).

3.3.2 SACCHARIDE ANALYSIS

Sugar analyses were conducted by means of HPLC with a ligand exchange chromatography (LEC) column in the Central Analytical Laboratory of Technische Universität Hamburg-Harburg. The technical specifications and the operating conditions of this system are stated in Table 3.2.

Table 3.2: Specifications of the HPLC system for the analysis of saccharides

Technical Specifications	HPLC	Macherey Nagel, Nucleogel®Sugar
	Column Type	Packed Column; L = 300 mm, ID = 7.8 mm Packing material: Cation exchange polymer
	Guard Column Type	Packed Column; L = 21 mm, ID = 4 mm
	Detector Type	Refractive Index
Operating Conditions	Eluent	Distilled Water
	Eluent Flow	0.5 ml/min
	Oven Temperature	72°C, isothermal

Pure demineralized and degasified water served as the eluent and was delivered with a piston pump (Merck-Hitachi-L7100) at a flow rate of 0.5 ml/min into a 6 way injection valve (Rheodyne 7725i). Product samples were first centrifuged at 13000 rpm to remove solid impurities. Subsequently the supernatant was passed through a filter unit (0.2 µm) prior to injection. A guard column was installed upstream of the separation column to remove further impurities, e.g. salts and peptides. Small amounts of the liquid samples were injected (injection

volume 20 µl) into the eluent flow and separated with a Nucleogel®Sugar column packed with a cation exchange polymer. This packing material is especially designed to separate mono- and disaccharides and the degradation products thereof. The components were identified with a refractive index detector (RI-IV LCD Analytical). Peak identification and quantification of the components detected with this system were accomplished by injecting standard solutions with known composition at different concentrations, in this way allowing to convert peak areas to concentration values. All samples were analysed in triplicate for reasons of reproducibility.

3.3.3 ANALYSIS OF CARBOXYLIC ACIDS

Carboxylic acids, especially acetic acid, are known to be refractory compounds [39] which are formed in larger quantities during hydrothermal treatment and have a major contribution to the residual DOC after oxidation [40]. Reaction effluents were therefore analysed for carboxylic acids with the system specified in Table 3.3.

Table 3.3: Specifications of the GC system for the analysis of carboxylic acids

Technical Specifications	Gas Chromatograph	Varian 3900
	Column Type	WCOT FUSED SILICA (25 m, ID = 0.32 mm, Coating: FFAP-CD, DF = 0.3 µm)
	Detector Type	Flame Ionisation Detector FID
Operating Conditions	Carrier Gas	Nitrogen
	Carrier Flow	1 ml/min
	Split Ratio	0 – 1 min splitless, 1 – 2 min: 1/100, after 2 min: 1/20
	Injector Temperature	220 °C
	Oven Temperature	60 °C (1 min) – 10 °C/min until 200 °C 200 °C (2 min)
	Detector Temperature	230 °C
	Injection Volume	0.5 µl

The system consisted of a gas chromatograph (Varian 3900) equipped with a capillary column (WCOT fused silica) and a flame ionisation detector operated at 220°C. The samples were acidified by 2 % phosphoric acid prior to injection. For each run a sample volume of 0.5 µl was injected using nitrogen as carrier gas. The temperature program was as follows: After an initial holding time of 1 min at 60°C the oven temperature was increased by a rate of 10°C/min to the final temperature of 200°C. By this method carboxylic acids higher than formic acid can be detected and quantified. Formic acid cannot be detected by FID but would require alternative methods like HPLC for detection.

3.3.4 GC-MS ANALYSIS OF DEGRADATION PRODUCTS

GC-MS analyses were run on selected effluents of the hydrothermal treatment of lignin, wheat straw, and naphthalene to identify and quantify main degradation products. The analyses were conducted at the Central Analytical Laboratory of Technische Universität Hamburg-Harburg according to the method described in Table 3.4.

Table 3.4: Specifications of the GC-MS system for the identification and quantification of products

Technical Specifications	Gas Chromatograph	Hewlett-Packard 5890 II
	Column Type	DB-5ms (30 m, ID = 0.25 mm, DF = 0.25 µm)
	Detector Type	MSD 5971A
Operating Conditions	Carrier Gas	Helium 5.5
	Column Pressure	65 kPa
	Split Ratio	Splitless
	Solvent	Dichloromethane
	Injector Temperature	300 °C
	Oven Temperature	70 °C (2min) – 5 °C/min (170°C) – 10 °C/min (290 °C) – 290 °C (10 – 15 min)
	Interface Temperature	280 °C
	Ionisation	EI (70 eV)
	Detector Temperature	182 °C
	Injection Volume	2 – 4 µl

The system used for the analyses was a HP5890 gas chromatograph with a HP5971A MS engine. The ionisation was accomplished by EI (70eV). A two-step temperature program was applied for separating the reaction products on a capillary column (DB-5ms): Starting temperature: 70°C (2 min) with a subsequent heating rate of 5°C/min to 170°C and a following heating rate of 10°C/min to 290°C and a final holding time of 10-15 min at 290°C. An aqueous sample of 4 ml was extracted with an equivalent volume of dichloromethane.

3.3.5 NAPHTHALENE ANALYSIS

The residual amount of naphthalene in the reaction effluents was determined quantitatively at the Institute for Thermal and Separation processes. After a single-stage extraction of 2 ml of effluent with an equivalent volume of toluene, the samples were subjected to the GC method described in Table 3.5.

Table 3.5: Specifications of the GC system for the quantification of naphthalene

Technical Specifications	Gas Chromatograph	Hewlett-Packard 5890
	Column Type	J & W DB5 (30 m, ID = 0.25 mm , DF = 0.1 µm
	Detector Type	Flame Ionisation Detector FID
Operating Conditions	Carrier Gas	Nitrogen
	Column Pressure	75 kPa
	Split Ratio	1/50
	Solvent	Toluene
	Injector Temperature	300 °C
	Oven Temperature	100 °C (2 min) – 10 °C/min until 320 °C 320 °C (7min)
	Detector Temperature	350 °C
	Injection Volume	1 µl

Pure naphthalene was extracted with toluene and injected into the chromatograph for the determination of the retention time. The quantification was accomplished by means of a calibration curve applying different naphthalene concentrations and evaluating the respective peak areas.

3.3.6 AMINO ACID ANALYSIS

The separation and detection of amino acids was accomplished by a RP-HPLC-system with derivatization of the amino acids prior to separation and fluorescence detection of the derivatives. The main specifications for this system are summarized in Table 3.6.

Table 3.6: Specifications of the HPLC system for the analysis of amino acids

Technical Specifications	HPLC	Merck, Superspher 4 RP18
	Column Type	Packed Column; L = 250 mm, ID = 4 mm
	Detector	Fluorescence, 340/420nm
Operating Conditions	Eluent	A: Sodium acetate; B: Methanol
	Eluent Flow	0.7 ml/min
	Eluent Mode	Isocratic, Gradient
	Oven Temperature	40°C, Isothermal

The effluents were treated with borate buffer and protein precipitant and were centrifuged at 16.000g. Afterwards the derivatization was performed with ortho-Phtaldialdehyde (OPA) and 15µl of the resulting reaction mixture were injected into the column.

Peak identification and quantification of the amino acids were accomplished by injecting external standards with known concentration of the amino acids. By injecting β-Alanin, which does not belong to the group of proteinogenic amino acids, as an internal standard, the peak area ratio of sample and standard solution could be determined, thus allowing to determine the amino acids concentration very accurately. This method is capable of detecting and quantifying all proteinogenic amino acids.

3.3.7 GAS PHASE ANALYSIS

For selected experimental runs, the off-gas of the hydrothermal treatment was characterized in terms of composition and volumetric flow rate. The composition of the gas phase was analyzed with a gas chromatograph (model Perkin Elmer 8500) equipped with a heat conductivity detector (HCD). Gas samples were taken from a gas mouse with a gas tight syringe and were immediately injected in the GC operated in off-line mode. The technical details of the gas chromatograph are depicted in Table 3.7.

Table 3.7: Technical specifications and mode of operation of GC analysis for gas phase measurements

Technical Specifications	Gas Chromatograph	Perkin Elmer 8500
	Column Type	Packed Column; L = 2m, ID = 2mm Packing: Propak Q 100-120 mesh
	Detector Type	Heat Conductivity Detector
Operating Conditions	Carrier Gas	Helium 4.6
	Carrier Flow	15 ml/min
	Oven Temperature	120°C, isothermal
	Injector Temperature	120°C
	Detector Temperature	120°C
	Injection Volume	400 µl

Helium (purchased from Westfalen AG) was chosen as the carrier gas since its thermal conductivity is distinctly different from those of most other gaseous components under the operating conditions stated above, thus allowing the identification of main constituents like carbon dioxide, nitrogen, and methane. Peak identification was accomplished by injecting

standard samples of the pure components and measuring their retention times. The quantitative analysis of the effluent gas composition was done according to the area percentage method, which leads to the determination of the quantitative ratio of the components instead of absolute concentration values.

4 EXPERIMENTS ON MODEL COMPOUNDS

Isolated cellulose and lignin were selected as model compounds for real lignocellulosic biomass, since they are the main constituents of plant biomass beside polyose (hemicellulose). Cellulose and lignin amount to approximately 50 % and 25 % of woody biomass, respectively. Polyose was not treated separately in this work, since it is known to be much more readily degradable due to its less crystalline structure than cellulose and its lower degree of cross-linking compared to lignin.

The main objective of the work with model compounds was to gain information about the achievable degree of liquefaction and about main degradation products. It was further intended to develop a suitable model for the description of the liquefaction kinetics and the kinetics of product formation. In case of cellulose, the acidification by adding carbon dioxide was studied as a supplementary technique to enhance the rate of hydrolysis. Lignin was treated at both hydrolytic and oxidative conditions by applying hydrogen peroxide. The oxidation of lignin was conducted to show the feasibility of a complete removal of any insoluble carbon of lignocellulosic biomass. In addition, the partial oxidation of lignin was studied with respect to the formation of valuable degradation products.

4.1 Liquefaction of cellulose

A systematic study of the liquefaction of pure cellulose in subcritical and near-critical water was conducted for two reasons. Firstly, cellulose is the most abundant biopolymer in the world and the most important constituent of plant derived biomass. Cellulose accounts for the main part of the fibre fraction of the waste specified by ESA, so that it can be considered as a proper model compound for the conversion of plant biomass. Secondly, cellulose was employed to elucidate the feasibility of enhancing the conversion to water-soluble products by adding carbon dioxide. By this means the pH can be lowered and acid-catalysed reactions will presumably proceed at faster reaction rates. The acid-catalysed pathway of cellulose hydrolysis is illustrated in Figure 4.1.

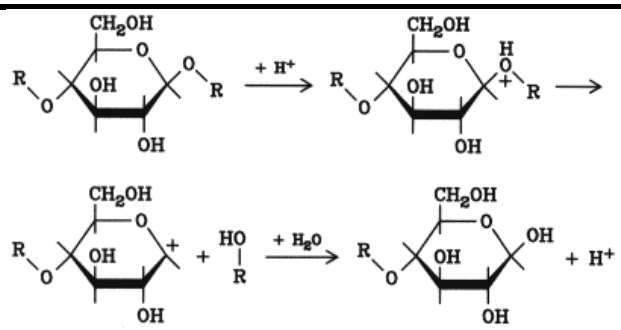

Figure 4.1: Reaction scheme of the acid-catalysed pathway of cellulose hydrolysis

The main objective was the conversion of cellulose to water-soluble degradation products. Therefore, a detailed parameter study on the continuous liquefaction of cellulose was conducted, covering temperatures from 240 to 374°C at residence times in the order of a few seconds to three minutes and initial cellulose concentrations of 0.5 to 1 wt-%. Carbon dioxide was added at different concentrations with respect to saturation in order to investigate the influence of acidification by carbonic acid on the degradation behaviour.

Based on the experimental studies, a kinetic description of the cellulose degradation and the formation of main degradation products was accomplished.

4.1.1 KINETICS OF CELLULOSE DEGRADATION

Discussion of results on cellulose liquefaction:

Continuous experiments on the liquefaction of pure cellulose were conducted with an initial cellulose concentration of 0.5-1 wt-% in the feed suspension, which yielded a cellulose concentration of 0.1-1 wt-% at the reactor inlet, depending on the mass flow ratios of feed and pure water flux. For this diluted system the reaction kinetics were assumed to be independent of the solid concentration and the evaluation in terms of residence time was performed using the properties of pure water [41].

The degree of liquefaction was calculated as the conversion of insoluble carbon to soluble carbon. Assuming that cellulose exhibits a negligible solubility in water, which was confirmed by own measurements, the degree of liquefaction on a carbon basis can be written as follows:

$$f = \frac{DOC_{out}}{TOC_{in}} \qquad (4.1)$$

with DOC_{out} denoting the soluble carbon at the outlet and TOC_{in} the insoluble carbon at the inlet of the flow reactor. The degree of liquefaction equals the degree of cellulose conversion **in case of negligible gas formation**.

The dissolved organic carbon content of the effluent was determined analytically by DOC measurement. The total organic carbon at the inlet of the reactor was calculated on the basis of the amount of cellulose and the cellulose composition. For this purpose, the theoretical portion of carbon in pure cellulose (44.4 wt-%) was corrected for a factor of 0.98 in order to account for impurities. In addition, the dry matter content of cellulose was measured as 95 %, such that the concentration of carbon in cellulose was taken as 41.4 wt-% for calculations.

The degree of liquefaction versus time at temperatures from 240 to 260°C is depicted in Figure 4.2.

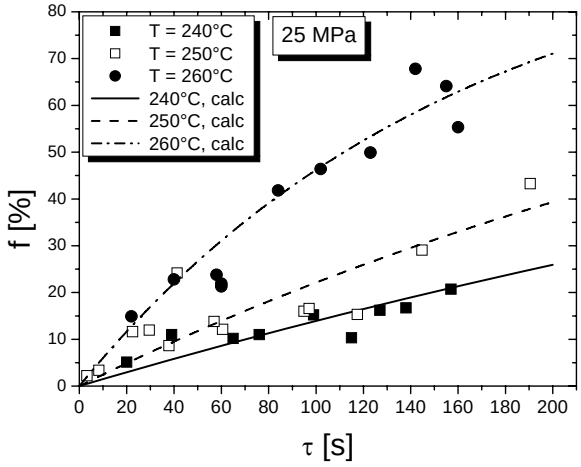

Figure 4.2: Degree of liquefaction of cellulose on a carbon basis at 240-260°C, initial cellulose concentration: 0.5 wt-%, the kinetics were calculated according to a first order approach

It can be inferred that the degree of liquefaction increases with temperature and reaction time. Cellulose is substantially liquefied at a temperature of 240°C, yielding degrees of liquefaction of about 20 % at a residence time of three minutes. A further extension of residence time was not possible because of technical limitations with respect to the available reactor volume and the feasible flow rates.

The degree of liquefaction progressively increases with temperature. At 260°C, about 60 % of the influent carbon were liquefied at a reaction time of 160 s. The experimental data reveal a still increasing tendency of liquefaction at the conditions applied. In order to study the feasibility of a complete liquefaction of any carbon, additional experiments were conducted in the same time range but at higher temperatures. The results of cellulose hydrolysis at temperatures of 270°C and 280°C are shown in Figure 4.3

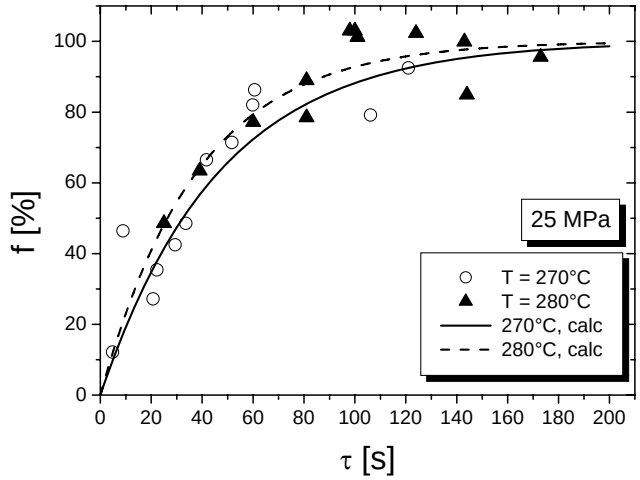

Figure 4.3: Degree of liquefaction of cellulose on a carbon basis at 270-280°C, initial cellulose concentration: 0.5 wt-%, the kinetics were calculated according to a first order approach

As compared to the results before, the cellulose degradation is strongly enhanced by a further increase in temperature. At a temperature of 280°C, essentially all carbon is liquefied at reaction times of 100-120 s. These results prove that pure cellulose can be efficiently degraded to water-soluble products by hydrolysis in water at elevated temperatures and pressures. A further increase in temperature led to even more rapid degradation kinetics, as illustrated by the results of experiments at 290°C and 310°C shown in Figure 4.4.

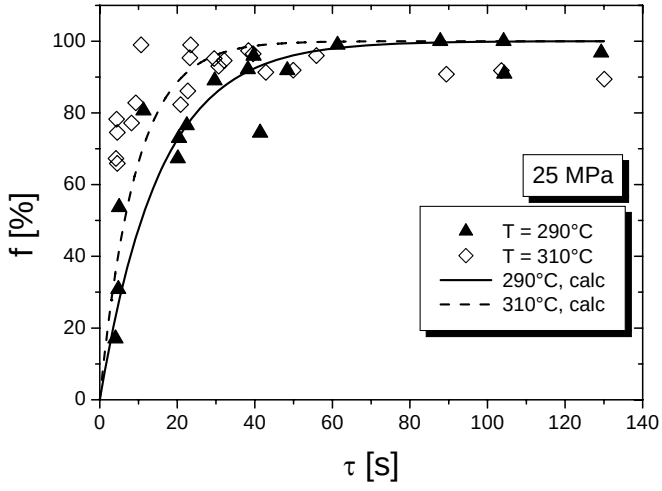

Figure 4.4: Degree of liquefaction of cellulose on a carbon basis at 290-310°C, initial cellulose concentration: 0.5 wt-%, the kinetics were calculated according to a first order approach

At a temperature of 290°C, a complete liquefaction could be achieved within residence times of 60 to 80 s, while at 310°C a complete conversion to soluble products was accomplished after 20 to 30 s. Although the rate of liquefaction initially was further enhanced by a temperature increase, the degree of liquefaction seems to decline with prolonging reaction time at 310°C. This observation can be attributed to different possible explanations, e.g. experimental uncertainties, formation of product gases, and secondary reactions to insoluble products. Experimental uncertainties as a reason for this observation are unlikely. The plausibility of the experiments was checked by calculation of the respective carbon balances. In addition, blank tests on the continuous processing of cellulose at ambient temperature were conducted. A comparison of the expected and the real cellulose concentration in the effluents did not reveal significant deviations, which might have been due to sedimentation and accumulation of insoluble matter in the apparatus.

Cellulose and primary reaction products are known to further decompose to gaseous products in sub- and supercritical water [42]. The gasification of glucose to yield carbon dioxide, hydrogen, and methane is illustrated in Figure 4.5.

$$C_6H_{12}O_6 + 6H_2O \rightarrow 6CO_2 + 12H_2$$

$$C_6H_{12}O_6 \rightarrow 3CH_4 + 3CO_2$$

Figure 4.5: Reaction schemes of glucose gasification in sub- and supercritical water

The formation of methane is the preferred reaction pathway at lower temperatures, while the production of hydrogen proceeds in the supercritical region. A substantial conversion to gas species is, however, usually accomplished at much higher temperatures (400-500°C) and residence times in the order of hours. This finding could be supported by own gas measurements at temperatures of 350 to 375°C and residence times from 20 to 40 s, which yielded a contribution of gas species to the carbon balance of about 1 wt-%. A marked gasification of cellulose can therefore be excluded at the conditions applied.

The decrease in liquefaction at higher temperatures and prolonged residence times is presumably due to the formation of insoluble products. Such compounds could be formed because of secondary or competing, free-radical reactions. This assumption was supported by visual observations. Effluents, which were treated at temperatures exceeding 300°C, showed precipitation of fine, brownish particulates after a short time at room temperature.

In contrast to temperature, the operating pressure had a negligible influence on cellulose degradation at the conditions applied. The hydrolysis of cellulose was studied for three different pressure levels at 15 MPa, 20 MPa, and 25 MPa, and temperatures of 250°C and 290°C. The results for 290°C are depicted in Figure 4.6.

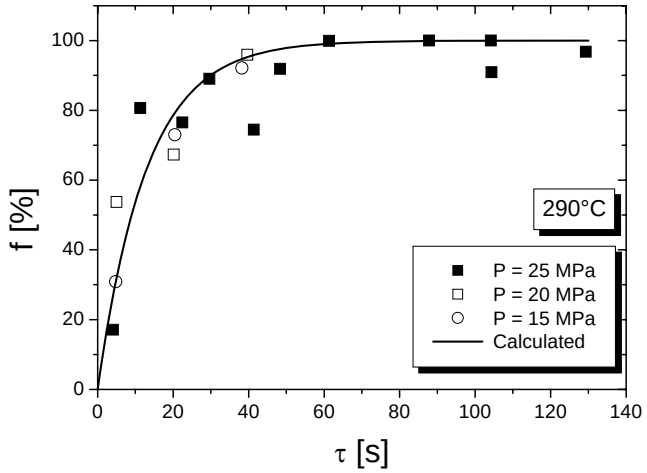

Figure 4.6: Influence of pressure on the degree of cellulose liquefaction, initial cellulose concentration: 0.5 wt-%

As can be seen, a marked influence of pressure cannot be distinguished at a temperature of 290°C. This result can be explained by the fact, that water still has the character of an incompressible fluid even at temperatures in the range of 300°C. The density of pure water at 300°C [41] changes from 742.9 kg/m^3 at 25 MPa, to 734.8 kg/m^3 at 20 MPa, and 725.7 kg/m^3 at 15 MPa, which corresponds to a weak decrease in density of 1.1 % and 2.3 %, respectively. Accordingly, physico-chemical properties associated with density, e.g. the dielectric constant, dissociation and reaction constants, do not change significantly with pressure.

In order to assess the plausibility of the results, a mass balance check was performed for a larger number of experiments. For this purpose, the total organic carbon of the effluent, being the sum of dissolved and insoluble carbon in the liquid phase, was measured by TOC analysis. The measured values were compared to the calculated influent carbon to elucidate whether the carbon balance was fulfilled. The calculation for 50 experiments yields a mean relative deviation of 9.5 % with respect to influent and effluent carbon. The values fluctuate arbitrarily rather than showing a clear tendency towards a higher or lower effluent carbon content as compared to the calculated influent carbon. This deviation might well be due to inaccuracies in the TOC analysis itself and not necessarily to experimental errors, since the injection of solid-bearing suspensions into the TOC-analyser could not be accomplished as reproducibly as the analysis of filtrated samples.

Due to the high density of data points, not every single experiment could be repeated in duplicate or triplicate. The reproducibility of experiments was checked by means of selected experiments, representing typical operating conditions. Experiments at 240°C and 120 s, 260°C and 160 s, as well as 280°C and 80 s were done in duplicate. In addition, an experiment at 260°C and 60 s was repeated in triplicate. The degrees of conversion and the relative

deviation from the respective mean values were calculated and averaged over all experiments. The resulting mean relative deviation was 6.6 %, which is satisfactory taking into account that the analysis of effluents was also afflicted with uncertainties.

Kinetic modelling:

The experimental data on the liquefaction of pure cellulose were modelled using a global rate law, with the reaction order of cellulose being unity. For such an irreversible first order reaction, the rate of reaction can be expressed as follows:

$$r = -kC_0(1-f) \qquad (4.2)$$

with k denoting the reaction rate constant and C_0 being the initial cellulose concentration. For modelling the degree of liquefaction by the concept of an ideal plug flow reactor, the following assumptions are made [43]:

- isothermal conditions
- plug flow in axial direction
- no gradients in radial direction (temperature, pressure, concentration)
- no axial dispersion

The assumption of isothermal conditions is justified because of the negligible temperature difference between the reactor inlet and outlet. The experiments were conducted at high axial velocities, with typical Reynolds numbers in the range of 3,000 to 8,000. It can therefore be assumed that axial diffusion is negligible compared to convection and that the turbulent regime accounts for plug flow and negligible radial gradients.

Due to the low compressibility of water and the low cellulose concentration , the fluid density can be assumed as constant along the reactor. At these conditions, the degree of cellulose liquefaction in an ideal plug flow reactor can be expressed as follows:

$$f = 1 - \exp(-k \cdot \tau) \qquad (4.3)$$

and after rearrangement:

$$-\ln(1-f) = k \cdot \tau \qquad (4.4)$$

In case the rate of conversion can accurately be described by a first order kinetic, the reaction rate constant can be read as the slope of a straight line in a ln(1-f) versus τ diagram. Such a diagram is depicted in Figure 4.7 for the temperature range from 240 to 310°C.

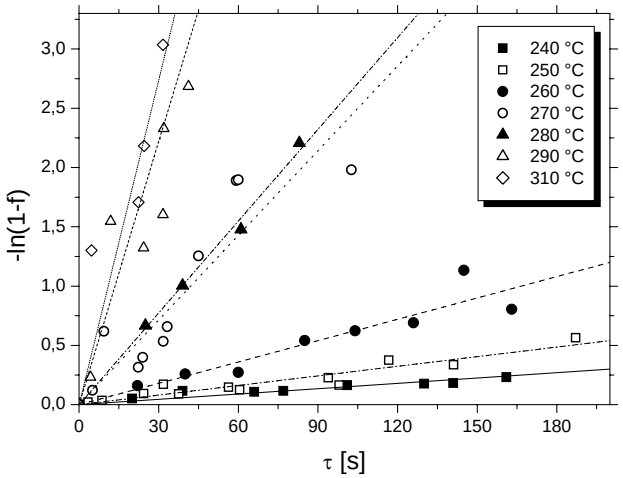

Figure 4.7: Determination of the reaction rate constant from the respective conversion data

As can be seen, the experimental data can reasonably be reflected by straight line relationships. Accordingly, the kinetics of cellulose liquefaction can satisfactorily be described by a global first order rate law. This approach is especially applicable for lower temperatures, where the data very accurately obey a linear relationship.

The reaction rate constants at different temperatures can be determined by reading the values of the slope of the straight lines. These values are stated in Table 4.1.

Table 4.1: Reaction rate constants of cellulose liquefaction at different temperatures

T [°C]	240	250	260	270	280	290	310
k(T) [1/s]	0.0015	0.0025	0.0062	0.0214	0.0263	0.0647	0.1086

A common approach to express the temperature dependence of the reaction rate constant is the Arrhenius' law:

$$k_{(T)} = k_0 \cdot \exp(-\frac{E_{C,A}}{R \cdot T}) \qquad (4.5)$$

with k_0 being the pre-exponential factor and E_A the activation energy of the reaction.

Accordingly, these kinetic parameters can be determined by plotting ln(k(T)) versus the reciprocal temperature and reading the ordinate intercept and the slope of the straight line. The Arrhenius' plot with the respective values of the pre-exponential factor and the activation energy is shown in Figure 4.8.

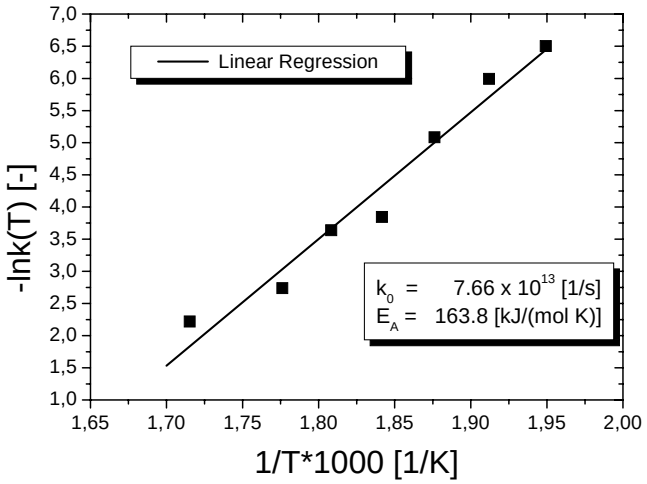

Figure 4.8: Determination of kinetic parameters from the Arrhenius' approach

The straight line was obtained by linear regression of the reaction rate constants at different temperatures. As can be seen, the calculated straight line is in good accordance with the values of the reaction rate constants. Hence, the Arrhenius' law can be applied to the liquefaction of cellulose in subcritical water.

Summing up the results of this parameter study, it can be concluded that the kinetics of cellulose conversion in subcritical water can accurately be described by a global first order rate law.

4.1.2 PRODUCT FORMATION

Beside the kinetics of cellulose hydrolysis, the investigation of product formation was of special interest. The examination of product formation included the identification and the description of temperature and time dependence of main degradation products. A detailed knowledge of product formation is important to optimise reaction conditions with respect to the selective production of desired compounds, e.g. glucose as a valuable product of the hydrolysis of lignocellulosic materials.

The liquid effluents of cellulose hydrolysis were analysed for saccharides and secondary degradation products thereof as well as for carboxylic acids. Figure 4.9 shows a chromatogram of cellulose degradation products.

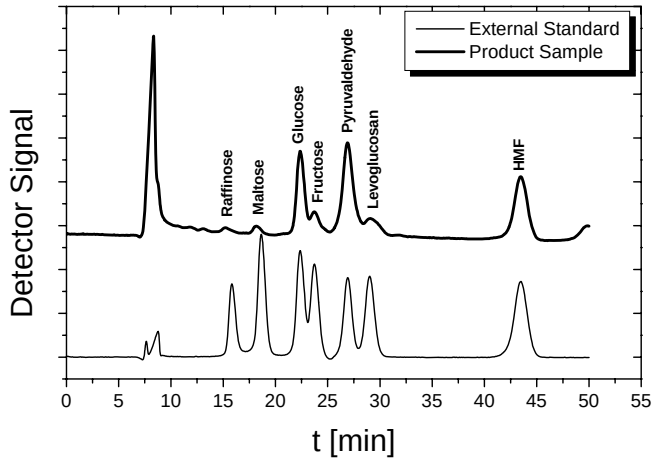

Figure 4.9: Chromatogram of saccharide analysis, experimental conditions: 25 MPa, 290°C, 62 s

It can be inferred that glucose, being the monomeric building block, as well as fructose, which is formed from glucose by isomerization reactions, could be detected in significant amounts. In addition pyruvaldehyde, levoglucosan, and hydroxymethylfurfural (HMF) were formed as secondary reaction products of cellulose hydrolysis. At lower temperatures and residence times, water-soluble oligosaccharides could also be detected as partial hydrolysis products, but not be quantified because of poor peak resolution.

The parameter study showed that glucose, pyruvaldehyde, and HMF are major reaction products of cellulose hydrolysis. These compounds were, however, not stable under operating conditions due to secondary decomposition reactions. The main objective of the studies on product formation was to derive practical conclusions for engineering purposes, e.g. process design and process optimisation, rather than achieving a thorough understanding and modelling of the exact reaction mechanism. Hence, the yields of main degradation products were modelled according to the approach of a simple consecutive reaction. This approach is illustrated in Figure 4.10 considering glucose.

$$\text{Cellulose} \xrightarrow{k_{G,f}} \text{Glucose} \xrightarrow{k_{G,d}} \text{Secondary products}$$

Figure 4.10: Simplified reaction scheme for glucose formation and secondary decomposition

Under the assumption, that both the rate of formation and the rate of decomposition are of first order, the concentration of glucose can be calculated as follows:

$$C_G = \frac{k_f}{k_d - k_f} C_{C,0} \left[\exp(-k_f t) - \exp(-k_d t) \right] \qquad (4.6)$$

with $C_{C,0}$ denoting the initial cellulose concentration and k_f and k_d the rate constants of formation and decomposition, respectively.

The yield of degradation product i on a carbon basis was defined as the ratio of carbon bound in species i to the theoretically possible amount, which was calculated from the initial cellulose concentration.

$$Y_i = \frac{C_i}{TOC} \qquad (4.7)$$

This formula is also valid in case of gas production. The reaction rate constants of formation and decomposition could be determined by fitting equation 4.6 to the experimentally determined yields. Figure 4.11 shows the yield of glucose and HMF as a function of time at 250 to 310°C.

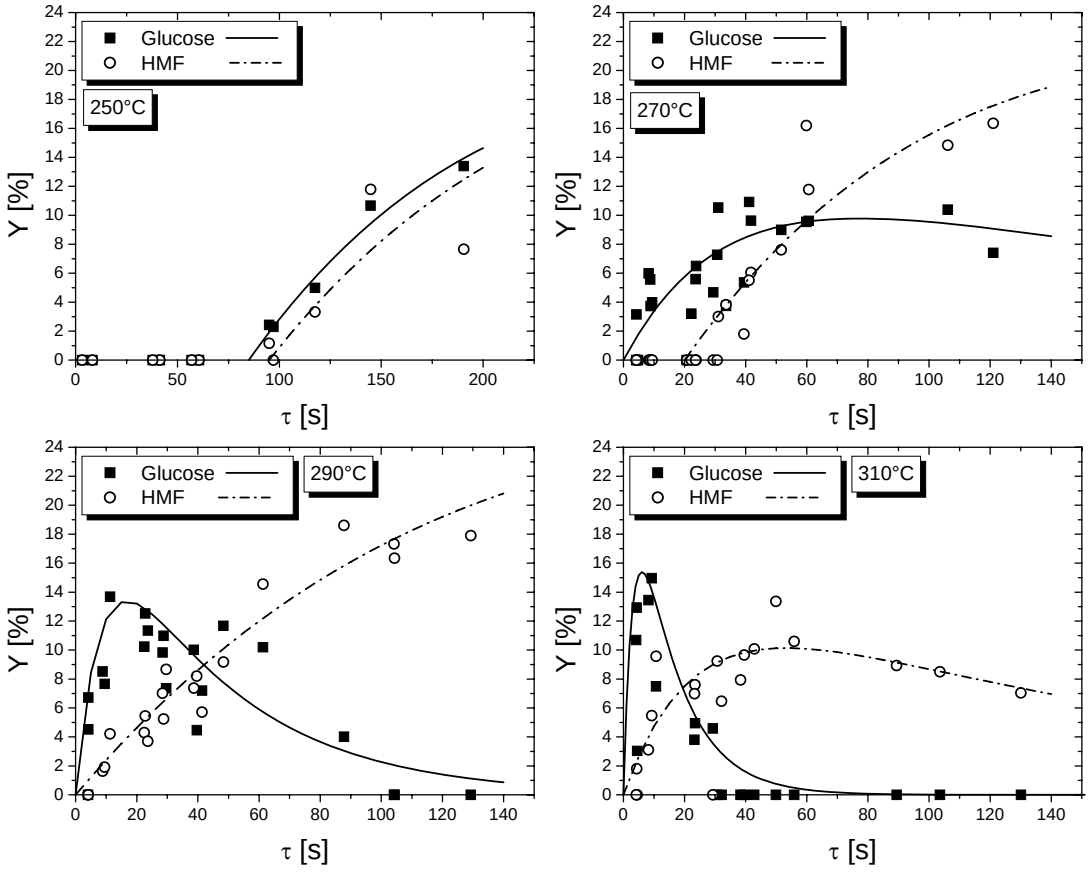

Figure 4.11: Yields of selected degradation products versus time, T: 250-310°C, P: 25 MPa

It can be inferred that the glucose yields follow the typical pattern of a consecutive reaction. Glucose was detected in quantifiable amounts with a substantial lag of about 80 s at 250°C, which can be attributed to the slow liquefaction kinetics and the low rate of cleavage of glycosidic bonds at this temperature. Within the residence time studied, the yields of glucose showed a still increasing tendency. A temperature increase to 270°C led to a marked acceleration in glucose formation, showing an immediate increase of glucose concentration. A maximum could be observed at 60 to 80 s, with a subsequent decline of glucose yields. This maximum was shifted to shorter residence times and higher glucose yields with a further increase in temperature, as can be concluded from the experiments at 290°C and 310°C. While at 290°C maximal glucose yields of 13 to 14 % could be attained after reaction times of about 20 s, glucose formation reached a maximum of 16 % in less than 10 s at 310°C. Glucose is obviously instable under the conditions applied and accordingly consumed by consecutive reactions.
Regarding the formation of HMF, a similar course could be observed. The HMF yields lag, however, behind the respective glucose yields, indicating that HMF is formed from cellulose by secondary rather than primary reactions. At a temperature of 310°C, HMF is also subject to secondary decomposition. The same pattern could be observed for pyruvaldehyde.

The experimental data could satisfactorily be reflected by the curves in the figure, which were calculated under the assumption of a consecutive reaction with a first order rate law for formation and decomposition. The respective values for the rate constants of formation and decomposition are stated in Table 4.2.

Table 4.2: Rate constants of formation and decomposition for main degradation products

T	Glucose		HMF		Pyruvaldehyde	
[°C]	k_f [1/s]	k_d [1/s]	k_f [1/s]	k_d [1/s]	k_f [1/s]	k_d [1/s]
250	0.002	0.006	0.0018	0.005	0.001	0.007
270	0.004	0.03	0.003	0.008	0.0017	0.01
290	0.024	0.12	0.0025	0.005	0.0036	0.013
310	0.075	0.31	0.006	0.043	0.015	0.045

Additional data were derived from experiments at 240, 260, and 280°C. It was further attempted to perform measurements for residence times exceeding three minutes in the lower temperature region (240-270°C), in order to confirm the kinetic data for declining product yields. Because of limitations with respect to the available reactor volume and the minimal required flow rate of the metering pump, such measurements were not possible in fully continuous mode. Hence, the residence time in the tubular reactor was extended by closing a check valve at the outlet of the cooler and simultaneously switching off the metering pump. This approach was, however, associated with highly non-ideal conditions. Due to the significant temperature gradients between the reactor on the one hand and the cooler and the supply line on the other hand, thermal convection led to substantial dilution and back-mixing

effects in the tubular reactor. The results of these experiments were therefore disregarded in the kinetic evaluation.

Based on the kinetic parameters of product formation, the selectivity of main products can be predicted. The selectivity states the amount of carbon transformed to degradation product i with respect to the overall degree of conversion.

$$S_i = \frac{Y_i}{f} = \frac{C_i}{DOC} \qquad (4.8)$$

This formula is only valid in case of negligible gas production.

Figure 4.12 shows the predicted selectivity of glucose formation as a function of residence time for different temperatures.

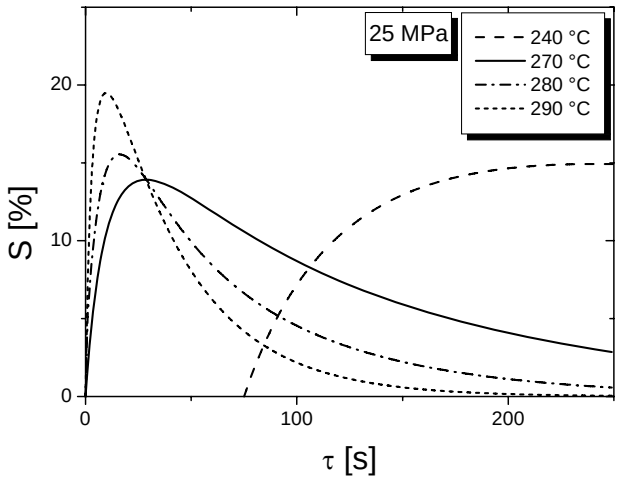

Figure 4.12: Calculated selectivity of glucose formation as a function of reaction time for different temperatures

The predicted curve for 240°C appears to overestimate the attainable selectivity. This can presumably be attributed to the fact that in this temperature region experimental data were available for increasing glucose yields, only. As can be seen, the maximum in glucose selectivity is shifted to shorter residence times with increasing temperature. The maximal attainable selectivity exhibits increasing values with temperature.

This finding is in accordance with results of other works [44, 45] on cellulose hydrolysis at temperatures from 320 to 400°C. The results described in literature also show increasing glucose yields with increasing temperature at very short residence times. The authors ascribe this observation to an increase in the rate of cellulose decomposition compared to the values of

glucose degradation. The respective rate constants of cellulose and glucose decomposition are depicted in Figure 4.13.

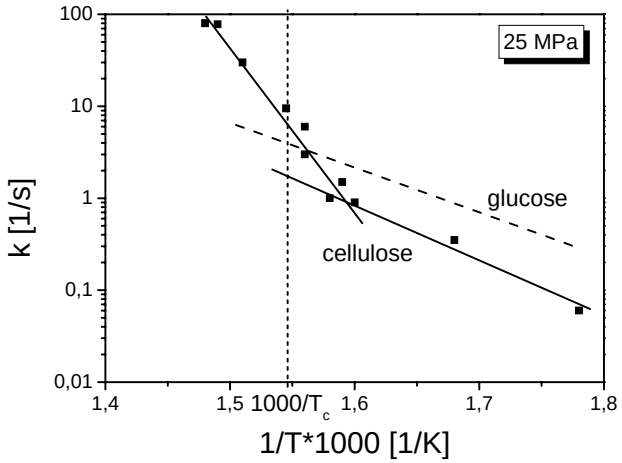

Figure 4.13: Rate constants of cellulose and glucose degradation in sub- and supercritical water [45]

Based on the literature data, the rate constant of cellulose decomposition shows a sharp bend at near-critical conditions. As a result, the decomposition of cellulose and the associated formation of glucose proceed faster than the secondary degradation of glucose in this region. Such a sharp bend in an Arrhenius' plot indicates a deviation of the actual reaction rate from the apparent one, which usually is a result of mass transfer limitations. The authors explain this observation by a drastically increased solubility of cellulose under near-critical conditions.

The reported glucose yields amounted to maximal 50 % at 400°C and 25 MPa. This value was, however, stated for a very short residence time of 0.0025 s. After a reaction time of 0.15 s, glucose was completely consumed by secondary reactions according to the authors. Based on the results of own measurements and literature data, the hydrolysis of cellulose can optimally be performed at high temperatures and very short residence times in the order of seconds, in case the selective formation of glucose is intended.

Beside the analyses of saccharides and degradation products thereof, samples of the experiments on cellulose hydrolysis were analysed for carboxylic acids. Acetic, propionic, as well as isobutyric and n-butyric acid could be detected and quantified. However, only acetic acid had a significant contribution to the total carbon of the effluents.

The ratio of carbon bound in acetic acid to the total effluent carbon is depicted in Figure 4.14.

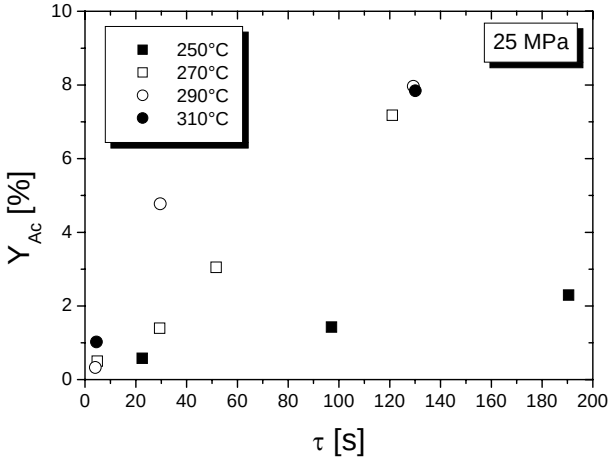

Figure 4.14: Yield of acetic acid as a product of cellulose hydrolysis versus time

The results reveal the presence of considerable amounts of acetic acid, which may be an explanation for the marked decrease in pH of the effluents. This is especially valid for temperatures higher than 250°C, where the course of acetic acid content shows a steep increase with residence time. At 380°C and a residence time of 6 s, acetic acid contributed to 6 % of the total carbon.

In average, about 50 % of the total carbon could be determined by detection and quantification of cellulose degradation products. The unrevealed portion of the carbon balance can presumably be attributed to the contribution of partial hydrolyzates at lower temperatures and the formation of various secondary reaction products with increasing temperature.

4.1.3 CATALYTIC INFLUENCE OF CO_2-ADDITION

Carbon dioxide was added to the influent suspension as a supplementary means to enhance the rate of cellulose conversion in water at elevated temperatures and pressures. Based on the results of the hydrolytic degradation of starch [29], carbon dioxide was believed to promote the acid-catalysed reaction pathway of cellulose hydrolysis by the formation and dissociation of carbonic acid. Such an approach offers the advantage of an easy recovery of carbon dioxide by expansion and subsequent re-utilisation in a closed cycle.

Experiments were conducted at different CO_2-concentrations, corresponding to a range of 25 to 100 % with respect to the saturation level. The saturation concentration of carbon dioxide in the aqueous phase was calculated from equilibrium data for the system water/CO_2 at elevated temperatures and pressures [35, 46]. The density of carbon dioxide was taken from literature data [47] and calculated according to [48]. The influence of acidification by carbon dioxide on

both the hydrolysis kinetics and the product formation was investigated and compared to cellulose hydrolysis in pure water.

Figure 4.15 shows the effect of carbon dioxide on the liquefaction of cellulose at different levels of saturation.

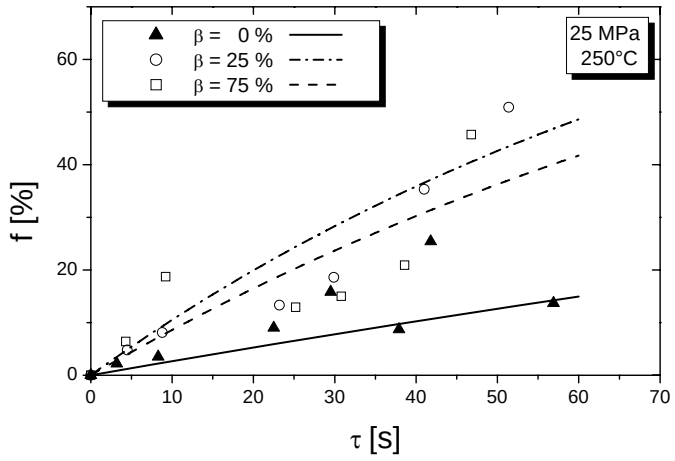

Figure 4.15: Liquefaction of cellulose at varying levels of CO_2-saturation

The curves were calculated in analogy to the kinetic modelling of cellulose liquefaction in pure water. It can be inferred that the addition of carbon dioxide results in a rate enhancement of cellulose hydrolysis at 250°C. Regarding the acidification at varying saturation levels, a difference cannot be observed within the range of experimental uncertainty. This finding can presumably be explained by the fact that the pH initially drops sharply and lowers progressively slower with increasing carbon dioxide addition. Because of the logarithmic character of the pH, the continuing addition of carbon dioxide does not significantly contribute to a further decrease in pH and associated rate enhancement of acid catalysed reaction steps at the conditions applied.

The influence of acidification by carbon dioxide as a function of temperature is depicted in Figure 4.16 and Figure 4.17.

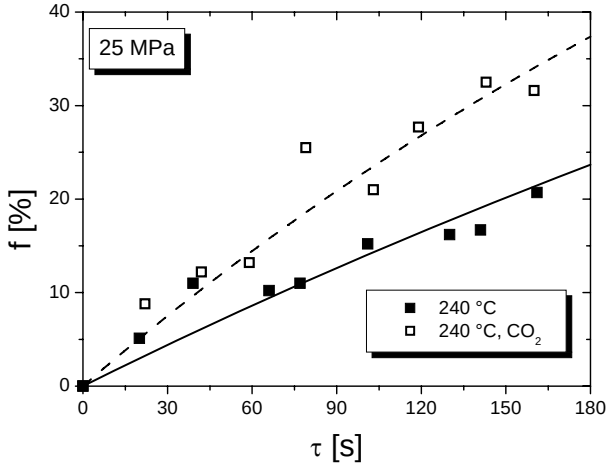

Figure 4.16: Liquefaction of cellulose at 240°C and varying amounts of carbon dioxide, β: 0-75 %, initial cellulose concentration: 0.5 wt-%

The addition of carbon dioxide yields a significant rate enhancement of cellulose liquefaction at 240°C. This catalytic effect diminishes with increasing temperature, as can be inferred from the respective degrees of liquefaction at 260°C and 280°C. A comparison for the system water/CO_2 and pure water shows a still slightly increased rate of hydrolysis at 260°C, while at 280°C no differences in hydrolysis kinetics could be determined.

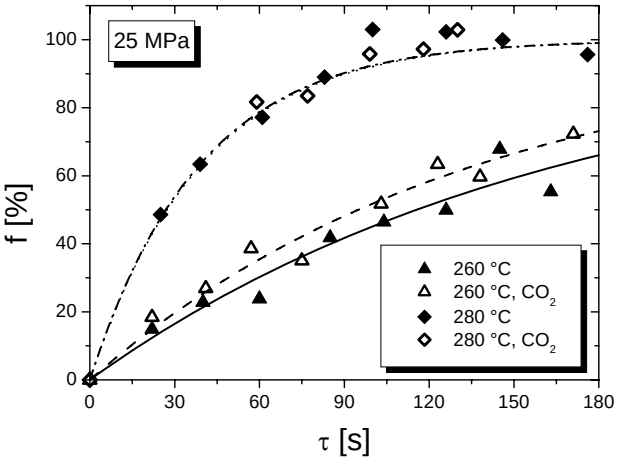

Figure 4.17: Liquefaction of cellulose at 260-280°C and varying amounts of carbon dioxide, β: 0-100 %, initial cellulose concentration: 0.5 wt-%

The decreasing catalytic influence of carbon dioxide with increasing temperature can presumably be attributed to two facts. On the one hand, the associated drop in pH of saturated

water/CO_2 mixtures decreases with increasing temperature, which leads to a less pronounced rate enhancement compared to the already increased rate of reaction at higher temperatures. On the other hand, acidic compounds are rapidly formed in the course of reaction, which could be confirmed by the analysis of carboxylic acids and measurements of the effluent pH. Figure 4.18 shows the pH of reactor effluents of cellulose hydrolysis at temperatures of 270°C, 290°C, and 310°C, respectively.

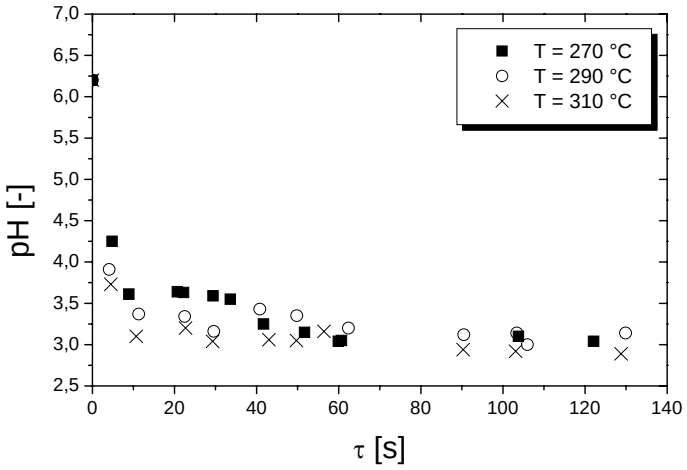

Figure 4.18: pH of reactor effluents after hydrolytic treatment, the times stated refer to the residence time in the reactor, the pH was measured off-line at ambient conditions with a conventional pH probe

As can be seen, the pH of the effluents drops sharply to values below 3.5 after reaction times of a few seconds. For short reaction times, the drop in pH is more pronounced at higher temperatures, while the temperature effect decreases with increasing time. The low pH values cannot be attributed to carbonic acid, but to the formation of carboxylic acids, e.g. acetic acid, in the course of reaction. Acetic acid is a much stronger acid than carbonic acid, meaning that the dissociation of carbonic acid under operating conditions has a rather minor contribution to the pH compared to the acidic compounds formed during reaction. Accordingly, the catalytic effect of carbon dioxide addition lessens with increasing reaction temperature, as could be observed in the liquefaction of cellulose.

A marked rate enhancement of cellulose hydrolysis by carbon dioxide addition could be determined at temperatures from 240 to 260°C. The kinetic modelling of cellulose liquefaction in the system water/CO_2 was done in accordance with the method applied for pure water. The resulting reaction rate constants are shown in Figure 4.19 along with the values for pure water.

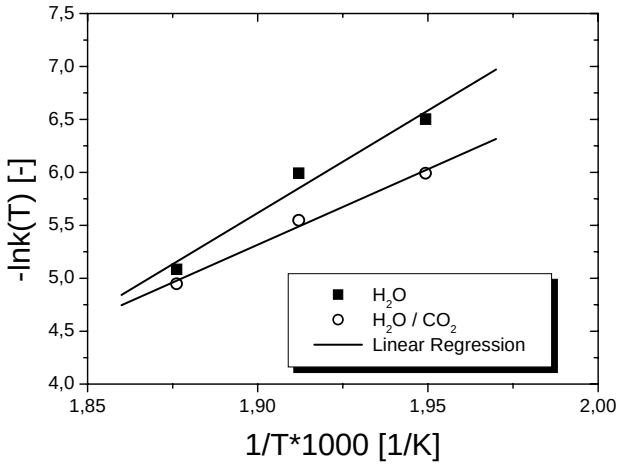

Figure 4.19: Arrhenius' plot of cellulose hydrolysis in water and water/carbon dioxide mixtures

The reaction rate constants of cellulose hydrolysis in the system water/CO_2 are higher than those for pure water at temperatures of 240 to 260°C. The lines in the Arrhenius' plot approach one another with increasing temperature, so that no further enhancement in the rate of liquefaction could be obtained by adding carbon dioxide at temperatures higher than 270°C.

A comparison of the respective reaction rate constants is depicted in Table 4.3.

Table 4.3: Reaction rate constants of cellulose hydrolysis in water/CO_2 and pure water

T [°C]	240	250	260
$k(T)_{CO2}$ [1/s]	0.0025	0.0039	0.0071
k(T) [1/s]	0.0015	0.0025	0.0062

The catalytic effect of acidification could not only be stated with respect to the liquefaction kinetics, but it could also be observed regarding the product formation. Glucose yields could be significantly increased by acidification in the temperature range from 240 to 260°C. Figure 4.20 shows the course of glucose yields in water/CO_2 and pure water.

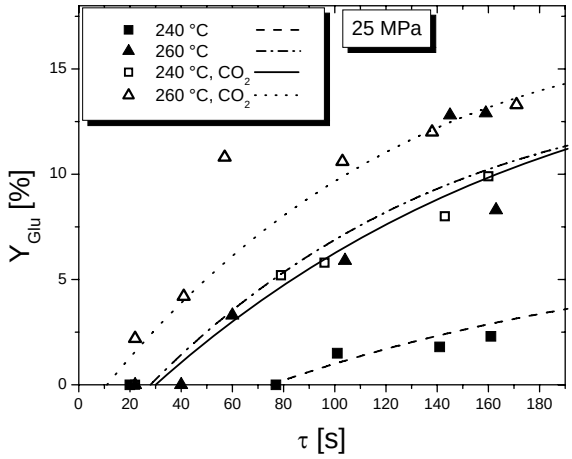

Figure 4.20: Glucose yields in water, water/carbon dioxide, β: 0-87 %

Compared to hydrolysis in pure water, the onset of glucose formation is shifted to shorter residence times due to the faster cleavage of glycosidic bonds. Glucose is also formed at higher yields. The differences in time and yield are less pronounced at 260°C because of the lessening catalytic effect at higher temperatures.
Regarding secondary reaction products, the yields of HMF were enhanced at 260°C, while in case of pyruvaldehyde no catalytic influence could be observed.

In line with the kinetics of cellulose liquefaction, the degree of CO_2-saturation did not exhibit a measurable effect on the formation of glucose. Figure 4.21 shows the respective glucose yields at two levels of carbon dioxide addition.

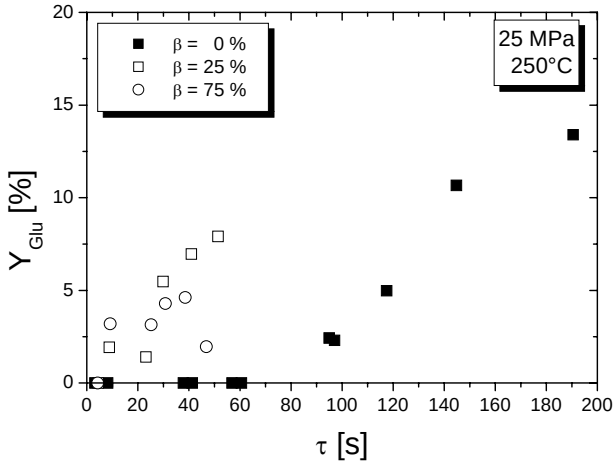

Figure 4.21: Glucose yields at varying levels of CO_2-saturation

Compared to the non-catalysed hydrolysis in pure water, the glucose yields are enhanced by acidification with carbon dioxide. A difference in glucose yields at concentrations of 25 % and 75 % with respect to saturation could, however, not be stated.

The investigation of the hydrolysis of crystalline cellulose yielded a number of very important conclusions with respect to the conversion of lignocellulosic biomass. Pure cellulose can readily be liquefied in subcritcal water at reaction times in the order of seconds to minutes without the addition of a catalyst. The hydrolysis kinetics are enhanced with increasing temperature, while a marked gas formation could not be observed at the conditions applied. Cellulose is degraded to saccharides, mainly glucose, as well as secondary reaction products, e.g. HMF, pyruvaldehyde, and carboxylic acids. Both the liquefaction kinetics as well as the kinetics of product formation could be described by global first order approaches.

The acidification by carbon dioxide led to a rate enhancement of cellulose hydrolysis. The rate of liquefaction as well as the formation of glucose were catalyzed by the dissociation of carbonic acid. The catalyzing effect of carbon dioxide lessens with temperature. A pronounced influence of CO_2-concentration with respect to saturation could not be observed.

4.2 Lignin Conversion

Lignin was chosen as a model compound for real biological waste, since it is one of the main components in plant biomass. Furthermore, lignin is known to exhibit a good thermal stability and, hence, it constitutes the most persistent component of woody biomass to both biological and thermo-chemical degradation. Beside the conversion of lignin by hydrolysis in near-critical water, the oxidative treatment using hydrogen peroxide was also investigated in this work. The objectives were to reveal the degree of liquefaction achievable by hydrolysis and to compare them to the results of lignin oxidation in terms of carbon conversion and product formation. Oxidation experiments were conducted at varying amounts of oxidant with respect to the stoichiometric demand, corresponding to conditions of partial oxidation, of oxidation providing the stoichiometric demand, and to conditions of oxidation with excess supply of oxidant. This study was intended to show the feasibility of a close to complete mineralization of lignin by conversion to carbon dioxide and water, mainly. Such a conclusion would demonstrate that the hydrothermal processing of plant biomass constitutes a stand-alone alternative rather than a supplementary technology to biological degradation.

4.2.1 HYDROLYTIC DEGRADATION

Experiments on the hydrolysis of lignin were conducted with organosolv lignin, which is essentially water insoluble at ambient conditions. Because of the fact that isolated lignin in general exhibits a more condensed, cross-linked structure than lignin contained in plant biomass, it was assumed that isolated lignin is more recalcitrant to hydrothermal degradation than lignin bound in real lignocellulosic wastes. The organosolv lignin was therefore treated semi-continuously in fixed bed mode at near-critical, non oxidative conditions, in order to increase the attainable reaction temperature and to extend the time available for reaction.

In the beginning, the effluents of the fixed bed were directly passed to the double-pipe heat exchangers and thus cooled down immediately. With this operating mode and preset holding temperatures of 370°C-380°C, degrees of liquefaction on a carbon basis in the range of 20-25 % could be achieved. A mass balance check yielded an essentially complete recovery of total carbon in the effluent, which in turn means that the lignin became water-soluble in near-critical water and passed the sinter metal inlet (mean pore diameter ~0.5 µm). At ambient conditions, however, about 75 % of the carbon were present in form of a water-insoluble, very finely suspended phase.

These results show that organosolv lignin completely dissolves in near-critical water and undergoes significant chemical modification. To confirm these findings, a test run was conducted at ambient temperature but otherwise identical conditions. The amount of lignin recovered in the fixed bed after the end of the experiment quantitatively equalled the amount prior to the experiment. In addition, the reactor effluent was analysed with respect to its DOC, but it did not contain any carbon-bearing substances. This blank test proves that lignin was completely retained in the fixed bed and was neither dissolved in water nor transported through the filter unit by the flow of water at ambient temperature.

Based on these conclusions, a high-temperature oven with an additional 20 ml of reaction volume was connected to the outlet of the fixed bed to increase both reaction temperature and residence time of the effluents in the reaction zone. By this modification, it was intended to degrade the lignin, which became soluble and passed the fixed bed under operating conditions, to hydrolysates which were still soluble under ambient conditions. With this set-up outlet temperatures up to 500°C could be realized. The results of these experiments show that the temperature increase led to an increase in degree of liquefaction up to 40 % at an outlet temperature of 450°C, while at even higher outlet temperatures the degree of liquefaction seemed to be inversely affected by temperature. The portion of water-soluble carbon in the effluent decreased from about 40 % (450°C) to 14 % (480°C) and 5 % (490°C). The mean residence time of the reaction mixture at operating conditions was between 35-40 s for all experiments. The actual solvent ratio could not be determined for the fixed bed experiments because of the fact that essentially all lignin became soluble under operating conditions.

The decrease in water-soluble carbon can be partly attributed to the formation of gaseous species, which was confirmed by gas phase measurements. Carbon dioxide and methane could

be determined qualitatively in the off-gas of lignin hydrolysis. Beside the transformation of carbon to the gas phase, the build-up of carbon-rich residues during the non-oxidative treatment could be observed. Carbon-like residues were recovered in all experiments. In case of the experiments with the high-temperature oven, the pure water stream was rapidly heated up before entering the fixed bed. These conditions led to the formation of black residues in the fixed bed, which where insoluble even under operating conditions. The solid, sometimes bituminous, material resulted in severe operating problems due to clogging of pipes and the backpressure regulator. The residues had to be removed subsequently by mechanical and chemical cleaning with acetone.

One possible explanation for this phenomenon is the recombination of reactive lignin fragments to form water-insoluble residues. The influence of such secondary reactions of reactive degradation products on the portion of water-insoluble lignin after hydrothermal treatment was investigated by [49]. Results of the hydrothermal treatment of poplar wood lignin in terms of the amount of insoluble residues are depicted in Figure 4.22.

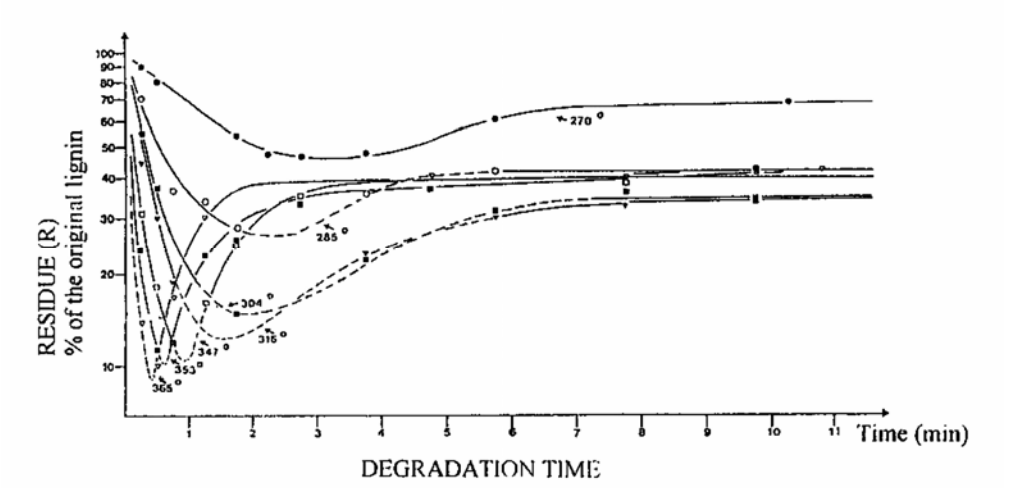

Figure 4.22: Hydrothermal degradation of lignin, yield of insoluble reaction products [49]

In this work, effluent samples were first washed with water and dissolved in an acetone-water mixture in a second step. The results demonstrate that the solubility of reaction products increases rapidly with temperature at first. There is a minimum with respect to the portion of insoluble reaction products, which can be inferred from the renewed increase in solid residues with time. This observation was attributed to secondary reactions and it is in line with own experiments, which showed a decreasing degree of liquefaction at higher temperatures and prolonged residence times. The residence time could, however, not be varied systematically at such high temperatures due to the limited reaction volume and the low water density. The low water density at high temperatures presumably leads to free radical reactions, leaving sticky pyrolysis products in the reactor, rather than ionic pathways.

The results discussed in literature and own experiments point to the conclusion that a complete liquefaction of isolated lignin by non-catalysed hydrolysis in pure high-temperature water is not feasible. At lower temperatures in the well-subcritical region, where the cleavage of the most widespread linkage, the β-O-4-bond, by hydrolysis should yield a high degree of degradation, the portion of insoluble residues is still in the range of 30-40 %. The formation of insoluble residues cannot be prevented even under optimised conditions. Furthermore, the treatment in pure water does not lead to the selective production of valuable compounds but to a broad product spectrum. This finding was derived from GC-MS analyses of soluble reaction products.

The chromatogram showed the existence of numerous degradation products in considerable concentrations. Although some major classes of degradation products could be identified, e.g. phenols, phenol derivatives, and other aromatic substances, a complete identification and quantification of all reaction products is virtually impossible.

It can be concluded that the hydrothermal treatment of lignin in pure water does neither result in a complete conversion nor in the selective formation of desired reaction products. Treatment of lignin in high temperature water led to the build-up of carbon-rich residues, which eventually resulted in reactor clogging and prevented the attempted continuous processing. Summing up these aspects, the non-catalysed hydrolysis of lignin in pure water does not appear to be a promising approach. Accordingly, the oxidative destruction of lignin was studied in the following.

4.2.2 OXIDATIVE DESTRUCTION

Based on the results of lignin degradation by hydrolysis, the oxidative treatment of lignin was investigated as a means to completely remove any insoluble carbon. Water-soluble alkali lignin was used in these studies, since the continuous processing of insoluble organosolv lignin was hampered by the formation of lignin coagulates in the feed vessel and lignin deposition in the reactor.

Hydrogen peroxide was used as the oxidant. It was directly introduced to the feed vessel and delivered to the reactor together with lignin. The stoichiometric amount of hydrogen peroxide was calculated on the basis of the structural formula and the elementary composition of lignin. The experiments were conducted at different amounts of hydrogen peroxide, corresponding to half the stoichiometric demand, one time and twice the stoichiometric demand. This parameter variation was done in order to elucidate the influence of both partial and complete oxidation on the amount of dissolved carbon and on the formation of main degradation products. The mean residence time could not be systematically varied due to the limited volume of the continuous flow reactor and the low fluid density at elevated temperatures. The time in the reaction zone was between 5 to 17 s for all experiments.

The degree of conversion of pure alkali lignin to gaseous products on a carbon basis is shown in Figure 4.23.

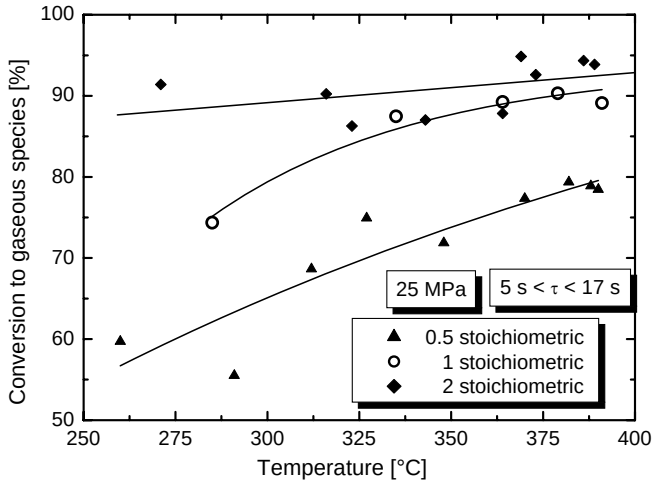

Figure 4.23: Conversion of alkali lignin to gaseous species on a carbon basis, influence of amount of oxidant and temperature, initial lignin concentration: 1 wt-%

The conversion to gaseous species was calculated on the basis of the aqueous phase analysis. This approach was feasible since no solid residues possibly contributing to the carbon balance were observed in the effluents. Providing at least half the stoichiometric demand yielded solid-free effluents at the temperatures applied.

The conversion to gaseous species increases with increasing temperature at hydrogen peroxide concentrations corresponding to half the stoichiometric and the stoichiometric demand. Supplying twice the stoichiometric amount yields only a very minor increase of gaseous products with increasing temperature. The portion of gaseous products is essentially constant and contributes to about 90-95 % of the total influent carbon, meaning that the residual DOC is about 5-10 % of the influent carbon at overstoichiometric hydrogen peroxide supply and temperatures ranging from well-subcritical to near-critical conditions.

It can be concluded that the stoichiometric and overstoichiometric oxidant supply lead to a nearly complete oxidation of lignin in less than 20 s. About 10 % of the influent carbon remains in the liquid effluents as DOC at temperatures up to 390°C. In order to identify these refractory compounds samples of the liquid effluents were subjected to GC-analyses.

Acetic acid is known to be a relatively stable intermediate in the total oxidation of organic wastes in water at elevated temperatures and pressures. The amount of carbon bound as acetic acid with respect to the total dissolved carbon in the liquid effluents is depicted in Figure 4.24.

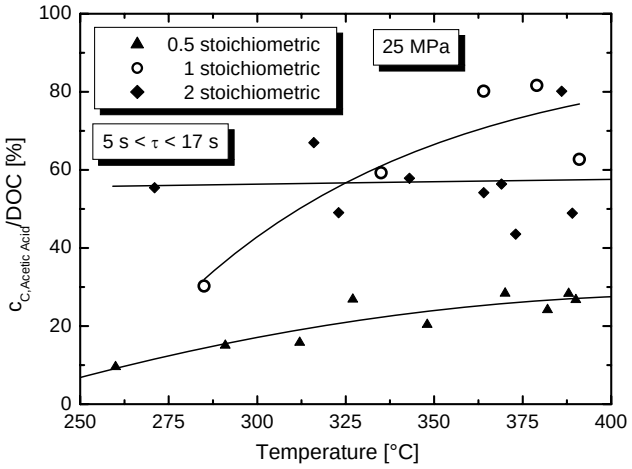

Figure 4.24: Oxidative conversion of alkali lignin, portion of carbon bound as acetic acid to total dissolved carbon in the effluent, initial lignin concentration: 1 wt-%

The results show that acetic acid constitutes the main degradation product providing the stoichiometric demand and an overstoichiometric amount of hydrogen peroxide, respectively. As can be seen, the portion of carbon bound in acetic acid increases with temperature, which confirms that acetic acid is a relatively stable intermediate in hydrothermal oxidation even at temperatures in the near-critical region. At stoichiometric oxidant supply, acetic acid contributes to up to 80 % of the dissolved carbon at near-critical conditions, while at overstoichiometric conditions acetic acid amounts to about 50-60 % on average. These values are, however, subject to larger deviations due to the almost complete oxidation and the low absolute concentrations of dissolved organic carbon. In contrast, the partial oxidation providing half the stoichiometric demand results in much lower acetic acid concentrations, contributing to 20-30 % of the dissolved carbon at near-critical conditions. This is probably due to the formation of partial oxidation products, which are not as highly oxidized as acetic acid.
Carboxylic acids higher than acetic acid have a comparatively minor contribution to the dissolved carbon.

Samples of the oxidative treatment of lignin were further analysed by GC-MS in order to identify and quantify oxidation products other than carboxylic acids. For each level of oxidant supply, three samples were analysed, covering conditions from well-subcritical to near-critical temperatures. An overview of the samples and the respective operating conditions is given in Table 4.4.

Table 4.4: Oxidative degradation of lignin, overview of samples selected for GC-MS analyses, the amount of oxidant α is stated with respect to the stoichiometric demand

Run No	Temperature [°C]	α [%]
AL 9	271	200
AL 12	323	
AL 8	389	
AL 21	285	100
AL 22	335	
AL 25	391	
AL 10	260	50
AL 17	327	
AL 7	390	

In case of the stoichiometric and overstoichiometric oxidant supply at higher temperatures (AL 12, AL 8, AL 22, AL 25), no further degradation products could be detected in quantifiable amounts due to the very low residual dissolved carbon content. For run AL 9, some organic compounds could be identified but not quantified because of the low absolute concentrations.

For the partial oxidation supplying half the stoichiometric demand, compounds other than carboxylic acids could be identified. The partial oxidation products identified were mainly phenol, phenol derivatives, benzoic acid, benzaldehyde and derivatives thereof, as well as alkylbenzenes.

In total, about 30 % of the total dissolved carbon could be identified in case of partial oxidation. The remaining carbon can probably be attributed to formic acid and other short-chain polar substances, which could not be detected by GC-MS due to the liquid/liquid extraction step with toluene and dichloromethane, respectively.

Summing up these aspects, the near-critical water oxidation can be regarded as a very efficient means to convert lignin to soluble and gaseous substances. In case of stoichiometric oxidant supply, lignin can be readily converted to gaseous species, leaving only about 10 % of the total influent carbon in the aqueous phase. In addition, a high selectivity for the formation of acetic acid, being in the range of 80 % at near-critical conditions, was observed. Acetic acid constitutes a desired decomposition product in biological systems since it can be readily converted by micro-organisms. The selective formation of other valuable reaction products with high yields in the course of hydrothermal degradation of lignin could not be accomplished in this work, although products like phenols and vanillin were produced in significant concentrations during partial oxidation. Especially at lower temperatures in the range of 260 to 330°C, phenol, benzoic acid, and vanillin were the preferred reaction products beside carboxylic acids.

Although these products were formed with higher selectivity, the respective yields were in the range of one percent on a carbon basis, only. Future work could be dedicated to the optimisation of reaction conditions in order to increase the overall yield of these aromatic substances.

Despite the fact that it was not possible to base a thorough description of the reaction kinetics on the experiments with lignin, the experimental results still offer valuable information with respect to the degradation behaviour of real lignocellulosic waste.

5 CONVERSION OF REAL BIOMASS

Based on the findings of the model compound studies with pure cellulose and lignin, real lignocellulosic wastes were treated in water at elevated temperatures and pressures. Wheat straw was subjected to hydrothermal conversion, since it has a rather well-known composition and can serve as an example for high-lignin content crop-derived biomass. Investigations on the conversion of crop plants are of special interest and increasing importance, as the sustainable utilisation of whole plants would open new potentials for the use of lignocellulose as a feedstock for valuable chemicals. One thinkable process is the hydrolysis of lignocellulosic materials in high-temperature water to yield saccharides, which can subsequently be converted to ethanol by fermentation.

Wheat straw was treated by hydrolysis to gain information on the degradation kinetics and product formation. In addition, supplementary techniques, e.g. the acidification by carbon dioxide and the introduction of an oxidant, were applied. The addition of carbon dioxide was believed to result in a rate enhancement of the degradation of the cellulose fraction, as could be observed in the hydrolysis of pure cellulose. On the basis of the experiments with lignin, it was known that lignin is remarkably resistant to thermo-chemical treatment and cannot be completely converted by hydrolysis. Wheat straw was therefore subjected to both non-oxidative and oxidative conditions in order to accomplish a complete removal of any insoluble matter.

Beside the investigations on wheat straw, solid biomass with complex composition was studied in this work. The biomass specified by ESA represents a model waste containing inedible parts of higher plants, e.g. wheat straw, cabbage, soya, as well as algae and faecal material, which contains similar material as kitchen waste and is representative of typical human organic waste in a space environment. Due to the presence of nitrogen-bearing compounds, particularly in cabbage and algae, the evaluation of degradation studies was not restricted to the transformation of carbon but also included the calculation of nitrogen balances (see section 5.2.1)

Beyond the kinetic description and the characterization of degradation products, the biodegradability of the effluents is a prerequisite for implementing the hydrothermal process in a biological loop system. Hence, effluents of the hydrothermal treatment of biomass were applied to biological degradation. For this purpose, indigestible residues of a mesophilic methane reactor of Partner 1 were transformed at near-critical conditions and subjected to a series of fermentation tests. The aim of these closed loop experiments was to exclude any detrimental effects of the degradation products on micro-organisms, which might be due to inhibitory or toxic properties, and to determine the overall efficiency of the combined process.

5.1 Hydrothermal degradation of wheat straw

Due to its significant amount of lignin and its lignocellulosic structure, wheat straw was the probably most persistent ingredient of the model waste specified by ESA. Wheat straw was therefore employed as a real waste in the investigation of the addition liquefaction technologies. Experiments were carried out over a wide temperature range from subcritical to supercritical conditions with and without adding carbon dioxide as a catalyst. Also, experiments on the oxidative destruction of wheat straw in near-critical water were performed.

Experiments were carried out in fully-continuous mode, typically with an initial solid concentration of about one percent by weight. Additionally, some experiments were conducted in fixed bed mode in order to increase the reaction time of water-insoluble solids by retaining them in the high temperature zone of the apparatus.

5.1.1 DEGRADATION BY HYDROLYSIS IN WATER AND WATER-CO_2

Experiments in water/carbon dioxide mixtures were conducted in the subcritical, near-critical and supercritical region of water. In contrast to the cellulose conversion experiments, a beneficial effect of the addition of carbon dioxide could not be detected. The results of these experiments are shown in Figure 5.1 together with the data for pure water as the reaction medium.

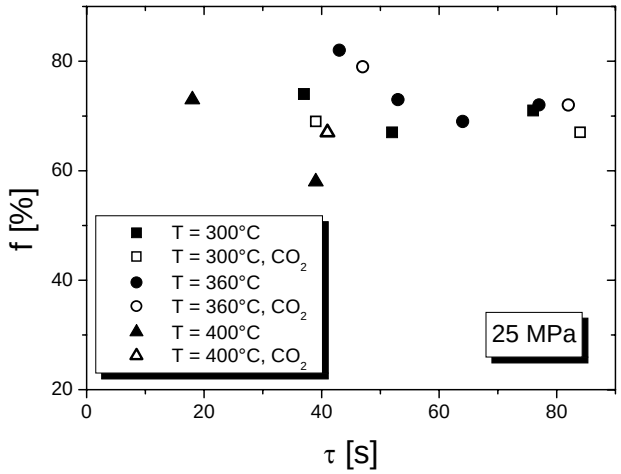

Figure 5.1: Conversion of wheat straw to water-soluble carbon in water, water/carbon dioxide, f: DOC_{out}/C_{in}, CO_2-concentration with respect to saturation: ~ 70 %, initial solid concentration: 1 wt-%

The degree of liquefaction f was calculated as the ratio of dissolved carbon in the effluent to the total influent carbon assuming negligible gas production. A difference in the degree of liquefaction on a carbon basis could not be determined within the range of experimental uncertainties, meaning that a residual portion of the wheat straw was not as susceptible to changes in pH as cellulose at the conditions applied.
The hydrolytic treatment of wheat straw in the absence of an oxidant did not return solid-free effluents. The results of the experiments with wheat straw did neither reveal a distinct temperature dependence nor a clear influence of reaction time at these conditions. The results in terms of the degree of liquefaction are depicted in Figure 5.2.

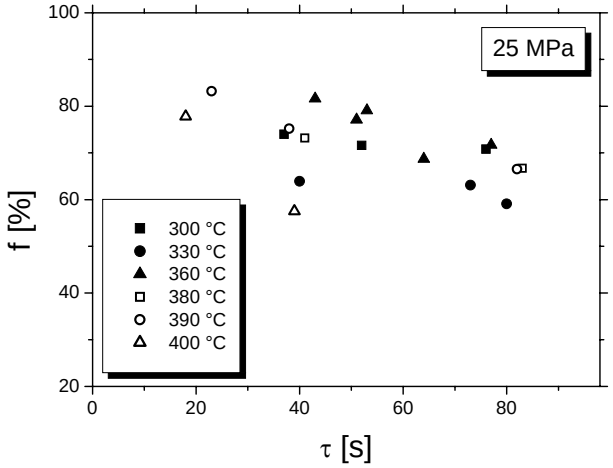

Figure 5.2: Conversion of wheat straw to water-soluble carbon, f: DOC_{out}/C_{in}, initial solid concentration: 1 wt-%

In average a portion of about 20-30 % of the influent carbon could not be converted to water-soluble carbon, independently of temperature. This fraction is in the order of the lignin content of wheat straw, which amounts to roughly 20 % of the total carbon. Furthermore it appears that the degree of conversion in average slightly decreases with increasing reaction time. One possible explanation for this observation may be the evolution of carbon-bearing gas species. Another reason might be the renewed formation of carbon-rich, insoluble material due to the repolymerisation of reactive radicals at higher temperatures and residence times.

In order to evaluate the contribution of gaseous products to the carbon balance, gas phase measurements were conducted with respect to composition and volumetric flow rate. In addition, the total influent carbon was compared to the carbon load of the reactor effluents. The ratio of carbon in the effluents to the influent carbon is depicted in Figure 5.3.

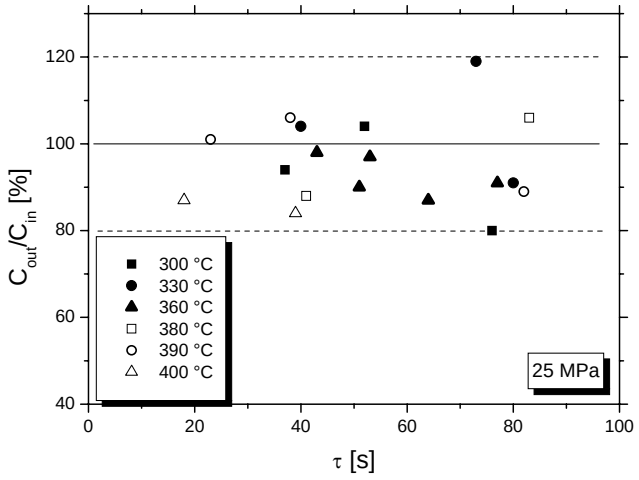

Figure 5.3: Carbon balance of experiments on wheat straw, C_{out}: measured carbon of soluble and insoluble reaction products, C_{in}: calculated carbon content according to elementary analysis

As can be seen, the values fluctuate rather than showing a clear temperature or time dependence. In average, the carbon content in the effluents seems to be slightly lower than the influent carbon. These values are, however, subject to uncertainties due to experimental and analytical inaccuracies, e.g. incomplete mixing, solids deposition, as well as errors in the determination of the carbon content. It can be concluded that the formation of product gases has a minor contribution in the hydrolysis of wheat straw at the conditions applied. This finding was confirmed by gas phase measurements for selected experiments in the near-critical region. Based on these measurements, less than one percent of the carbon was transformed to carbon dioxide. Accordingly, a portion of 20 to 30 % of the influent carbon was still present as insoluble carbon in the effluents.

In addition to the fully-continuous experiments a number of runs were conducted in fixed bed mode. For these experiments it was initially intended to calculate the degree of conversion by determining the weight loss of the solids trapped in the fixed bed. The results, however,

showed that this approach was not feasible due the fact that essentially all solid particulates dissolved in water at operating conditions. The effluents were therefore collected in different fractions and analysed for the concentration of dissolved organic carbon.

The results revealed that the main part of the carbon was collected in the first fraction during the heating up of the fixed bed to the desired holding temperature, while in the second, constant temperature phase only a very minor carbon concentration could be detected. Presumably, the carbon was successively converted to water-soluble substances during the heating up phase and instantaneously cooled down in the heat exchanger. In these experiments a degree of liquefaction of close to 100 % could be obtained at temperatures from 370 to 380°C. These results support the assumption that the degree of liquefaction decreases with progressive reaction time at higher temperatures and that the conditions applied in the continuous experiments were not optimal with respect to liquefaction. A possible explanation for this behaviour is the recondensation of reactive fragments to form insoluble products, as it was reported in the degradation of lignin [49, 50].

5.1.2 OXIDATIVE TREATMENT

Following the experimental study on lignin conversion under oxidative conditions, wheat straw was subjected to hydrothermal treatment in sub- and near-critical water. This study was aimed at answering the question, whether the results of the model compound studies can be transferred to a real, insoluble bio-waste. In accordance with the lignin study, wheat straw was treated both by partial oxidation, providing half the stoichiometric demand, as well as by total oxidation, supplying twice the stoichiometric amount of hydrogen peroxide. In addition, experiments under hydrolytic conditions, without adding any oxidant, were conducted to compare both processes in terms of residual carbon content and main degradation products.

The stoichiometric amount of hydrogen peroxide was calculated on the basis of the structural formula and the elementary composition of wheat straw. The effluents were characterized in terms of the ratio of dissolved carbon to the total influent carbon and the contribution of carboxylic acids to the solubles. The effluent DOC was measured directly, while the influent carbon was calculated on the basis of the elementary analysis of the input material.

The results of the wheat straw experiments in terms of the residual dissolved carbon content are depicted in Figure 5.4.

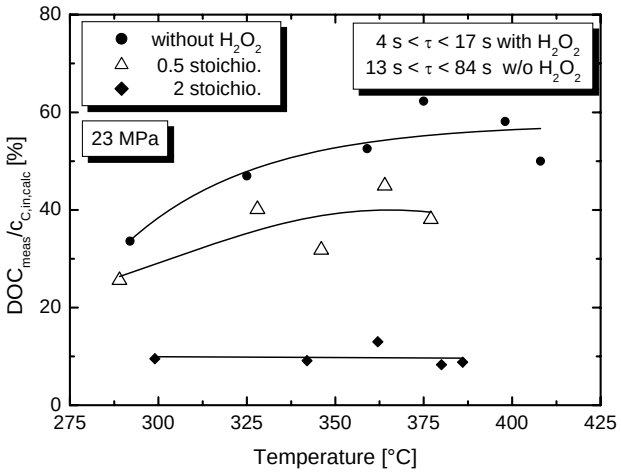

Figure 5.4: Conversion of wheat straw to water-soluble substances, influence of amount of oxidant and temperature, initial solid concentration: 1 wt-%

It can be inferred that the degree of liquefaction under non-oxidative conditions increases with temperature up to 60 % in the near-critical region. These results are in line with the experiments on the non-oxidative destruction of wheat straw discussed before, which yielded a maximum degree of liquefaction of about 70-80 % under optimised conditions. The effluents of all of the non-oxidative runs still contained solids. A marked gas evolution could not be observed. Thus, it can be concluded that about 40 % of the influent carbon was still present as insoluble carbon after non-oxidative treatment.

In contrast, the oxidative destruction of wheat straw returned essentially solid-free effluents. Except of the run with half the stoichiometric amount of hydrogen peroxide at a temperature below 300°C, all effluents were solid-free. In case of the partial oxidation, about 35-40 % of the total influent carbon were liquefied, meaning that the remaining portion was converted to gaseous species.

Supplying twice the stoichiometric demand results in a residual dissolved carbon content of about 10 %, essentially independent of the temperature applied. As in case of pure lignin, about 90 % of the influent carbon were transformed into gaseous substances within residence times of less than 20 s.

The effluents of wheat straw degradation were analysed with respect to the content of carboxylic acids, saccharides, and aromatic reaction products.

The results of the acetic acid analyses are shown in Figure 5.5.

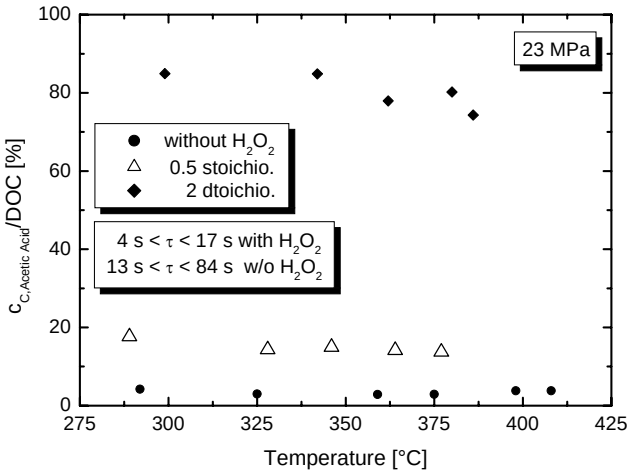

Figure 5.5: Wheat straw conversion, portion of carbon bound as acetic acid to total organic carbon, initial solid concentration: 1 wt-%

Acetic acid had a very minor contribution to the dissolved organic carbon at non-oxidative conditions, roughly amounting to 5 % of the total dissolved carbon. In contrast, supplying half the stoichiometric amount led to an increase in acetic acid concentration to 15-20 %. This portion seems to be independent of temperature over a wide range from well-subcritical to near-critical conditions. Increasing the amount of oxidant to twice the stoichiometric demand led to the selective formation of acetic acid, which is produced with a selectivity of about 80 %.

In accordance with the studies on pure lignin, acetic acid is a relatively stable intermediate in the total oxidation of wheat straw. In order to completely eliminate any residual DOC in the effluents, the operating range would have to be adjusted to higher temperatures and residence times. However, the complete conversion to gaseous products was beyond the scope of this work. The selective formation of acetic acid by providing excess oxidant is an attractive alternative to complete gasification as acetic acid can be readily degraded by micro-organisms.

Saccharides could not be detected with the exception of low glucose concentrations in some of the experiments. Based on the results of the cellulose studies, saccharides were presumably decomposed by secondary reactions at the temperatures and reaction times applied in wheat straw conversion.

Selected samples of both hydrolytic and oxidative conditions were analysed by GC-MS for the identification of further degradation products. As in case of lignin oxidation, mainly phenolic substances, benzoic acid, benzaldehyde and derivatives thereof, as well as ketones could be identified.

The results of wheat straw conversion resemble the findings of the model compound studies with lignin in many aspects. With respect to a complete conversion to soluble products, the hydrolytic treatment is not capable of achieving a degree of liquefaction higher than 80 %. The degree of liquefaction shows the tendency to decrease with increasing temperature and prolonged reaction times. The addition of carbon dioxide did not show any beneficial influence on the reaction kinetics in the temperature range studied.

In order to completely remove any insoluble matter, oxidation techniques need to be applied. Supplying twice the stoichiometric demand of oxidant leads to a nearly complete removal of any organic carbon, leaving a residual carbon content of only about 10 % in the liquid phase. This residual carbon can mainly be attributed to acetic acid, which is formed with a high selectivity and contributes to 80-90 % of the carbon. Supplying half the stoichiometric amount of oxidant also yields a complete conversion of insoluble material at near-critical temperatures and residence times of less than 20 s.

These results prove the feasibility of a complete conversion of insoluble lignocellulosic wastes by treatment in sub- and supercritical water to form water-soluble and gaseous degradation products.

5.2 Degradation of complex biomass samples

The feasibility of a complete conversion of lignocellulosic biomass at high-space time yields was shown by the studies on cellulose, lignin, and wheat straw. By the degradation of complex biomass samples additional aspects were addressed. One important question regarding the overall concept of the combined process of thermo-chemical and biological degradation is the determination of the optimum sequence of treatment steps. The hydrothermal conversion of biomass can both serve as a pre-treatment, to rapidly degrade all waste components and to produce biodegradable hydrolyzates, and as an after-treatment following biological conversion, to destroy the most recalcitrant, indigestible waste components, only.

Both approaches were investigated in this work. The former concept, the hydrothermal degradation of all waste components as a pre-treatment to subsequent biological conversion, was studied with the waste specified by ESA. This investigation was also intended to provide information on the conversion of nitrogen-bearing compounds in sub- and supercritical water.

The latter concept, the implementation of the hot-water treatment following biological digestion, was investigated by means of closed-loop experiments. For this purpose, the substrate specified by ESA was first degraded in a mesophilic methane reactor of Partner 1 at Ghent University. Indigestible solid residues were withdrawn from the reactor and sent to Hamburg for hydrothermal treatment and characterization of effluents. The hydrolyzates of these experiments were subsequently subjected to fermentation again in order to study the

biodegradability and to determine the overall efficiency of the concept. Additionally, solid residues of Partner 2 were degraded.

The biological innocuousness of the hydrothermal effluents was investigated by standard sterility tests. Furthermore, some preliminary studies on the hydrolysis of proteins in water at elevated temperatures and pressures were conducted. The destruction of the primary amino acid sequence and the associated occurrence of free amino acids in the effluents indicate the loss of activity of biological contaminants and provide information on the contribution of amino acids to the dissolved nitrogen.

5.2.1 DEGRADATION OF MODEL WASTE SPECIFIED BY ESA

The model waste specified by ESA was processed continuously at an initial solid concentration of one weight percent on a dry matter basis, since higher solid concentrations complicated the pumping of the suspension. Because of its composition and its lower content of lignocellulosic material, the waste was treated by hydrolysis in pure water, only.

The results of the liquefaction experiments in terms of the carbon balance are summarized in Table 5.1.

Table 5.1: Experimental results on model waste specified by ESA, computation of carbon balance, P = 25 MPa, initial solid concentration: 1 wt-%

Run No	T [°C]	τ [s]	C_{in} [mg/l]	$C_{out,l}$ [mg/l]	$C_{out,sol}$ [mg/l]	$C_{out,sol}/C_{out,l}$ [%]	$C_{out,g}/C_{in}$ [%]	$(C_{out,l}+C_{out,g})/C_{in}$ [%]
ESA 1	300	23	3918	3925	2184	55.64	n.d.	100
ESA 2	307	23.6	3925	3507	2552	72.77	0.8	n.d.
ESA 3	344	25.9	3800	3724	2652	71.21	2.5	101
ESA 4	350	28.7	3722	3674	2945	80.16	2.1	101
ESA 5	352	28.4	3761	3746	3089	82.46	2.0	102
ESA 6	360	27.9	3918	-	3321	87.11	2.7	n.d.
ESA 7	340	50.9	-	3603	3419	94.89	n.d.	n.d.
ESA 8	340	25.9	n.d.	3762	2824	75.10	2.6	n.d.

Except for the last run, the faecal material was omitted and the other substrate ingredients were adjusted according to their ratios as specified by ESA. The effluent of run ESA 1 was reintroduced into the reactor (run ESA 2) in order to extend the residence time within the

reactor. The same approach was applied to the effluent of run ESA 6, which was used as new feed for run ESA 7.

The experimental temperature and the residence time calculated on the basis of the reactor outlet temperature are stated. The values reported in column 4 are calculated influent carbon concentrations based on the molecular composition analysis. Columns 5 and 6 report the measured total carbon concentration in the liquid effluent and the respective values of the dissolved carbon content. The ratio of these concentrations serves as a measure to evaluate the degree of liquefaction based on the carbon balance.

Since the experiments were conducted in a relatively narrow pressure range, the influence of the experimental temperature and the mean residence time on the conversion to soluble carbon components can be studied. A comparison of the first two runs yields an increase of the degree of liquefaction from 56 % to 73 % by increasing the residence time from 23 s to 46 s at a reaction temperature of 300°C. The degree of liquefaction shows an increase with increasing experimental temperature at comparable residence times, as can be inferred from the results of run ESA 3 – ESA 6, giving a degree of liquefaction of about 87 % at a temperature of 360°C and a residence time of 28 s. Even higher conversions can be achieved by further extending the reaction time. This can be concluded from the results of run ESA 7, which yields a degree of liquefaction of about 95 % by treating the effluents of run ESA 6 for another 51 s at a temperature of 340°C. The last experiment was done in the presence of faecal material. Compared to run ESA 3, which was conducted at nearly identical conditions, the degree of liquefaction is slightly higher than in case of the absence of faecal material, which points to the fact that faecal material is more readily decomposed.

The values stated in column 8 report the amount of carbon detected in the gas phase with respect to the calculated influent carbon. As can be inferred from the results of these measurements, the amount of carbon in the gas phase only has a minor contribution, being in the range of 2-3 % of the total carbon introduced into the system.

A comparison of the total effluent carbon, expressed as the sum of the total carbon of the liquid effluent and the gas phase carbon, with the calculated influent carbon is given in the table. The results of this calculation reveal a very good agreement of calculated influent and measured effluent carbon. The matching carbon balance shows that the experimental determinations are very reliable with respect to their accuracy.

The ratio of the chemical oxygen demand of the soluble effluent to the total effluent was also determined. Comparing these results with the respective carbon ratios, it can be concluded that the ratio of the oxygen demand is lower than the carbon ratio for all experiments. This can possibly be explained by the presence of highly oxidised compounds, which are soluble in the aqueous phase.

Comparing these results with those from the studies on lignin and wheat straw, it can be seen that the hydrolysis of the model waste yields much higher degrees of liquefaction than in case

of lignin and wheat straw, which can be attributed to the much lower content of lignocellulose in the model waste. Some ingredients, e.g. algae, do not have any lignocellulosic structures at all. This again shows that lignocellulose is the most persistent fraction of biomass.

In order to calculate the nitrogen mass balance for these experiments, the total nitrogen content of the influents and effluents was measured by means of a TOC, TN analyser. In addition, the ammonia nitrogen concentrations were determined using Dr. Lange N-NH_4 cuvette tests. The results of these analyses are summarized in Table 5.2.

Table 5.2: Experimental results on model waste specified by ESA, computation of nitrogen balance

Run No	$N_{in,calc}$ [mg/l]	$N_{in,meas}$ [mg/l]	$N_{in,sol}$ [mg/l]	N_{out} [mg/l]	$N_{out,sol}$ [mg/l]	N-$NH_{4,out}$ [mg/l]	N-$NH_{4,out,sol}$ [mg/l]	N_{out} /$N_{in,meas}$	$N_{out,sol}$ /$N_{in,calc}$	(N-NH_4 /N)$_{out,sol}$
ESA1	307	405	82	426	283	42.5	40.3	1.05	0.87	0.14
ESA2	n.d.	n.d.	n.d.	457	313	48.0	46.5	n.d.	n.d.	0.15
ESA3	298	405	82	437	323	61.1	59.5	1.08	1.03	0.18
ESA4	292	344	129	392	268	53.6	52	1.14	0.87	0.19
ESA5	295	362	79	401	289	57.4	56.9	1.11	0.93	0.20
ESA6	307	n.d.	130	n.d.	341	86.1	84.0	n.d.	1.06	0.25
ESA7	n.d.	n.d.	n.d.	n.d.	323	81.6	82.5	n.d.	n.d.	0.26
ESA8	376	n.d.	n.d.	475	401	76.5	72.0	n.d.	1.02	0.18

The conditions of the experimental runs correspond to those stated in Table 5.1. The calculation of the influent nitrogen concentrations is based on the analysis of the molecular composition of the substrate components. The values of the measured total and soluble nitrogen concentrations of feed and effluent and the respective ammonia nitrogen concentrations of the effluent are reported.

A comparison of the calculated influent nitrogen concentrations with the measured values reveals a discrepancy of 15-25 %. This is partly due to the fact that the dissolved nitrogen was not considered in this calculation. For low partial pressures the solubility of gases in water can be expressed by Henry's law:

$$x_{N_2} = p_{N_2} \cdot H_{N_2,l}$$

where x is the fraction of the gas in water, p is the partial pressure of the gaseous component and H is the Henry coefficient. For the system N_2-H_2O at atmospheric pressure and a temperature of 298 K, the Henry coefficient is 0.00065 mol_{N2}/(kg bar) [51] yielding a concentration of about 15 mg N_2 per litre of water. When this portion is taken into account by adding the amount of dissolved nitrogen, the deviation decreases to values of 11-23 %. This discrepancy is probably due to inaccuracies in the determination of the total nitrogen content of

the influent. However, nitrite and nitrate were not looked for in these studies but might also contribute to the nitrogen balance.

The nitrogen balance expressed in terms of total effluent to influent nitrogen shows a slight mismatch, which is in the range of 5-15 %. Since the total nitrogen concentration does not decrease but increase, this deviation can only be explained by analytical inaccuracies. Because of the fact that the measured values for total nitrogen seem less reliable than the calculated ones, the degree of liquefaction with respect to nitrogen is computed based on the theoretical values derived from the molecular composition analysis. These values are reported as the ratio of the soluble nitrogen to the calculated total influent nitrogen. With the values of the soluble nitrogen corrected for the gaseous nitrogen dissolved in the liquid phase, it can be concluded that those compounds of the feed which contain nitrogen are readily liquefied. This can be inferred from the fact, that the degree of liquefaction based on the nitrogen balance is higher than the respective values calculated from the carbon balance for all experiments. This is probably due to the fact that the most difficult to degrade substances, e.g. lignocellulosic materials, contain little nitrogen. As a conclusion, the nitrogen-bearing compounds, e.g. polypeptides, seem to be more susceptible to hydrolytic attack than lignocellulose at the conditions applied. The measurement of ammonia nitrogen shows that nitrogen in the ammonia form amounts to about 15-25 % of the total nitrogen present in the liquid phase, which leaves about 80 % of the liquefied nitrogen in form of unidentified reaction products. For closing the nitrogen balance, separate studies on the conversion of polypeptides were conducted in order to assess the contribution of free amino acids to the portion of unknown nitrogen.

As a result, the model waste specified by ESA can be readily converted by hydrothermolysis without the addition of a catalyst or an oxidant. Degrees of liquefaction up to 90-95 % could be obtained on a carbon basis. Carbon in form of gas species had a minor contribution and amounted to less than three percent. Regarding the nitrogen balance, even higher degrees of liquefaction up to 100 % could be achieved. Both the carbon and the nitrogen balance could be closed satisfactorily. Based on these findings, the conclusion is drawn that the hydrothermal conversion of complex biomass is a suitable process for the production of soluble hydrolyzates, which can be utilised by subsequent biological treatment.

5.2.2 CLOSED LOOP EXPERIMENTS

The concept of implementing the hydrothermal process in a biological system was also investigated by means of closed-loop experiments. For this purpose, the substrate specified by ESA was first degraded in a mesophilic methane reactor of Partner 1 at Ghent University in order to remove the main part of the carbon. By means of this mesophilic digestion, about 70-80 % of the initial carbon load could be converted to biogas. Indigestible solid residues were withdrawn from the reactor and sent to Hamburg for hydrothermal treatment. The hydrolyzates

were subjected to fermentation again in order to study the biodegradability and to determine the overall efficiency of the concept.

Loop 1:

In the first set of closed loop experiments, the indigestible residues were treated at hydrolytic conditions to generate hydrolyzates with increased solubility and biodegradability. The results of the liquefaction experiments in terms of the carbon balance are summarised in Table 5.3.

Table 5.3: Hydrothermal treatment of indigestible residues from a methanogenic bioreactor, P = 25 MPa, initial solid concentration: 0.5 wt-%

No	T [°C]	τ [s]	$C_{sol.out}/C_{in}$ [%]
LI 1	360	25.1	73.9
LI 2	366	39.7	56.4
LI 3	360	38.8	57.1
LI 4	301	87.2	44.8
LI 5	319	45.2	58.7
LI 6	406	> 35	57.2

All experiments were conducted with initial solid concentrations of about 0.5 weight percent on a dry matter basis. The experimental temperature and the residence time calculated on the average of inlet and outlet temperature are stated. The values reported in column 4 are the ratios of dissolved effluent carbon to total influent carbon. The dissolved carbon was measured by means of a TOC-analyser. The total influent carbon was calculated on the basis of the influent solid concentration and the carbon content of the solid material, which was determined by composition analysis with a CNS-analyser. The ratio of dissolved carbon to total influent carbon serves as a measure to evaluate the degree of liquefaction based on the carbon balance.

The experiments were conducted in a very narrow pressure range, such that the influence of the experimental temperature and the residence time on the conversion to soluble carbon components could be studied. Comparing run LI 1 and LI 2, the degrees of conversion were surprisingly inconsistent, since run LI 1 yielded a comparatively high conversion though temperature and residence time were lower than for run LI 2. This may only be explained by the fact that for run LI 1 the solid material was taken from a different batch of reactor residues from Ghent University, while all other runs were conducted with residues from the same batch. Based on the experimental runs it seems that the first batch of residues was containing more readily degradable components than the second one.

Run LI 2 and LI 3 were conducted at nearly identical experimental conditions in order to check the reproducibility of the experiments. Comparing the degrees of liquefaction it can be concluded that the results differ less than 1 % with respect to the conversion and therefore are in very good agreement. Run LI 4 was performed at a much lower temperature of 300°C and

yields a significantly lower degree of liquefaction of 45 %, though the residence time of 87 s was much longer than for the other runs.

For run LI 5 the conversion to soluble components was essentially the same as for run LI 2 and LI 3, although the mean temperature was much lower. This may be explained by the fact that for this particular experiment the temperature at the reactor inlet and outlet exhibited a relatively large deviation, meaning that the outlet temperature was in the same range as for run LI 2 and LI 3. This finding points to the assumption that the solid residues contained a certain fraction which could not be liquefied by increasing the residence time within a narrow range at temperatures of about 360°C. Even an increase in temperature to 406°C, which is well above the critical temperature of pure water, did not result in a higher degree of liquefaction within the residence time employed in the experiments. As a conclusion, about 40 % of the carbon are very difficult to liquefy without a further increase in residence time.

The facts that the residues of the methane reactor were not biodegradable any further and that they could not be converted by hydrolysis in supercritical water pointed to the assumption, that the solid biomass contained a significant amount of lignocellulosic material. In order to reveal the contribution of fibrous material to the dry weight of the residues, a standardised method for the determination of cellulose, polyose, and lignin according to [52] was conducted. The analysis for the quantitative determination yielded a total fibre content of 54 % by weight with respect to the dry mass of the residues. Lignin amounted to 15 % of the dry weight of the residual biomass. Hence, the residues could not be completely liquefied by hydrothermolysis due the high content of lignocellulosic material.

In order to check the plausibility of the experiments, the effluent solid of run LI 6 was analysed with respect to its carbon content. By determining the solid concentration of the effluent and knowing the carbon content of the solid phase, the contribution of the solid carbon to the total effluent carbon could be calculated. Summing up the solid carbon and the dissolved carbon yielded about 91 % of the expected total carbon based on the substrate composition and the respective influent concentration. This slight mismatch might be partly explained by carbon converted into the gas-phase.

For the calculation of nitrogen mass balances, the total nitrogen content of the influents and effluents was measured by means of a TOC, TN analyser. In addition, the ammonia nitrogen and nitrate concentrations of the effluents were determined by photometric analysis. The results of these analyses and the ratio of COD in the liquid phase to the total effluent COD are summarized in Table 5.4.

Table 5.4: Hydrothermal treatment of indigestible residues from a methanogenic bioreactor, computation of nitrogen balance

No	$COD_{sol.out}$ /COD_{tot} [%]	$N_{sol.out}$ /N_{in} [%]	NH_4-N [mg/l]	NO_3-N [mg/l]	NH_4-N+NO_3-N /$N_{sol.out}$ [%]
LI 1	59.9	n.d.	n.d.	n.d.	n.d.
LI 2	56.7	97.1	38.5	21.1	56.7
LI 3	67.5	92.8	37.0	22.7	62.1
LI 4	67.6	75.7	44.5	25.6	57.0
LI 5	61.7	103.9	41.8	20.6	45.8
LI 6	66.4	110.0	87.5	46.3	55.3

The notation of the experimental runs corresponds to the measurements described before. The calculation of the influent nitrogen concentrations is based on the analysis of the molecular composition of the substrate. The values of the measured soluble nitrogen concentrations of the effluent and the respective ammonia nitrogen and nitrate concentrations of the effluent are reported.

It can be concluded that the degree of liquefaction based on the nitrogen balance is higher than the respective degree based on the carbon balance, which means that nitrogen is more readily converted into soluble components than carbon. Except for run LI 4, which was conducted at a significantly lower temperature, essentially all nitrogen initially present in the solid phase was converted to water-soluble components in the course of the reaction. This finding is in line with the results of the studies on the original model waste, for which a close to complete liquefaction of nitrogen could be achieved, too. Regarding the composition of the water soluble, nitrogen-bearing components, nitrogen in the ammonia and nitrate form amounts to about 60 % of the total nitrogen detected in the liquid phase. This means that there still is a significant amount of unknown species which contributes to the soluble nitrogen. For this reason, additional experiments with bovine serum albumin were conducted in order to clarify if nitrogen bound in polypeptides can be detected at the conditions employed in the experiments (see section 5.4.1).

Loop2:

Based on the results of the hydrolytic degradation of indigestible residues, it could be concluded that the addition of an oxidant was required to accomplish a complete removal of any insoluble matter. Therefore, experiments at oxidative conditions supplying twice the stoichiomentric demand of oxidant were conducted. Both effluents from Partner 1 and Partner 2 were treated in the frame of these additional closed loop experiments.

The effluents were characterized in terms of the ratio of dissolved carbon to the total influent carbon and the contribution of carboxylic acids to the solubles. The effluent DOC was measured directly, while the influent carbon was calculated on the basis of the elementary analysis of the input material. Larger quantities of the effluents in the litre range were distributed to Ghent University to feed the methane reactor and close the loop. The results of the closed loop experiments are depicted in Table 5.5.

Table 5.5: Closed loop experiments with solid residues of a methane reactor from Ghent University (run LII 1-4) and fibrobacter compartment (run LII 5-8) on a carbon basis: P = 25 MPa, amount of oxidant α is given with respect to the stoichiometric demand, initial solid concentration: 1 wt%

Run No	T [°C]	τ [s]	α [%]	$DOC_{out, meas}$ / $TC_{in, calc}$ [%]	C_{acids} / C_{diss} [%]
LII 1	398	8	200	7.2	112.7
LII 2	289	10	200	15.1	2.1
LII 3	372	50	0	35.4	3.4
LII 4	331	60	0	11.7	12.7
LII 5	413	8	200	9.3	84.2
LII 6	350	15	200	7.5	59.3
LII 7	385	29	0	39.5	12.9
LII 8	320	43	0	27.4	6.1

It can be inferred that the degree of liquefaction under non-oxidative conditions (run LII 3-4, LII 7-8) was markedly lower than in case of the first loop experiments, which resulted in conversions of about 60 %. A possible explanation for this finding might be changes in composition of the solid residues, which shows that the results of the degradation of complex biomass strongly depend on the actual composition and are not as reproducible as the experiments with model compounds.
The non-oxidative experiments yielded a degree of liquefaction of 35-40 % at near- and supercritical conditions, while the hydrolytic treatment at well-subcritical conditions led to conversions of 27 % and 12 %, respectively. Carboxylic acids amounted to less than 13 % of the dissolved carbon.

In contrast, the oxidative destruction resulted in only slightly coloured, initially solid-free effluents. After a short time at room temperature the formation of tiny cords and subsequent precipitation of small amounts of solid material could be observed, which might be due to secondary reactions of reactive products. The residual dissolved carbon content was in the range of 7-15 % for both materials under oxidative conditions.

A significant difference could be observed with respect to the amount of carboxylic acids under subcritical and supercritical conditions. At well-subcritical conditions (300°C) only a small portion of the dissolved carbon could be attributed to carboxylic acids, which was probably a result of larger quantities of partially oxidized compounds. A temperature increase led to an increase in selectivity of carboxylic acids, such that at near- and supercritical

conditions the majority of the dissolved carbon was present in form of acids (run LII 1. LII 5, LII 6).

These results evidence that supercritical water oxidation is a suitable technology for the efficient conversion of biologically non-degradable materials to water-soluble substances and gaseous species within very short residence times. Also, the operating conditions can be optimized to selectively produce readily-degradable end products such as acetic acid. Hence, the hydrothermal treatment of complex biomass containing lignocellulose can be used as a pre-treatment to convert all waste components as well as an after-treatment to degrade the most persistent constituents, only. The biodegradability of the hydrolyzates derived from the after-treatment is discussed in the following.

5.3 Biodegradability of hydrolyzates

One of the main objectives of this work was the conversion of real biomass to products which show an increased availability to biological degradation. This does not necessarily mean that all waste components need to be completely converted to water-soluble or gaseous species by hydrothermal treatment, but it is also desired to produce hydrolyzates which are accessible to further biological attack. Most studies dealing with hydrothermal degradation of biomass are focused on the reaction kinetics and mechanisms, whereas only a limited number of works is also dedicated to the subsequent biological treatment of the effluents [53, 54, [55].

Short-term fermentation tests:

The effluents of the hydrothermal reactor were fed to a methanogenic bioreactor at the Institute of Bioprocess and Biochemical Engineering (Prof. Dr.-Ing. H. Märkl) in order to investigate the biodegradability and to prove the non-toxicity of the hydrolyzates. Two short-term fermentation tests were done, the first one running for a period of 8 days and the second one for more than 2 weeks. In both cases the thermophilic biomass population, originating from a sewage treatment facility, was operated at a temperature of 50°C with sludge withdrawal, turbid water separation, and subsequent sludge recirculation. In these studies, effluents from the hydrolysis of the waste specified by ESA were delivered to the bioreactor.

Test 1:

The first fermentation was conducted in a 2 L reactor with an operating volume of about 1.3 L. In total, an effluent volume of 200 ml per day was fed at 4 rates of 50 ml each, yielding a residence time of about 6-7 days in the bioreactor. Figure 5.6 reports the biogas production in the course of the fermentation, with day 0 being the starting point of feeding the effluents from the thermal degradation. The effluents were taken from degradation experiments without the

addition of fecal material. Prior to the fermentation of the effluents the bioreactor was run with effluents from a delicatessen producer. This substrate was obtained from the production of salads and had a high mayonnaise content, thus bearing a high protein and fat load.

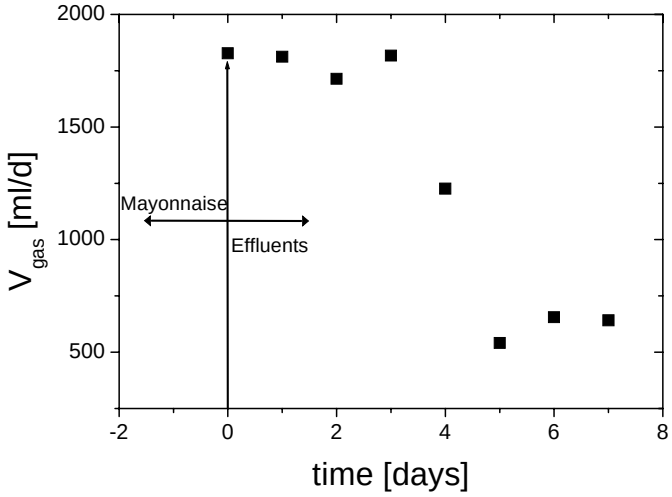

Figure 5.6: Fermentation test 1: Biogas production

It can be concluded that the change of substrate from the mayonnaise, having a higher carbon load, to the reactor effluents resulted in a decrease in biogas production after an adaptation period of several days. Afterwards the gas production stabilized at values of about 600 to 700 ml/d.

Biogas composition and pH values were determined during the fermentation by means of a photometer and a pH probe, respectively, and are shown in Figure 5.7.

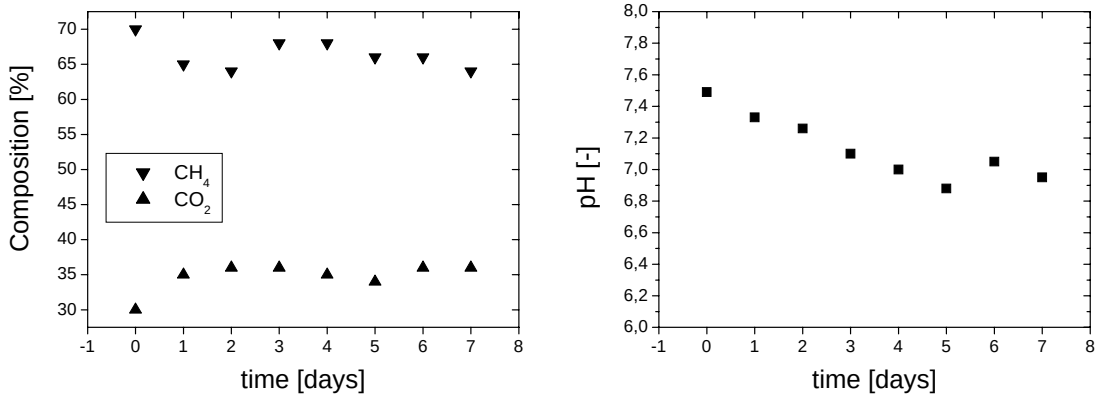

Figure 5.7: Fermentation test 1: Biogas composition (left) and pH values (right)

The results of these measurements show a stable biogas composition of approximately 65 % methane and 35 % carbon dioxide. The course of the pH over time exhibits a very slight decrease, which may point to an incomplete consumption of acids. The fluctuations of gas production and pH are, however, very minor.

Test 2:

A second fermentation test was conducted using effluents from a thermal degradation experiment which was run with a feed containing all substrate components. The aim of this experiment was to prove a stable operation of the methanogenic bioreactor for more than two weeks and to characterize the effluents in terms of TOC and COD in order to determine the biodegradability of the liquefied material.

The effluents were treated in a 1 L reactor with a feeding of 100 ml of reactor effluents per day. After a period of 10 days, corresponding to one mean residence time, the effluents were collected and analysed in terms of COD and TOC. The specific biogas production with respect to the reactor volume and the course of the pH value during the fermentation are depicted in Figure 5.8.

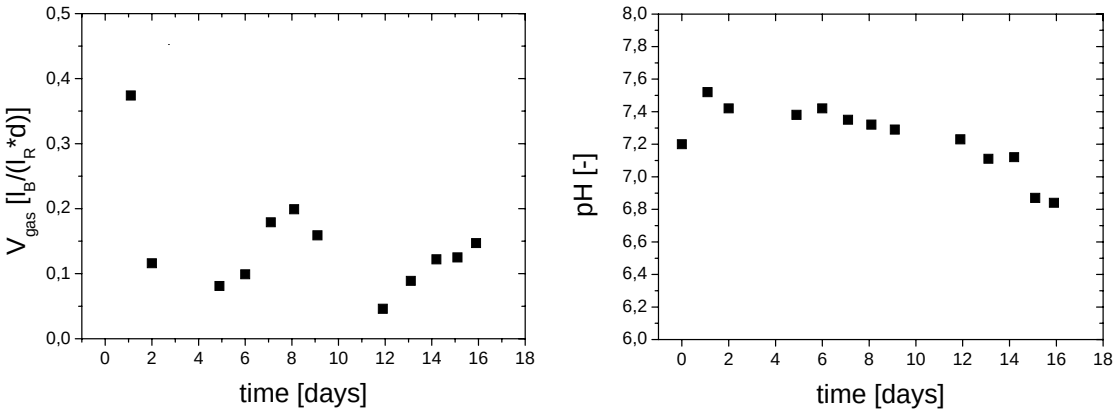

Figure 5.8: Fermentation test 2: Biogas production versus time (left), pH value (right)

The results reveal that the reactor effluents could be used as sole feed without the addition of any supplementary substrate. The biogas production fluctuates around a mean value of about 0.15 of litres of biogas per litre of reactor volume and day. The pH value shows, again, a slight decrease with increasing fermentation time.

The respective DOC and TOC values for the reactor influent and effluent are reported in Table 5.6.

Table 5.6: TOC and COD reduction in bioreactor after 10 days

	TOC [mg/l]	COD [mg/l]
Feed	3713	10760
Effluent (Filtrate)	529	1640

The major part of the influent load was consumed in the methanogenic bioreactor, which can be concluded from the reduction of the respective TOC and COD values. However, this short-term fermentation test could not reasonably be balanced, since the reactor was filled with sludge, having a higher carbon load, prior to the experiment and only about one reactor volume was exchanged before the first effluent sample was collected.

The results of these short-term fermentations prove that the effluents of the hydrothermal reactor did not show any directly toxic or inhibitory effects on the micro-organisms of the methanogenic reactor. The effluent components were readily converted and depicted a high availability to biological degradation. An exact evaluation of the bio-availability as compared to the original substrate was, however, not possible due to the limited duration of the tests which did not account for the adaptation time to the new feed.

5.4 Biosafety of effluents

The biosafety of the effluents of the liquefaction compartment plays an important role in the overall concept of MELISSA. The first compartment is not only responsible for a complete conversion of any insoluble waste produced by the crew, but it is also designed to produce effluents which are hygienic, free of biological contaminants, and harmless with respect to the chemical species formed in the course of degradation.

The former aspect, the biological innocuousness, was investigated by applying standard sterility tests to check if any organisms were still present after hydrothermal treatment. In addition, protein degradation experiments were conducted. These studies were aimed at the question whether polypeptides contained in the waste undergo chemical modifications or leave the reactor essentially unaltered. The degradation of proteins, indicated by the determination of free amino acids and partial hydrolyzates, points to a loss of activity and the destruction of pathogens.

5.4.1 PROTEIN DEGRADATION

At that point in time, only a very limited number of works on the degradation of amino acids and proteins by hydrothermal treatment was available [56], [57]. Hence, protein degradation experiments were conducted in order to determine the degree of hydrolysis of polypeptides at operating conditions. This study served the purpose of clarifying if organically bound nitrogen in form of amino-groups has a significant contribution to the still unidentified portion of soluble nitrogen. Furthermore, the destruction of polypeptides and the occurrence of free amino acids may be regarded as evidence that the reactor effluents are sterile.

Bovine serum albumin was employed in the experiments on the hydrolysis of polypeptides, since this protein exhibits a well-defined and known structure and has a limited solubility in water. The experimental conditions covered temperatures from 230°C up to 350°C at a constant pressure of 25 MPa and residence times from 40 s to 130 s. The effluents were analysed with respect to the concentration of free amino acids and the yield of selected amino acids was calculated on the basis of the albumin sequence. In addition, effluents of the hydrothermal treatment were subjected to a complete hydrolysis by hydrochloric acid in order to cleave the bonds of any partial hydrolyzates present in the effluent. By this means, the total amount of the respective amino acids in the effluent can be determined. It is further possible to estimate the portion of amino acids still bound in polypeptides compared to free amino acids. Besides, the amount of amino acids which was degraded due to secondary reactions can be calculated by this approach. Figure 5.9 shows a chromatogram obtained from one of the experimental runs.

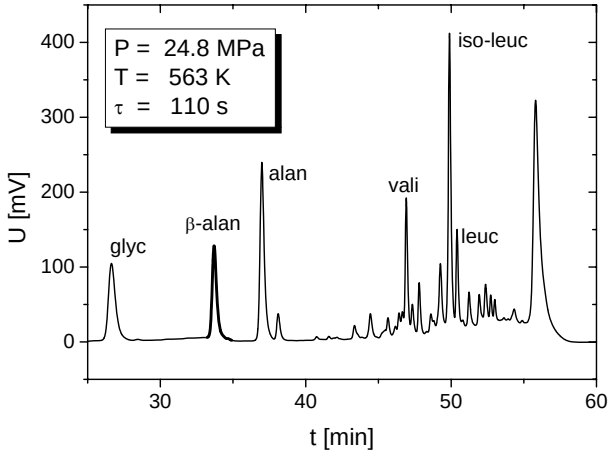

Figure 5.9: Chromatogram obtained from HPLC-analysis of reactor effluents

The chromatogram reports the existence of free amino acids at a temperature of 290°C and a residence time of 110 s. The peak indicated by the bold line is caused by β-alanine as the internal standard. Especially glycine, alanine, histidine, phenylalanine, valine, iso-leucine and

tyrosine could be detected in significant concentrations. Comparing the actual concentrations with the theoretically possible ones from the albumin sequence, the yield of these amino acids exceeded 10 %. The yield of iso-leucine was about 60 %, the yields of alanine and glycine were 40 % and 45 %, respectively. In contrast, at a temperature of 350°C and a residence time of 85 s no free amino acids except for iso-leucine and phenylalanine could be detected in significant amounts, which is probably due to the decomposition of free amino acids at increasingly high temperatures.

In order to further study the degree of albumin degradation, the reactor effluents were subjected to a complete hydrolysis with hydrochloric acid for 16 h at a temperature of 110°C. In this way the amount of the different amino acids in the hydrolyzates can be compared to the amounts in the influent, which are calculated from the albumin sequence. By subtracting the amounts of free amino acids in the effluents from the respective amounts in the hydrolyzates, the amount of the different amino acids bound in peptides can be determined and related to the original amount in the influent. The ratio of free amino acid in the effluents and the amino acid in the hydrolyzates with respect to the calculated influent amino acid content is depicted in Figure 5.10 for alanine and phenylalanine.

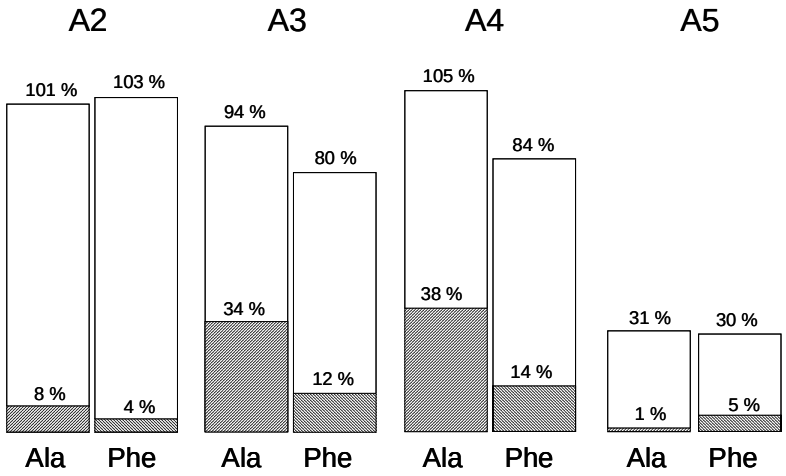

Figure 5.10: Total amount of amino acid in hydrolyzate and amount of free amino acid in effluent with respect to the influent amount for Alanine (Ala) und Phenylalanine (Phe). Initial albumin concentration: 0.5 wt-%: Conditions: P = 250 bar; A2: T = 250°C, τ = 129 s; A3: T = 290°C, τ = 65 s; A4: T = 290°C, τ = 111 s; A5: T = 350°C, τ = 85 s

The results show that the concentration of alanine in the hydrolyzate equals the calculated alanine concentration based on the albumin sequence up to 290°C, while for the experimental run at 350°C a significant decrease of the alanine concentration could be observed. This behaviour can probably be attributed to the fact that alanine is not thermally stable at such temperatures and decomposes due to secondary reactions. This assumption is further underlined by the results of the free amino acids in the effluents which increases up to 290°C with increasing residence time but drastically drops at 350°C. The same behaviour could be

observed in case of phenylalanine save that phenylalanine appears to be less stable than alanine and already shows a noticeable degradation at 290°C.

It can be inferred from the results that hydrolysis of peptide bonds occurs at the operating conditions and the residence times employed in the conversion of the model waste specified by ESA and the indigestible residues from the methane reactor of Partner 1. From this view, the protein content of micro-organisms present in the substrate definitely is not only altered with regard to the secondary and tertiary structure, but also with respect to the destruction of the primary structure, the amino acid sequence. This should be evidence that the effluents of the hydrothermal treatment can be considered as being sterile, thus ensuring an additional hygienic barrier in the system.

While the degradation of proteins proceeds with increasing temperature and residence time due to the hydrolysis of the peptide bonds, experiment A 5 shows that there still is a residual amount of about 30 % of amino acids bound in peptides at conditions which resemble those of the biomass degradation experiments. Therefore it may well be that soluble protein fragments have a contribution to the nitrogen detected in the liquid phase.

The yields of selected amino acids as function of temperature and residence time were further investigated by additional continuous experiments. Because of the increasing decomposition of free amino acids at higher temperatures, the experiments were conducted in a temperature range from 230 to 290°C and reaction times from 40 to 130 s. Beside the hydrolysis in pure water, the acidification by carbon dioxide was applied at concentrations of 50 to 100 % with respect to saturation. The yields of selected amino acids are shown in Figure 5.11.

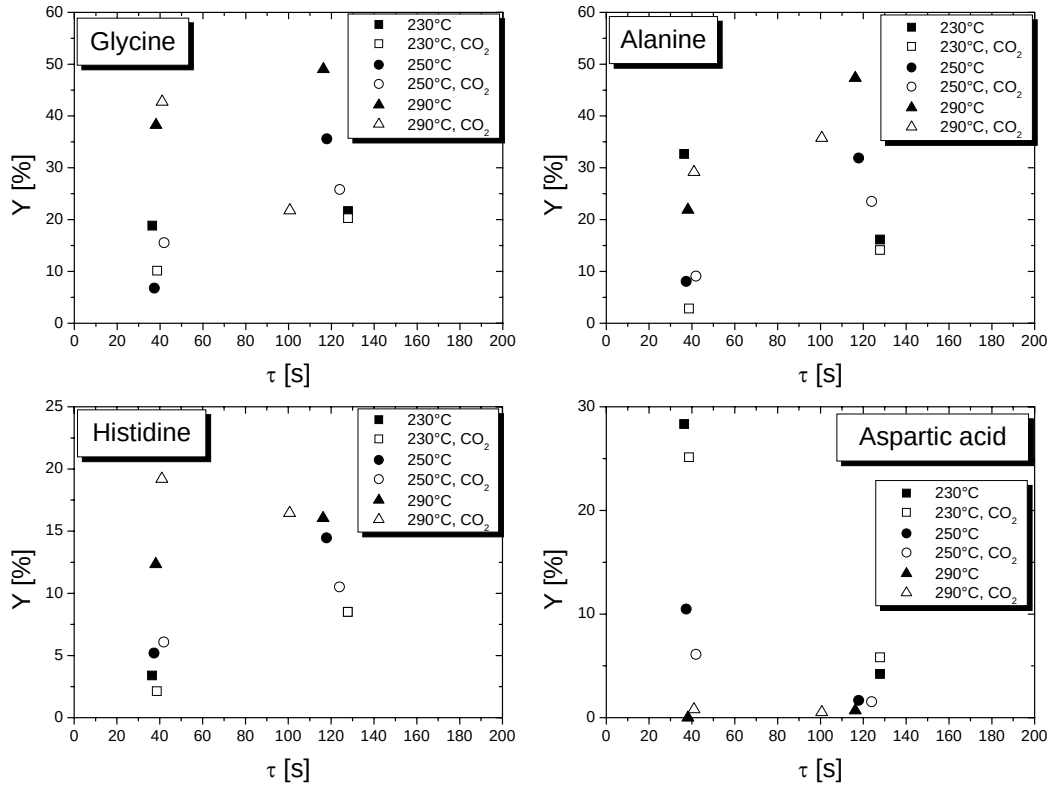

Figure 5.11: Continuous hydrolysis of bovine serum albumin, yields of selected amino acids were calculated as the ratio of free amino acid in effluent to theoretical concentration of respective acid according to albumin sequence, P: 25 MPa, initial albumin concentration: 0.5 wt-%

As can be seen, selected amino acids could already be detected at 230°C and a reaction time of 40 s, which in turn means that bovine serum albumin was substantially degraded at such conditions. Glycine and alanine were formed with high yields of up to 40 to 50 %, while histidine and aspartic acid were produced at a maximum yield of 20 to 30 %. A clear influence of acidification by carbon dioxide could not be found on the basis of the limited number of experiments.

Although the density of data points for these preliminary studies is not sufficiently high to derive detailed kinetics of the product formation, some general tendencies can be observed. At the conditions applied, the yields of glycine, alanine, and histidine increase with increasing temperature and residence time, while the yield of aspartic acid rapidly drops at higher temperatures and prolonged reaction times. Accordingly, the amino acids under consideration exhibit markedly different thermo-chemical stabilities. In case of aspartic acid, the rate of reaction of secondary decomposition appears to be much faster than the primary formation by hydrolysis of peptide bonds with increasing temperature. Hence, an optimisation of process conditions with respect to the formation of all amino acids is impossible. Because of the

opposite influence of temperature and reaction time on the yields of different amino acids, an optimisation would need to be restricted to a selected number or a class of amino acids.

Furthermore, it is not clear whether the differences in yields of selected amino acids can solely be explained by their thermal stability, e.g. the rate of decomposition due to secondary reactions. It may also be that the rate of formation varies from amino acid to amino acid, which would mean that the peptide bonds in the amino acid sequence exhibit different susceptibilities to hydrolytic attack. Such differences might be due to functional groups of neighbouring amino acids, having different electronegativity or size. A detailed kinetic description would therefore require investigations on the decomposition of free amino acids as well as a characterization of the partial hydrolyzates in terms of mean size and composition.

A further characterization of the protein hydrolyzates and investigations on the exact reaction mechanisms were, however, beyond the scope of this work. Nonetheless, amino acids and protein hydrolyzates find widespread applications in increasingly growing markets [58], [59], such that an optimisation of reaction conditions regarding the production of valuable free amino acids or protein hydrolyzates would be interesting from both a scientific and an economical point of view. On the other hand, the hydrothermal treatment could also be employed to degrade and remove proteins in cleaning applications, e.g. the removal of organic matter from bone material [60].

5.4.2 STERILITY OF EFFLUENTS

In addition to protein degradation experiments, the sterility of the effluents could be proven by applying standard sterility tests, which are based on the growth of micro-organisms and their detection on different nutrient agars.

By rinsing the effluents over the agar plates and subsequent incubation, colonies become visible in case the effluents were contaminated by micro-organisms. Two different tests were employed, one for the detection of yeasts and moulds (Envirocheck®Contact YM (R) and one for the total viable counts (Envirocheck®Contact TVC). Neither one showed any signs of colonies after incubation, which is further evidence that the high temperature treatment imposes an additional hygienic barrier on the system and ensures biosafety.

5.4.3 DESTRUCTION OF PCBS AND PAHS

The effluents of the hydrothermal treatment of biomass were shown to be absolutely biosafe. No biological contaminants like pathogens were present at the conditions applied, due to the

sterilizing effect of high-temperature water. However, not only biological contaminants might have a detrimental influence on micro-organisms or humans, but also reaction products formed during hydrothermal degradation. In this context, the question was addressed whether the conversion in sub- and supercritical water might possibly transform organic substances into reaction products which exhibit a toxicity higher than that of the input material.

Polychlorinated biphenyls (PCBs) and polycyclic aromatic hydrocarbons (PAHs) were selected for these studies. PCBs and PAHs are usually not present in lignocellulosic biomass in significant concentrations, but they are regarded as insusceptible to biological degradation and thus as biologically persistent. As a result of their biological inertness, they can accumulate in biological systems without showing immediately toxic effects on the organisms employed. Accordingly, it was investigated whether thermo-chemical treatment in sub- and supercritical water substantially alters these compounds, which could in principle lead to an increased toxicity of degradation products due to the decreased biological persistency. The discussion of conversion of PCBs in high-temperature water was limited to a literature survey because of governmental restrictions in handling this class of compounds. Experiments on the degradation behaviour of PAHs were performed with naphthalene, since it has the simplest structure of all PAHs and is therefore especially suitable for studying the product formation. The experimental conditions were similar to those of the experiments on lignocellulose in order to elucidate if PAHs undergo significant alterations at the conditions applied in the conversion of biomass.

Destruction of PCBs:

Based on early works in the 1980s [61], several research groups have studied the feasibility of destroying PCB-contaminated hazardous wastes in sub- and supercritical water. This research was aimed at the treatment of highly concentrated wastes, e.g. oils from capacitors or electrical transformers, where PCBs have been applied in large quantities in the past. The most important results are summarized below, emphasizing the degree of PCB-conversion and the characterization of decomposition products.

The destruction of PCBs under both oxidative and alkaline conditions was studied in [62]. In this investigation a PCB mixture containing mainly DiCB and HeptaCB as well as measurable amounts of MonoCB, OctaCB, NonaCB and DecaCB was used. Of this mixture about 100-1000 µg were loaded along with 11 ml of water into a microautoclave (44ml volume) made of Hastelloy C-276 for the oxidative treatment. For these studies the autoclave was filled with oxygen providing an overstoichiometric amount of oxidant. For the non-oxidative treatment, the autoclave was loaded with 11 ml of sodium hydroxide solution and flushed with argon. The results of both destruction processes in terms of the degree of conversion, stated as the destruction efficiency, are given in Figure 5.12.

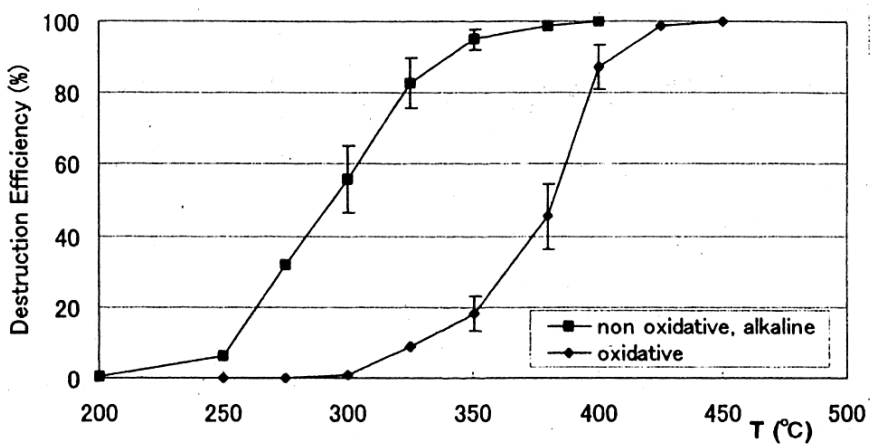

Figure 5.12: Destruction efficiency of PCB in subcritical and supercritical water under oxidative and alkaline conditions, 15 min [62]

The results reveal a remarkable thermo-chemical stability of the PCBs used in this study. In case of the oxidative treatment, temperatures in the near-critical region led to a PCB-destruction of about 50 % at a treatment time of 10 min. An essentially complete conversion could be observed at temperatures markedly exceeding 400°C. In contrast, the non-oxidative, alkaline treatment led to higher destruction efficiencies at given operating temperature.

In addition to the destruction efficiency, the authors studied the product formation, which was shown to be dependent on operating temperature and treatment time. The toxicity of the effluents was assessed in terms of toxic equivalency and compared to the influent PCB mixture. During the early stage of the reaction, the formation of polychlorinated dibenzofurans (PCDF) could be observed, while no polychlorinated dibenzodioxins (PCDD) could be detected. The temporary increase in PCDF concentration results in an increase in toxic equivalency of the reaction mixture as compared to the inlet PCB mixture. However, the treatment at prolonged reaction times and elevated temperatures results in the subsequent destruction of PCDFs, since this class of compounds is not stable but constitutes an intermediate product only. This finding is in line with the results from other research groups who could show the ability of supercritical water to destroy PCDFs and PCDDs.

In fact, an increase in reaction time from 15 to 60 min at 400°C led to a drastic decrease in toxic equivalency. At a temperature of 450°C, reaction times exceeding 15 min resulted in PCDF-concentrations below the detection limit. These results prove the ability to convert a biologically persistent class of substances to harmless end products by employing SCWO-technology, provided that the operating conditions are carefully selected when expecting any significant PCB-levels in the influent.
Based on the experimental results the authors propose a reaction mechanism and illustrate possible initial reaction pathways.

The destruction of a single-chlorinated biphenyl, namely 3-chlorobiphenyl, is reported in [63]. In this study the PCB was converted in a continuous flow reactor by adding hydrogen peroxide as the oxidant. It is stated that PCB-conversions higher than 99.9 % can be obtained at a temperature of 400°C and residence times exceeding 10 seconds in case an excess of oxidant is provided. The authors present a table of reaction products for an experiment in which half the stoichiometric demand of hydrogen peroxide was used. Again, various PCDFs could be detected in small amounts, but no PCDDs were found in the effluents.
The oxidative conversion of a tetra-chlorinated biphenyl in the presence of methanol was investigated in [64]. In this work an isothermal plug-flow reactor with achievable residence times of 3.11 seconds at 500°C and 25.6 seconds at 400°C was employed for the destruction of PCB in the presence of hydrogen peroxide as the oxidant. The authors come to the conclusion that adding methanol to the influents enhances the rate of PCB destruction, possibly by promoting the dechlorination step due to the formation of reactive intermediates originating from the methanol. Regarding the product formation, no PCDFs were detected in the presence of methanol as a co-solvent. Based on the experimentally derived data a rate equation for the destruction of PCBs along with possible reaction pathways is given.

In addition to the oxidative destruction of PCBs, the non-oxidative dechlorination of PCBs by means of supercritical water hydrolysis in the presence of sodium hydroxide as an alkali catalyst was also studied in [65]. The transformation of PCBs was conducted in a batch type reactor with an internal volume of 9 cm^3, which was loaded with 10 mg of PCBs and 1.3 g of water giving a reaction pressure of about 30 MPa at a temperature of 450°C. Two different PCBs were studied with respect to the dechlorination at varying amounts of sodium hydroxide and the decomposition at different hydrogen peroxide concentrations. The reaction time was set at 20 min at a constant temperature of 450°C for all experiments. The results of these studies are depicted in Figure 5.13.

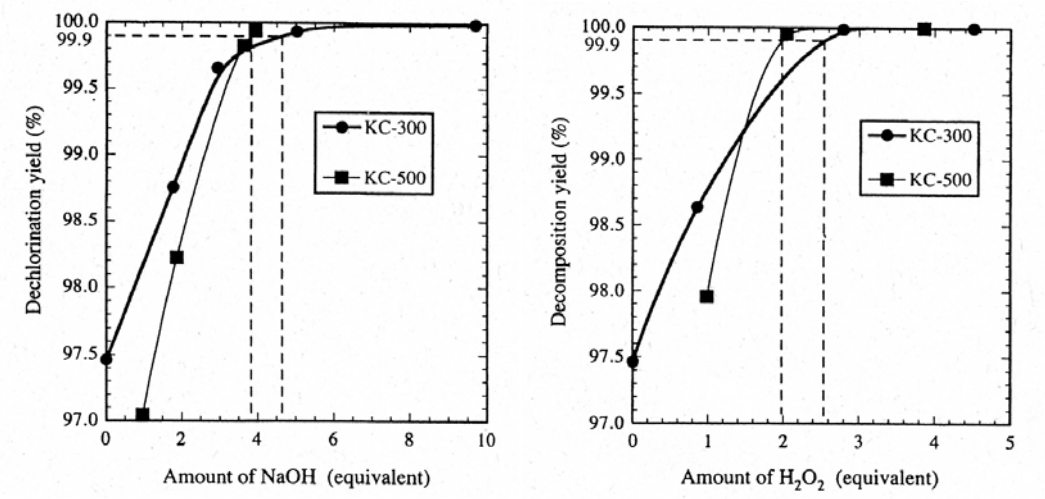

Figure 5.13: Dechlorination of pure PCBs with SC-water + NaOH, 723 K, 30 MPa, 20 min, PCB/water = 1 wt% (left); Decomposition of pure PCBs with SC-water + H_2O_2, 723 K, 30 MPa, 20 min, PCB/water = 1wt% (right) [65]

It can be inferred that adding sodium hydroxide increases the degree of dechlorination from 97.5 % to values higher than 99.9 %. Major decomposition products of the dechlorination were phenol, biphenyl, and hydroxybiphenyl. Although no oxidizing reagent was charged to the reactor, the total organic carbon content decreased to about half the initial value, which was probably due to the formation of gaseous species.

Regarding the oxidative destruction of biphenyls, an amount of 2-3 times the stoichiometric demand results in an essentially complete decomposition at the conditions applied.

Destruction of PAHs:

Experiments were performed on the hydrothermal decomposition of polycyclic aromatic hydrocarbons, since the use of PCBs is prohibited due to governmental restrictions. Naphthalene was employed in the model compound studies because it is classified as being irritating but non-toxic. In addition, it constitutes the simplest compound of all polycyclic aromatic hydrocarbons and is therefore especially suitable for studying the product formation in the course of the hydrothermal transformation.

Experiments were conducted systematically varying the operating temperature and the amount of hydrogen peroxide with respect to the stoichiometric demand. The results of these experimental runs applying an initial naphthalene concentration of 0.5 wt% and a pressure of 25 MPa are shown in Table 5.7.

Table 5.7: Naphthalene conversion to soluble products on a carbon basis: P = 25 MPa, the amount of H_2O_2 is given with respect to the stoichiometric demand, initial solid concentration: 0.5 wt-%

Run No	T [°C]	τ [s]	α [%]	$DOC_{out, meas}$ / $TC_{in, calc}$ [%]	C_{acids} / DOC_{out} [%]
N 1	375	65	0	8.8	2.3
N 2	263	79	0	3.9	5.2
N 3	384	7	200	1.9	28.3
N 4	375	11	200	2.9	72.6
N 5	292	12	200	4.2	54.2
N 6	380	8	200	5.7	51.8
N 7	302	10	200	14.8	37.0
N 8	384	7	50	60.5	1.9
N 9	375	8	50	23.9	5.1
N 10	384	6	50	31.9	6.3

For run N 1 and N 2 an additional reaction unit was coupled to the tubular reactor to extend the reaction time. These runs show that naphthalene is relatively stable under non-oxidative conditions. At well-subcritical conditions (263°C) only 4 % of the inlet carbon is converted to water-soluble substances, while in the near-critical region (375°C) about 9 % of the total

carbon is liquefied at residence times exceeding one minute. The effluents of these experiments exhibit a characteristic naphthalene odour and are similar in appearance to the influent suspension. These observations indicate that naphthalene is only degraded to a minor extent by hydrolytic attack.

In contrast, the oxidative treatment (run N 3 - N 10) substantially transforms naphthalene within reaction times of about 10 seconds. The effluents of these experiments were absolutely solid-free, showing that naphthalene was converted completely to water-soluble substances and gaseous species. Supplying twice the stoichiometric demand (run N 3 – N 7) results in a degree of liquefaction of less than 6 %, meaning that the remaining carbon was completely mineralised. Especially the experiments conducted at near- and supercritical conditions exhibit a very minor contribution of dissolved carbon, which amounts to less than 3 % of the total influent carbon. Highly oxidized carboxylic acids, mainly acetic acid, account for a significant portion of the dissolved carbon, ranging from about 30 % to more than 70 %.

Applying half the stoichiometric demand of hydrogen peroxide results in a partial oxidation of naphthalene (run N 8 – N 10). In these experiments, a considerable portion of the total carbon could be detected as dissolved carbon (24-61 %). The amount of highly oxidized carboxylic acids is less (2-6 %) than in case of the runs with overstoichiometric oxidant supply.

These results were basically confirmed through quantitative measurements of the residual naphthalene by GC analysis. Measurable amounts of naphthalene could only be detected for the non-oxidative experiments (run N 1, N 2) and run N 10. In case of run N 1, the concentration of naphthalene determined by GC analysis exceeded the influent concentration, which is probably due to incomplete mixing of the suspension during the taking of the sample for the liquid-liquid extraction with toluene. The naphthalene conversion calculated for run N 2 is 16 %, which appears to be rather high when compared to the results of the DOC analysis (4 %). This might also be a problem of incomplete mixing in the sample vial, meaning that the amount of naphthalene in the aqueous phase used for liquid-liquid extraction deviates from the naphthalene content in the effluent suspension. Run N 10 exhibits a low residual naphthalene content corresponding to a degree of conversion of 99.1 %.

The data depicted in Table 5.7 reveal a significant portion of dissolved organic carbon, which cannot be attributed to carboxylic acids higher than formic acid. The contribution of formic acid cannot be assessed by GC-FID. Therefore, selected samples of the naphthalene experiments were analysed by GC-MS to identify further decomposition products.

Three samples (run N 1, N 7, and N 10) representing non-oxidative and oxidative conditions at different amounts of oxidant were selected. It can be concluded that no compounds other than naphthalene are present in significant amounts at non-oxidative conditions. This observation is in line with the results of the DOC analysis and the quantification of residual naphthalene by GC-FID. Apart of small amounts of residual naphthalene (3), phenol (1) and benzoic acid (2) could be identified as major degradation products of the partial oxidation. By means of a two-

point external calibration phenol, benzoic acid, and residual naphthalene could be analysed quantitatively. Along with the carboxylic acids these compounds amount to about 60 % of the dissolved organic carbon. The residual fraction can be partly attributed to further organic substances extracted by dichloromethane. Formic acid might have a significant contribution, too. In addition, it is very likely that polar, hydrophilic compounds other than carboxylic acids are formed in the course of the partial oxidation. This can be inferred from the detection of additional peaks by the GC method used to quantify carboxylic acids.

As compared to the partial oxidation, the oxidative destruction supplying excess oxidant (run N 7) yields less degradation products at a lower concentration level.

In order to identify further degradation products of the partial oxidation a sample volume of 20 ml (run N 9) was extracted with 20 ml of dichloromethane. The solvent was subsequently evaporated in a rotary evaporator and the residue re-solubilized in 1 ml dichloromethane. A list of substances identified in this highly concentrated sample is given in Table 5.8.

Table 5.8: Naphthalene oxidation products of run N 9: Partial oxidation at 375°C, 8 s

Substance	Retention time [min]	Substance	Retention time [min]
Benzaldehyde	5.04	Phenylacetic acid	14.72
Phenol	5.55	Pelargonic acid	14.83
Hydroxy-benzaldehyde	6.92	Methylpropylphenol	16.67
Methoxyphenol	7.93	Phenyl derivatives	et seqq.
Naphthalene	10.71	Hydroxymethoxy-benzaldehyde	17.42
Benzoic acid	14.30	Naphthalene derivatives	et seqq.
Methylbenzoic acid	14.68	Binaphthalene	33.35

The results reveal that a number of different decomposition products is formed in trace amounts during partial oxidation of naphthalene. A complete identification and quantification of all these substances is practically impossible.

Based on the results of the literature survey and own experiments, in can be concluded that PCBs as well as PAHs are modified at the conditions applied in the continuous treatment of lignocellulosic biomass. Naphthalene is degraded to a minor extent by hydrolysis, but decomposes to a number of degradation products at partial oxidation. At overstoichiometric oxidant supply, naphthalene undergoes essentially complete conversion.

Due to the multitude of PCBs and PAHs and the variety of decomposition products it cannot be completely excluded that a particular compound might be transformed to degradation products showing an increased toxicity. It is therefore recommended to apply SCWO at temperatures in the range of 550 to 600°C and reaction times in the order of minutes in case

PCBs are present in the input material in significant amounts. Such operating conditions are, however, not required for the degradation of lignocellulosic wastes, which was the scope of this work.

6 CONCLUDING REMARKS

In this work, model compounds like cellulose and lignin as well as real lignocellulosic biomass, e.g. a kitchen waste specified by ESA, wheat straw, and indigestible residues of a methanogenic bioreactor could be successfully converted by hydrothermolysis. Beside the substantial removal of insoluble carbon and nitrogen, this technology showed some further beneficial aspects. The hydrothermal reaction unit could be implemented in a system consisting of biological compartments without showing any inhibitory or detrimental effects on the microorganisms employed in the set-up. The effluents obtained from the hot water treatment exhibited a distinctly increased biodegradability, yielding an essentially complete conversion to biogas by subsequent methanogenic digestion. The hydrothermal effluents were absolutely sterile, meaning that the treatment in sub- and supercritical imposes a hygienic barrier to the overall system and guarantees the biosafety of effluents.

Pure cellulose could be completely converted to soluble degradation products in subcritical water in the order of seconds to minutes, without additional catalysts. The rate of liquefaction could be modelled by a global first order kinetic approach. Main degradation products of cellulose hydrolysis could be identified and quantified. The formation of glucose and secondary degradation products could be described by assuming the pattern of a consecutive reaction with both formation and subsequent decomposition being of first order. The modelling of glucose formation showed a shift of maximum glucose yields to shorter residence times with increasing temperatures and an increase in attainable yields with temperature. The addition of carbon dioxide led to a rate enhancement of cellulose hydrolysis.

Pure lignin as well as lignocellulosic biomass could not be completely liquefied by hydrolysis. The oxidation of lignocellulose in near-critical water in the presence of hydrogen peroxide led to the removal of essentially any DOC, leaving only about 10 % of the initial carbon load in the aqueous phase. In case of overstoichiometric oxidant supply, the residual DOC could almost exclusively be attributed to the formation of acetic acid as a refractory intermediate.

Based on the results of this work, important conclusions can be drawn with respect to the conversion of lignocellulosic materials in sub- and supercritical water. In case the removal of any insoluble matter is the primary aim, e.g. the destruction of excess sludge originating from domestic and industrial waste water treatment, oxidation in sub- and supercritical water can be employed as a stand-alone technology. The hydrolysis of lignocellulosic materials in high-temperature water can be applied as a supplement to biological degradation. It can either be used as a pre-treatment prior to digestion or following biological degradation to convert

indigestible residues, only. Due to the much increased biodegradability of the hydrolyzates, efficiencies up to 100 % can be achieved with respect to solid removal.

In case that the utilization of lignocellulosic materials as a feedstock for valuable degradation products is the main objective, a two step process is proposed. In a first step, cellulose and polyose could be liquefied at near-critical conditions and residence times in the order of seconds or fractions of a second. Such short residence times would be recommendable to maximize the yields of primary reaction products, e.g. saccharides, and to largely suppress the onset of secondary reactions. The insoluble, lignin-rich portion could afterwards be treated by partial oxidation to yield valuable aromatic compounds like phenolic substances and vanillin.

[1] Bobleter O.: Hydrothermal Degradation of Polymers Derived from Plants, Prog. Polym. Sci. 19 (1994) 797-841

[2] Final Report for 2004 Activity on MELISSA, ed. by Ch. Lasseur, I. Fedele; ESA/EWP-2092, April 2000

[3] Brunner G.: Gas Extraction, Springer Verlag New York, 1994

[4] Stahl E., Quirin K.W., Gerared D.: Verdichtete Gase zur Extraktion und Raffination, Springer Verlag, Berlin, 1987

[5] Brunner G.: Supercritical Fluids as Solvents and Reaction Media, Elsevier, Amsterdam, 2004

[6] Jessop P.G., Leitner W.: Chemical Synthesis using Supercritical Fluids, Wiley-VCH, Weinheim, New York, 1999

[7] Shaw R.W., Brill T.B., Clifford A.A., Eckert C.A., Franck E.U.: Supercritical Water – A Medium for Chemistry, Chem. Eng. News 69 (1991) 51, pp. 26-39

[8] Savage P.E., Gopalan S., Mizan T.I., Martino C.J., Brock E.E.: Reactions at Supercritical Conditions: Applications and Fundamentals, AICHE J. 41 (1995) 7, pp. 1723-1778

[9] Sealock L.J., Elliott D.C., Baker E.G., Butner R.S.: Chemical Processing in High-Pressure Aqueous Environments. 1. Historical Perspective and Continuing Developments, Ind. Eng. Chem. Res. 32 (1993) 8, pp. 1535-1541

[10] Brüll D., Kaul C., Krämer A., Krammer P., Richter T., Jung M., Vogel H., Zehner P.: Chemie in überkritischem Wasser, Angew. Chem. 111 (1999), pp. 3180-3196

[11] Kruse A.: Reaktionen in nah- und überkritischem Wasser, Nachrichten Forschungszentrum Karlsruhe Jahrg. 33 (2001), pp. 59-70

[12] Uematsu M., Franck E.U.: Static Dielectric Constant of Water and Steam, J. Phys. Chem. Ref. Data 9 (1980) 4, pp. 1291-1306

[13] Deul R., Franck E.U.: The Static Dielectric Constant of the Water-Benzene mixture System to 400°C and 2800 bar, Ber. Bunsenges. Phys. Chem. 95 (1991), pp. 847-853

[14] Brunner G.: Extraction and Destruction of Waste with Supercritical Water, in: Supercritical Fluids: Fundamentals for Application, Kiran E., Levelt Sengers J.M.H. (Eds.), Kluwer Academic Publishers, Dordrecht, The Netherlands, 1994, pp. 697-705

[15] Katritzky A.R., Allin S.M., Siskin M.: Aquathermolysis: Reactions of Organic Compounds with Superheated Water, Acc. Chem. Res. 29 (1996) 8, pp. 399-406
[16] Nowak K.: Reinigung kontaminierter Bodenmaterialien mit überkritischem Wasser, Dissertation, Hamburg, 1996
[17] Firus A.: Reinigung von Bodenmaterial durch Extraktion und Reaktion mit überkritischem Wasser und Kohlendioxid, Dissertation, Hamburg, 1996
[18] Marshall W.L., Franck E.U.: Ion Product of Water Substance, 0-1000°C, 1-10,000 Bars. New International Formulation and Its Background, J. Phys. Chem. Ref. Data 10 (1981) 2, pp. 295-304
[19] Bandura A.V., Lvov S.N.: The Ionization Constants of Water over a Wide Range of Temperatures and Densities, Proceedings of the International Conference on the Properties of Water and Steam, Toronto, Canada, 1999, pp. 96-103
[20] Römpp Chemie Lexikon, Georg Thieme Verlag Stuttgart, New York
[21] Xiang Q., Lee Y.Y., Pettersson P.O., Torget R.W.: Heterogeneous Aspects of Acid Hydrolysis of α-Cellulose, Appl. Biochem. Biotechnol. 105-108 (2003), pp. 505-514
[22] Bjerre A.B., Olesen A.B., Fernqvist T., Plöger A., Schmidt A.S.: Pretreatment of Wheat Straw Using Combined Wet Oxidation and Alkaline Hydrolysis Resulting in Convertible Cellulose and Hemicellulose, Biotechnol. Bioeng. 49 (1996) 5, pp.568-577
[23] Jones, J.: Synthese von Aminosäuren und Peptiden, VCH Verlagsgesellschaft Weinheim (1995)
[24] Montoneri, E.; Rizzi, G.; Rizzi, A.; Mordenti, A.; Bauli, A.; Riolfatti, M.; Pellegrini, L.: Hydrolysis of Tannery Wastes to Protein Meal for Animal Feedstuffs: A Process and Product Evaluation, J. Chem. Tech. Biotechnol., Vol. 59, pp. 91-99 (1994)
[25] Lin, X.; Shih, J.C.H., Swaisgood, H.E.: Hydrolysis of Feather Keratin by Immobilized Keratinase, Applied and Environmental Microbiology, Vol. 62, No. 11, pp. 4273-4275 (1996)
[26] Krammer P., Vogel H.: Hydrolysis of Esters in Subcritical and Supercritical Water, J. Supercrit. Fluids 16 (2000), pp. 189-206
[27] Kruse A.: Die Pyrolyse von tert.-Butylbenzol in überkritischem Wasser, Dissertation, Karlsruhe, 1994
[28] Bühler W. Dinjus E., Ederer H.J., Kruse A., Mas C.: Ionic Reactions and Pyrolysis of Glycerol as Competing Reaction Pathways in Near- and Supercritical Water, J. Supercrit. Fluids 22 (2002), pp. 37-53
[29] Liu K.: Zur Hydrolyse von Biopolymeren in Wasser und Kohlendioxid unter erhöhten Drücken und Temperaturen, Dissertation, Hamburg, 2000
[30] Moreschi S.R.M., Petenate A.J., Meireles M.A.A.: Hydrolysis of Ginger Bagasse Starch in Subcritical Water and Carbon Dioxide, J. Agric. Food Chem. 52 (2004) 6, pp. 1753-1758
[31] Hunter S.E., Savage P.E.: Acid-Catalyzed Reactions in Carbon Dioxide-Enriched High-Temperature Liquid Water, Ind. Eng. Chem. Res. 42 (2003) 2, pp. 290-294
[32] Misch B.: Reinigung mischkontaminierten Bodenmaterials und kontinuierliche Extraktion von Feststoffen mit überkritischen Fluiden, Dissertation, Hamburg, 2001

[33] Da Silva D.L.: Extraction of Heavy Metals from Contaminated Soil Material and Regeneration of Ion Exchange Resins and a Biosorbent by Means of Water and Carbon Dioxide, Dissertation, Hamburg, 2003

[34] Stegmann R., Brunner G., Calmano W., Matz G.: Treatment of Contaminated Soil, Springer Verlag Berlin Heidelberg, 2001

[35] Takenouchi S., Kennedy G.C.: The Binary System H2O-CO2 at High Temperatures and Pressures, Am. J. Sci. 262 (1964), pp. 1055-1073

[36] Read A.J.: The First Ionization Constant of Carbonic Acid from 25 to 250°C and to 2000 bar, J. Sol. Chem. 4 (1975) 1, pp. 53-70

[37] Toews K.L., Shroll R.M., Wai C.M., Smart N.G.: pH-Defining Equilibrium between Water and Supercritical CO_2. Influence on SFE of Organics and Metal Chelates, Anal. Chem. 67 (1995) 22, pp. 4040-4043

[38] Wissenschaftliche Tabellen Geigy, CIBA-GEIGY Limited, Basle, Switzerland

[39] Meyer J.C., Marrone P.A., Tester J.W.: Acetic Acid Oxidation and Hydrolysis in Supercritical Water, AIChE J. 41 (1995) 9, pp. 2108-2121

[40] Calvo L., Vallejo D.: Formation of Organic Acids During the Hydrolysis and Oxidation of Several Wastes in Sub- and Supercritical Water, Ind. Eng. Chem. Res. 41 (2002) 25, pp. 6503-6509

[41] Wagner W., Kruse A.: Properties of Water and Steam, International Association for the Properties of Water and Steam, Springer, Berlin, Germany, 1998

[42] Kruse A., Abeln J., Dinjus E., Kluth M., Petrich G., Schacht M., Sadri E., Schmieder H.: Gasification of Biomass and Model Compounds in Hot Compressed Water, Proceedings of the International Meeting of the GVC Fachausschuss "Hochdruckverfahrenstechnik", Karlsruhe, Germany, March 3-5, 1999, pp. 111-114

[43] Keil F.: Skriptum zur Vorlesung Chemische Reaktionstechnik I, Technische Universität Hamburg-Harburg

[44] Sasaki M., Adschiri T., Arai K.: Kinetics of Cellulose Conversion at 25 MPa in Sub- and Supercritical Water, AICHE J. 50 (2004) 1, pp. 192-202

[45] Sasaki S., Fang Z., Fukushima Y., Adschiri T., Arai K.: Dissolution and Hydrolysis of Cellulose in Subcritical and Supercritical Water, Ind. Eng. Chem. Res. 39 (2000) 8, pp. 2883-2890

[46] Tödheide K., Franck E.U.: Das Zweiphasengebiet und die kritische Kurve im System Kohlendioxid-Wasser bis zu Drucken von 3500 bar, Z. Phys. Chem. 37 (1963), pp. 387-401

[47] VDI-Wärmeatlas, VDI-Verlag, Düsseldorf, 1994

[48] Span R., Wagner W.: A New Equation of State for Carbon Dioxide Covering the Fluid Region from the Triple-Point Temperature to 1100 K at Pressures up to 800 MPa, J. Phys. Chem. Ref. Data 25 (1996) 6, pp. 1509-1596

[49] Bobleter O., Concin R.: Degradation of Poplar Lignin by Hydrothermal Treatment, Cellul. Chem. Technol. 13 (1979), pp. 583-593

[50] Saisu M., Sato T., Watanabe M., Adschiri T., Arai K.: Conversion of Lignin with Supercritical Water-Phenol Mixtures, Energy & Fuels 17 (2003) 4, pp. 922-928

[51] NIST Chemistry WebBook, Nationale Institute of Standards and Technolgy, http:///www.nist.gov

[52] Van Soest P.J.: Use of detergent in the analysis of fibrous feed II – A rapid method for the determination of fiber and lignin, J. Ass. Anal. Chem. 46 (1963), pp. 829-835

[53] Sakaki T., Shibata M., Miki T., Hirosue H., Hayashi N.: Reaction Model of Cellulose Decomposition in Near-Critical Water and Fermentation of Products, Bioresour. Technol. 58 (1996), pp. 197-202

[54] Schieder D., Schneider R., Bischof F.: Thermal Hydrolysis (TDH) as a Pretreatment Method for the Digestion of Organic Waste, Water Sci. Technol. 41 (2000) 3, pp. 181-187

[55] Bonmati A., Flotats X., Mateu L., Campos E.: Study of Thermal Hydrolysis as a Pretreatment to Mesophilic Anaerobic Digestion of Pig Slurry, Water Sci. Technol. 44 (2001) 4, pp. 109-116

[56] Walter W., Harke H.-P., Polchow R.: Das Verhalten von Glykokoll, Alanin, α-Aminobuttersäure, Leucin, Phenylalanin und Aspariginsäure unter hydrothermalen Bedingungen, Sonderdruck aus der Zeitschrift für Naturforschung 22b (1967) 9, pp. 931-937

[57] Susumu M., Kiyotaka H., Yutaka I., Isao S., Shinsuke M.: Production of Amino Acid or Peptide from Protein by Using Super Critical Water and Food, Feed, Medium for Culturing Microorganism and Medicine, Japanese Patent 09268166 A, 1997

[58] Izumi Y., Chibata I., Itoh T.: Herstellung und Verwendung von Aminosäuren, Angew. Chemie 90 (1978), pp. 187-194

[59] Chibata I., Kawashima K.: Use of Amino Acids in Medicine, in: Nutrition: Proteins and Amino Acids, Springer Verlag, 1990, pp. 273-284

[60] Doncheva D.: Entfernung von Proteinen aus Pferdeknochenmaterial mittels Extraktion in unter- und nahekritischem Wasser, Diplomarbeit, Technische Universität Hamburg-Harburg, 2004

[61] Modell, M., Sobczynski, S., Larson, J.: Supercritical Water Oxidation of Pulp Mill Sludges, MODEC-research report, Boston, 1991

[62] Weber R., Yoshida S., Miwa K.: PCB Destruction in Subcritical and Supercritical Water – Evaluation of PCDF Formation and Initial Steps of Degradation Mechanisms, Environ. Sci. Technol. 36 (2002) 8, pp. 1839-1844

[63] Hatakeda K., Ikushima Y., Ito S., Saito N., Sato O.: Supercritical Water Oxidation of a PCB of 3-Chlorobiphenyl Using Hydrogen Peroxide, Chem. Lett. (1997), pp. 245-246

[64] Anitescu G., Tavlarides L.L.: Supercritical Water Oxidation Reaction Pathway and Kinetics of Polychlorinated Biphenyls, Proceedings of the 2001 Conference on Environmental Research, Manhattan, Kansas, May 21-24 (2001), pp. 40-51

[65] Sako T., Sugeta T., Otake K., Kamizawa C., Okano M., Negishi A., Tsurumi C.: Dechlorination of PCBs with Supercritical Water Hydrolysis, J. Chem. Eng. Jpn. 32 (1999) 6, pp. 830-832